EXHIBIT A

Biomed Mass Spectrom. 1984 Feb;11(2):55-9.

Fast atom bombardment mass spectrometry of insulin, insulin A-chain, insulin B-chain, and glucagon.

Desiderio DM, Katakuse I.

Fast atom bombardment mass spectral data are presented for the polypeptides insulin, oxidized insulin A-chain, carboxymethylated insulin B-chain, and glucagon. The doubly-charged molecular ion of the intact insulin molecule produced with fast atom bombardment with xenon atoms is observed at a reduced accelerating voltage (4 kV).

PMID: 6372882 [PubMed - indexed for MEDLINE]

EXHIBIT B

mie (Lyon, France) for supporting this work and for supplying pure bromoxynil (sodium salt). We also thank G. S. Dangl and M. Griggs for tobacco transformation and regeneration, C. Shewmaker and J. O'Neal for providing the small subunit promoter vector plasmid pCGN631 (a precursor to plasmid pCGN1510), J. Kiser for chloroplast analysis, and S. Autry for plant spraying.

29 April 1988; accepted 9 August 1988

Single-Chain Antigen-Binding Proteins

ROBERT E. BIRD,* KARL D. HARDMAN, JAMES W. JACOBSON, SYD JOHNSON, BENNETT M. KAUFMAN, SHWU-MAAN LEE, TIMOTHY LEE, SHARON H. POPE, GARY S. RIORDAN, MARC WHITLOW

Single-chain antigen-binding proteins are novel recombinant polypeptides, composed of an antibody variable light-chain amino acid sequence (V_L) tethered to a variable heavy-chain sequence (V_H) by a designed peptide that links the carboxyl terminus of the V_L sequence to the amino terminus of the V_H sequence. These proteins have the same specificities and affinities for their antigens as the monoclonal antibodies whose V_L and V_H sequences were used to construct the recombinant genes that were expressed in *Escherichia coli*. Three of these proteins, one derived from the sequence for a monoclonal antibody to growth hormone and two derived from the sequences of two different monoclonal antibodies to fluorescein, were designed, constructed, synthesized, purified, and assayed. These proteins are expected to have significant advantages over monoclonal antibodies in a number of applications.

TYPICAL ANTIBODIES ARE COMPOSED of four polypeptide chains, two light chains of about 220 amino acid residues and two heavy chains of about 440 amino acids (*1*). These chains fold into domains of approximately 110 amino acids, assuming a conserved three-dimensional conformation (*2*). The domains associate to form discrete structural regions. The antigen binding or variable regions are formed by the interaction of the variable light (V_L) and variable heavy (V_H) domains at the amino termini of the chains. The first constant regions are formed by interaction of the remainder of the light chain and the first constant domain of the heavy chain. Two or three additional constant regions are formed by interaction of the two heavy chains. The heavy chain constant regions are responsible for effector functions, such as complement fixation and binding to receptors (*3*).

The high background present when intact antibodies have been used to image tumors is in large part due to the binding of the antibody to nontumor cells via the heavy chain constant regions (*4*). When Fab fragments, consisting of the variable region and the first constant region, have been used the background problem has been partially circumvented (*4*). Therefore, a better molecule to use as an imaging or delivery agent would be the Fv fragment, which consists of only the V_L and V_H domains. Unfortunately, there have been few reports of the successful isolation of Fv fragments by proteolytic digestion of intact antibody molecules (*5*).

The idea for the design and synthesis of single-chain antigen-binding proteins was conceived during attempts to circumvent problems encountered when expressing antibody genes in *Escherichia coli* and to avoid problems associated with reassociation of Fv fragments. These proteins consist of the V_L and V_H sequences synthesized as a single polypeptide chain, with the carboxyl terminus of the V_L linked by a designed peptide to the amino terminus of the V_H. Both chains are therefore expressed in equimolar concentrations, and the covalent linking of the two chains facilitates the association of the V_L and V_H domains after folding.

Determination of the three-dimensional structures of antibody fragments by x-ray crystallography has led to the realization that variable domains are each folded into a characteristic structure composed of nine strands of closely packed β-sheets. This structure is maintained despite sequence

Genex Corporation, 16020 Industrial Drive, Gaithersburg, MD 20877.

*To whom correspondence should be addressed.

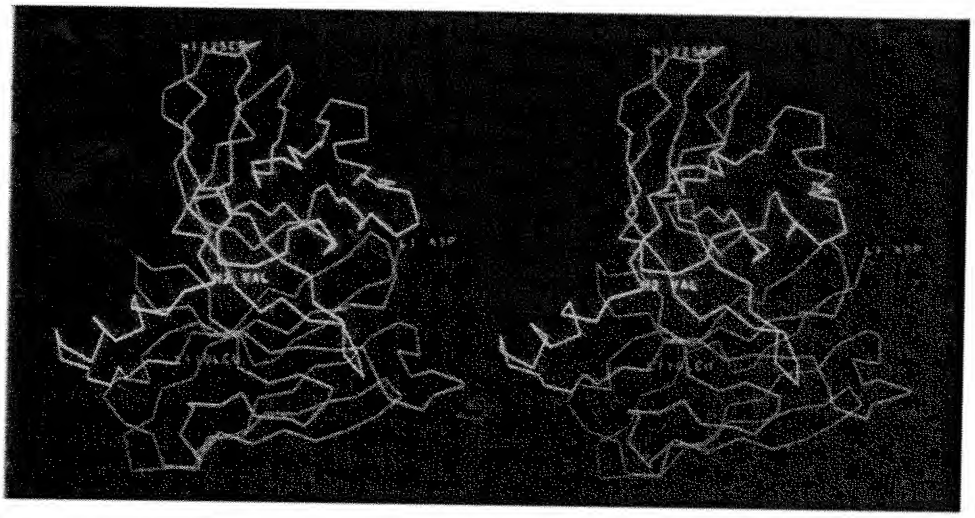

Fig. 1. An alpha-carbon model of the anti-BGH 3C2/59 single-chain antigen-binding protein. The V_L is red, the V_H is blue, and the linker is green. The model was generated by superimposing the sequences of the 3C2 V_L and V_H domains of the single-chain antigen-binding protein onto the structure of the variable region of MCPC603 (*9*). The sequence of the protein depicted is MENV LTQSPAIMSASPGEKVTMTCRASSSVS SSYLHWFQQKSGASPKLWIYSTSNLA SGVPARFSGSGSGTSYSLTISSVEAEDA ATYYCQQYSGYPLTFGAGTKLKESGS VSSEQLAQFRSLDVQLVESGGDLVKP GGSLKLSCAASGFTFISYGMSWVRQT PDKRLEWVATISSGGSTYTYYPDSVKG RFTISRDNAKNTLYLQMSGLKSEDTA MYYCARRITTVVLTDYYAMDYWGQ GTSVTVS; with the linker region underlined. Abbreviations for the amino acid residues are as follows: A, Ala; C, Cys; D, Asp; E, Glu; F, Phe; G, Gly; H, His; I, Ile; K, Lys; L, Leu; M, Met; N, Asn; P, Pro; Q, Gln; R, Arg; S, Ser; T, Thr; V, Val; W, Trp; and Y, Tyr. The linker, which in this case is derived from a segment of human carbonic anhydrase, spans from residue 105 of the V_L to residue 2 of the V_H with the use of the Kabat numbering system (*7*). The carboxyl terminus corresponds to residue 116 of the V_H, after which a stop codon was introduced. A methionine was inserted in front of the V_L for expression in *E. coli*. The single-chain antigen-binding proteins have been designated by the monoclonal name (for example, 3C2) with the number of the designed linker sequence after the diagonal mark (for example, 3C2/59).

variation in the V_L and V_H domains (*6*). Analysis of antibody primary sequence data has established the existence of two classes of variable region sequence: hypervariable sequences and framework sequences (*7*). The framework sequences are responsible for the correct β-sheet folding of the V_L and V_H domains and for the interchain interactions that bring domains together. Each variable domain contains three hypervariable sequences, which appear as loops at one end of the β-sheets. The six hypervariable sequences of the variable region, three from the V_L and three from the V_H, form the antigen-binding site and are therefore named the complementarity determining regions (CDRs).

The design of the single-chain antigen-binding protein was based on the assumption that the molecular interactions responsible for the conserved structure, determined by the framework sequences, would assure that proper folding of the individual V_L and V_H domains would occur when tethered by a short peptide linker. Linkers of different designs have been used to join the V_L and V_H sequences.

A computer-assisted method (*8*) was used in designing the first group of linkers. Since the variable domains of antibodies appear to have homologous three-dimensional structures, we based our modeling on the previously published structure of the Fab fragment of MCPC603, a mouse myeloma protein that binds phosphorylcholine (*9*). Design of the polypeptide linker was initiated by selecting specific amino acids, one near the carboxyl terminus of the V_L sequence and one near the amino terminus of the V_H sequence. A computer program was then used to search libraries of three-dimensional peptide structures derived from the Brookhaven Protein Data Bank for peptides of the proper molecular dimensions to span the distance in space between the selected amino acids. The number of potential peptides was reduced by specifying that the angle of the peptide bonds at the ends of the linker peptide match the angles of the bonds at the selected amino acids on either side of the linker. Structures of the remaining potential linker peptides were superimposed onto the MCPC603 variable region structure by computer graphics. The peptides that had a conformation that interfered with the Fv structure were discarded. This process was repeated with different amino acids as linker attachment sites to identify a number of peptides that could be used to link the V_L and V_H regions of antibodies to create single-chain antigen-binding proteins. The linker in single-chain antigen-binding proteins to bovine growth hormone (BGH), 3C2/59, and to fluorescein, 18-2-3/59, was designed by this method. A model of the three-dimensional structure of 3C2/59 protein is shown in Fig. 1.

Additional linkers were designed by the incremental addition of single amino acids or short peptides extending from the carboxyl terminus of the V_L to the amino terminus of the V_H. Some linkers were designed to minimize interactions with the Fv and others were designed to fit into a groove on the back of the Fv structure with the use primarily of alternating glycine and serine residues with glutamic acid and lysine residues included to enhance solubility. The linkers in the single-chain antigen-binding proteins to fluorescein 18-2-3/202 and 4-4-20/202′ were designed in this way. Linker 202 has the sequence EGKSSGSGSESKST. In the 4-4-20/202′ protein, an additional amino acid, Gln, is present between the linker and the V_H.

The first single-chain antigen-binding protein genes were constructed from the V_L and V_H sequences of 3C2, an immunoglobulin G1 (IgG1) monoclonal antibody to BGH (anti-BGH). Five versions of an anti-BGH single-chain gene containing different linkers were constructed and expressed in *Escherichia coli*. The resulting proteins were purified, renatured, and tested for their ability to bind to BGH immobilized on nitrocellulose or covalently linked to Sepharose. The anti-BGH single-chain antigen-binding protein containing a linker designated 59 (3C2/59) was chosen for further study based on its affinity for BGH-Sepharose.

When the 3C2/59 gene was expressed in *E. coli*, the single-chain protein accumulated in insoluble inclusion bodies. The 3C2/59 protein had an apparent molecular size of 26 kD as determined by SDS–polyacrylamide gel electrophoresis (SDS-PAGE). This compares favorably with the molecular size of 26,652 daltons calculated from the amino acid sequence. The 3C2/59 protein cross-reacted on immunoblots with antiserum prepared against purified 3C2 light chain.

The anti-BGH 3C2/59 protein was renatured and purified by affinity chromatography on BGH-Sepharose. The affinity-purified protein migrated as a single band of 26 kD when analyzed by SDS-PAGE under both reduced and nonreduced conditions. The amount of protein that was successfully folded and therefore able to bind to a BGH-Sepharose column varied between 5% and 30% in different experiments. To demonstrate that the affinity-purified protein retained binding activity after thiocyanate elution, the protein was analyzed again by chromatography on a second BGH-Sepharose column. More than 90% of this protein bound to BGH-Sepharose and was eluted with thiocyanate. Renatured single-chain protein produced from a modified 3C2/59 gene in which the sequence of five of the six hypervariable regions had been changed did not bind to BGH-Sepharose, demonstrating that binding of 3C2/59 protein to BGH occurs at the antigen-binding site.

The relative affinity of the purified 3C2/59 protein for BGH was determined by competition with Fab fragments isolated from the 3C2 monoclonal antibody. Increasing amounts of unlabeled Fab were mixed with [^{35}S]methionine-labeled 3C2/59 protein, and the mixture was incubated with BGH-Sepharose. After incubation, the amount of bound labeled protein was determined. The competition curves for two ex-

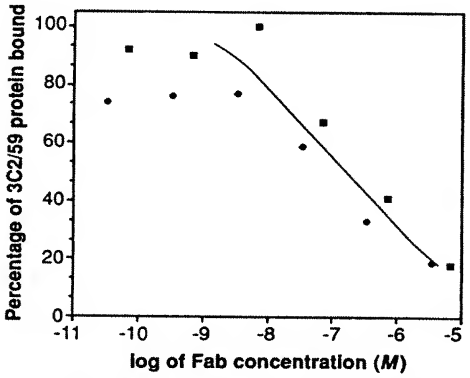

Fig. 2. The 3C2/59 gene was constructed for easy insertion into an *E. coli* expression vector such that an ATG codon is placed directly in front of the first codon of the light chain sequence. Expression is controlled by the hybrid λ phage promoter (*18*). The resulting strain containing the CI857 temperature-labile repressor gene and the expression plasmid was induced by raising the culture temperature to 42°C. Overnight growth of the expression strain GX6539 at 42°C resulted in the production of 3C2/59 protein at greater than 10% of the total cell protein. Cells that had been induced in the presence of [^{35}S]methionine were disrupted by two passes through a French Pressure Cell at 1600 psi. The crude inclusion bodies were recovered by differential centrifugation, dissolved in 50 m*M* glycine, *p*H 10.8, 9*M* urea, 1 m*M* EDTA, and 20 m*M* β-mercaptoethanol (*19*), and diluted to a final protein concentration of ~100 μg/ml in the same buffer. The diluted protein was renatured as described by Boss *et al.* (*19*). The renatured protein in phosphate-buffered saline (PBS) was bound to a BGH-Sepharose column and eluted with 3*M* sodium thiocyanate. After dialysis against PBS, 90% of the 3C2/59 protein bound to a second BGH-Sepharose column. We performed competition assays using 8×10^{-7}*M* 3C2/59 protein, BGH-Sepharose beads, and varying concentrations of Fab derived from the monoclonal antibody in a total volume of 175 μl. After washing, we counted individual wells containing the Sepharose beads in a Beckman liquid scintillation counter to quantitate binding. The results from two experiments are shown by the different symbols.

periments are shown in Fig. 2. The concentration of Fab that inhibited binding of 3C2/59 protein to BGH by 50% was $2 \times 10^{-7}M$, one-fourth the concentration of the labeled protein ($8 \times 10^{-7}M$), indicating that the equilibrium constant (K_a) of the 3C2/59 single-chain protein was within a factor of 4 of the K_a of the Fab.

Monoclonal antibodies to fluorescein were chosen for continued development of the single-chain antigen-binding protein technology because this antibody-antigen system has been well characterized (*10*).

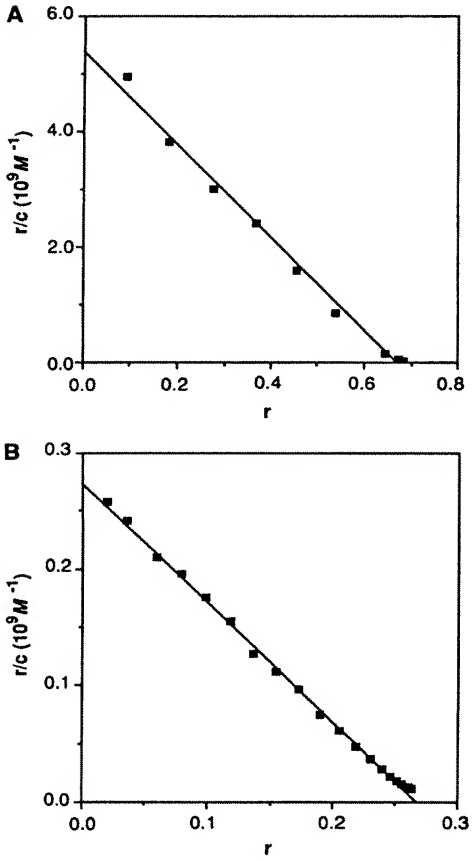

Fig. 3. Analysis of fluorescein binding affinities of the 4-4-20 Fab (**A**) and 4-4-20/202′ protein (**B**) by the use of a fluorescence quenching assay (*11*). The r represents the fraction of Fab or 4-4-20/202′ protein bound, and c represents the concentration of unbound fluorescein. A sample (590 μl) was placed in a 0.5-cm path-length cell, and 10-μl portions of $3.0 \times 10^{-7}M$ fluorescein were added to each sample and to buffer specimens (controls); the fluorescence was measured with a Perkin-Elmer LS-5 fluorescence spectrophotometer. Quenching maxima (previously determined) of 0.965 and 0.970 were used for the 4-4-20 Fab and 4-4-20/202′ protein analysis, respectively. We calculated protein concentrations from absorbance at 280 nm using calculated molar extinction coefficients at 280 nm (76,182 and $51,267 M^{-1}$ cm^{-1} for the 4-4-20 Fab and 4-4-20/202′ protein, respectively, based on the Trp and Tyr content of each protein sequence).

Several monoclonal antibodies with high affinity for fluorescein have been isolated, and quantitative assays for equilibrium constant determinations based on the quenching of fluorescein fluorescence have been described (*11*). Single-chain antigen-binding protein genes were constructed from the sequences of the variable domains of two different monoclonal antibodies to fluorescein: 18-2-3, an IgM (*12*), and 4-4-20, in IgG2a (*13*).

Binding measurements for each sample of anti-fluorescein Ig, Fab, or single-chain antigen-binding protein were performed by fluorescence quenching assays (*11*). An initial titration of the protein with fluorescein was used to determined the fluorescence quenching maximum (Q_{max}). An estimate of the K_a was then calculated from this titration to select protein and fluorescein concentrations for accurate determination of the K_a. For the monoclonal antibody 4-4-20, the reported values for Q_{max} and K_a are 96.4% and $1.7 \times 10^{10} M^{-1}$, respectively (*13*).

The 4-4-20/202′ protein, renatured from inclusion bodies, was concentrated, dialyzed against 20 m*M* tris, *p*H 8.5, loaded onto a DEAE-SPW high-performance liquid chromatography anion exchange column (LKB), and eluted with a linear gradient of 0 to 2*M* sodium acetate in 20 m*M* tris, *p*H 8.5. Binding data for samples of 4-4-20 Fabs and 4-4-20/202′ protein are shown in Scatchard plots (*14*) in Fig. 3, A and B, respectively. The K_as for the 4-4-20 Fab and the 4-4-20/202′ protein, calculated from the slopes in Fig. 3, are $8.0 \times 10^9 M^{-1}$ and $1.1 \times 10^9 M^{-1}$, respectively. The number of binding sites per molecule was determined from the *x*-intercept. Values of 0.68 and 0.27 indicate the fractions of active Fab and 4-4-20/202′ protein in the preparations under these conditions. Thus, the refolding and nonaffinity purification used for the 4-4-20/202′ protein produced 27% active protein with high affinity (*15*).

Kranz *et al.* (*13*) reported that the absorbance spectrum of fluorescein was shifted from a maximum at 493 nm to a maximum at 505 nm when the fluorescein was bound by the 4-4-20 monoclonal antibody. This shift ranged from about 500 to 525 nm for different antibodies to fluorescein. To test whether this shift occurred with fluorescein bound to a single-chain antigen-binding protein, we measured the fluorescence excitation spectra of the 4-4-20 monoclonal antibody, the Fab fragment prepared from this antibody, and the 4-4-20/202′ protein (Fig. 4). The 4-4-20/202′ protein caused a similar shift in excitation maximum from 493 to 505 nm as the monoclonal antibody and Fab, demonstrating that fluorescein was bound by the 4-4-20/202′ protein in a manner analogous to the monoclonal antibody.

The 18-2-3/59 and 18-2-3/202′ proteins also quenched the fluorescence of fluorescein. The Q_{max} of these proteins was equivalent to that of the 18-2-3 monoclonal antibody. Absolute K_a's were not determined for these proteins.

In summary, single-chain antigen-binding proteins were constructed from the variable region sequences of three different monoclonal antibodies and various linker peptides designed by computational methods and computer graphics. These proteins retain both the affinity and specificity of the starting monoclonal antibodies. The linker peptide that worked in one single-chain antigen-binding protein was also successful in a different protein, as in the anti-BGH 3C2/59 and antifluorescein 18-2-3/59 proteins. We are confident that we can produce active single-chain antigen-binding proteins with the sequence of any monoclonal antibody.

Winter and colleagues (*16*) showed that the specificity of a monoclonal antibody can be changed by substituting the hypervariable sequences of a mouse antibody into a human framework. It should also be possible to change the specificity of a single-chain antigen-binding protein by replacing the hypervariable sequences with those from a

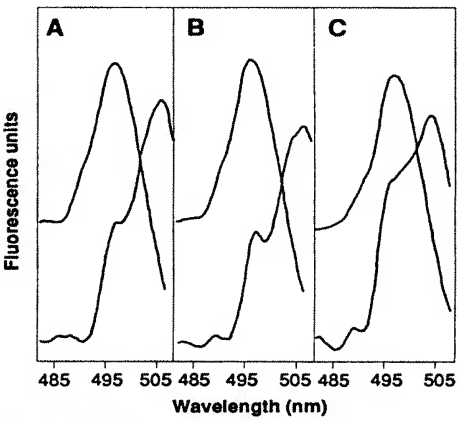

Fig. 4. The fluorescence excitation spectra were obtained on a Perkin-Elmer LS-5 fluorescence spectrometer connected to an R100 recorder and were determined at 2°C with 5-mm path-length microcuvettes in a thermostatted holder. Readings were obtained for samples (600 μl) of $5 \times 10^{-9}M$ free fluorescein (left peak in all panels) and the same concentration of fluorescein in the presence of (**A**) 10 μg/ml 4-4-20 monoclonal antibody, (**B**) 10 μg/ml 4-4-20 Fab fragment, and (**C**) 0.1 μg/ml 4-4-20/202′ protein. The fluorescence emission was monitored at 530 nm while the excitation wavelength was varied from 470 to 515 nm. The nominal absorption maximum of unbound, unquenched fluorescein is about 493 nm [left peak in (A) to (C)] and was monitored on a scale five times that of the protein-bound, quenched fluorescein samples (right peak).

monoclonal antibody having a different specificity. A logical step in the development of a clinically useful antitumor agent would be to insert the hypervariable sequences from antitumor antibodies generated in mice into a single-chain antigen-binding protein derived from human framework regions.

Single-chain antigen-binding proteins are expected to have advantages in clinical applications because of their small size. These proteins should be cleared from serum faster than monoclonal antibodies or Fab fragments. Because they lack the Fc portion of an antibody, which is recognized by cell receptors, they should have a lower background in imaging applications and they should be less immunogenic. They may penetrate the microcirculation surrounding solid tumors better than monoclonal antibodies. We foresee the use of single-chain antigen-binding proteins in applications for which monoclonal antibodies and antibody fragments are currently used, such as (i) imaging and therapy of cancers and cardiovascular or other diseases, (ii) separations, and (iii) biosensors.

The peptide linkers present in single-chain antigen-binding proteins can be designed with specialized function such as sites for the chelation of metals or the attachment of drugs or toxins for applications in imaging and therapy. In addition, it will be possible to design sequences into the linkers or at the carboxyl terminus for the attachment of the protein to solid supports for use in clinical assays, separations, and sensing devices.

Note added in proof: Since this report was submitted another paper dealing with similar technology has appeared (*17*).

REFERENCES AND NOTES

1. R. R. Porter, *Science* **180**, 713 (1973).
2. P. M. Schiffer *et al.*, *Biochemistry* **12**, 4620 (1973); R. S. Poljak *et al.*, *Proc. Natl. Acad. Sci. U.S.A.* **70**, 3305 (1973).
3. D. R. Davies and H. Metzger, *Annu. Rev. Immunol.* **1**, 87 (1983).
4. R. L. Wahl, C. Racker, G. W. Philpott, *J. Nucl. Med.* **24**, 316 (1983); P. J. Harwood *et al.*, *Eur. J. Cancer Clin. Oncol.* **21**, 1515 (1985).
5. J. Hochman, D. Inbar, D. Givol, *Biochemistry* **12**, 1130 (1973); J. Sen and S. Beychok, *Proteins* **1**, 256 (1986).
6. C. de Préval and M. Fougerdau, *J. Mol. Biol.* **102**, 657 (1976); E. A. Padlan, *Q. Rev. Biophys.* **10**, 35 (1977).
7. E. A. Kabat *et al.*, in *Sequences of Proteins of Immunological Interest* (National Institutes of Health, Bethesda, MD, 1987), pp. 1–261.
8. R. C. Ladner, U.S. Patent 4 704 692 (1987).
9. D. M Segal *et al.*, *Proc. Natl. Acad. Sci. U.S.A.* **71**, 4298 (1974); Y. Satow, G. H. Cohen, E. A. Padlan, D. R. Davies, *J. Mol. Biol.* **190**, 593 (1986).
10. E. W. Voss, Jr., in *Fluorescein Hapten: An Immunological Probe*, E. W. Voss, Jr., Ed. (CRC Press, Boca Raton, FL, 1984), pp. 3–20; J. N. Herron, D. M. Kranz, E. W. Voss, Jr., *Biochemistry* **25**, 4602 (1986); J. N. Herron, A. L. Gibson, E. W. Voss, Jr., A. B. Edmundson, *Fed. Proc.* **44**, 1328 (1985).
11. J. N. Herron, in *Fluorescein Hapten: An Immunological Probe*, E. W. Voss, Jr., Ed. (CRC Press, Boca Raton, FL, 1984), pp. 49–76.
12. D. W. Ballard, D. M. Kranz, E. W. Voss, Jr., *Proc. Natl. Acad. Sci. U.S.A.* **80**, 5071 (1983). The V_L and V_H cDNA sequences of the monoclonal antibodies to fluorescein were synthesized by priming on RNA isolated from hybridoma cells with oligonucleotides complementary to the first constant region of each chain. To verify that the isolated cDNA clones encoded the V_L and V_H chains, the amino acid sequences translated from the nucleotide sequences were compared with the amino-terminal amino acid sequences of the parent antibodies.
13. D. M. Kranz, J. N. Herron, E. W. Voss, Jr., *J. Biol. Chem.* **257**, 6987 (1982).
14. G. Scatchard, *Ann. N.Y. Acad. Sci.* **51**, 660 (1949).
15. The majority of experiments have produced K_a's within a factor of 2 of these values; therefore, log K_a's for the 4-4-20 IgG, Fab, and 4-4-20/202′ single-chain protein are 10.2, 9.9, and 9.0 ± 3, respectively. This corresponds to a difference in free energy between the Fab and 4-4-20/202′ protein of 1.1 ± 0.4 kcal mol^{-1}.
16. P. T. Jones, P. H. Dear, J. Fotte, M. S. Newberger, G. Winter, *Nature* **321**, 522 (1986); M. Verhoeyen, C. Milstein, G. Winter, *Science* **239**, 1534 (1988); L. Riechmann, M. Clark, H. Waldmann, G. Winter, *Nature* **332**, 323 (1988).
17. D. Scandella, P. Arthur, M. Mattingly, L. Neuhold, *J. Cell Biochem.* **9B**, 203 (1985).
18. J. S. Huston *et al.*, *Proc. Natl. Acad. Sci. U.S.A.* **85**, 5879 (1988).
19. M. A. Boss, J. H. Kenten, C. R. Wood, J. S. Emtage, *Nucleic Acids Res.* **12**, 3791 (1984).

20. This work was supported by NIH grants 1-R43-GM39662-01 and 1-R43-GM39646-01. We wish to thank R. C. Ladner for initiating the thought processes for this project and for designing the linker in 3C2/59. We thank K. C. Huynh-Pham, N. Essig, K. Knisely, and S. Small for technical assistance, D. Filpula and J. Nagle for DNA sequencing, P. Bryan and M. Pantoliano for discussions, and E. Voss for consultations on the antibody to fluorescein system. We also thank our colleagues for reading the manuscript.

11 May 1988; accepted 9 August 1988

Kaposi's Sarcoma Cells: Long-Term Culture with Growth Factor from Retrovirus-Infected CD4$^+$ T Cells

SHUJI NAKAMURA, S. ZAKI SALAHUDDIN, PETER BIBERFELD, BARBARA ENSOLI, PHILLIP D. MARKHAM, FLOSSIE WONG-STAAL, ROBERT C. GALLO*

Studies of the biology and pathogenesis of Kaposi's sarcoma (KS) have been hampered by the inability to maintain long-term cultures of KS cells in vitro. In this study AIDS-KS–derived cells with characteristic spindle-like morphology were cultured with a growth factor (or factors) released by CD4$^+$ T lymphocytes infected with human T-lymphotropic virus type I or II (HTLV-I or HTLV-II) or with human immunodeficiency virus type 1 or 2 (HIV-1 or HIV-2). Medium conditioned by HTLV-II–infected, transformed lines of T cells (HTLV-II CM) contained large amounts of this growth activity and also supported the temporary growth of normal vascular endothelial cells, but not fibroblasts. Interleukin-1 and tumor necrosis factor–α stimulated the growth of the KS-derived cells, but the growth was only transient and these factors could be distinguished from that in HTLV-II CM. Other known endothelial cell growth promoting factors, such as acidic and basic fibroblast growth factors and epidermal growth factor, did not support the long-term growth of the AIDS-KS cells. The factor released by CD4$^+$ T cells infected with human retroviruses should prove useful in studies of the pathogenesis of KS.

KAPOSI'S SARCOMA DEVELOPS IN the form of multifocal lesions consisting of characteristic spindle-shaped cells in a stroma of proliferating abnormal vessels, fibroblasts, and infiltrating leukocytes. An indolent form of KS occurs in elderly males in Mediterranean and African countries (*1, 2*) and a more aggressive, glandular form of the disease occurs in younger Africans. An aggressive form of KS is also associated with HIV-1 infection, primarily in homosexual men (*3, 4*), and with immune suppression due to other causes (*5*). A direct transforming involvement of HIV-1 in the development of AIDS-associated KS (AIDS-KS) is unlikely because genomic sequences of the virus have not been detected in KS tissues (*6*). Furthermore, no other viruses, environmental factors, or genetic factors have been convincingly linked to any form of KS (*4, 6, 7*). To gain insight into the nature of KS cells and to search for possible new etiological agents, we developed procedures for establishing cells from AIDS-KS in culture.

A number of growth factors, including endothelial cell growth supplement (ECGS) and fibroblast growth factors (FGF), that were previously shown to stimulate or sup-

S. Nakamura, S. Z. Salahuddin, B. Ensoli, F. Wong-Staal, R. C. Gallo, Laboratory of Tumor Cell Biology, National Cancer Institute, National Institutes of Health, Bethesda, MD 20892.
P. Biberfeld, Department of Pathology, Karolinska Institute, 10401 Stockholm, Sweden; and a Visiting Scientist at the Laboratory of Tumor Cell Biology, National Cancer Institute, National Institutes of Health, Bethesda, MD 20892.
P. D. Markham, Department of Cell Biology, Bionetics Research, Inc., Rockville, MD 20850.

*To whom correspondence should be addressed.

EXHIBIT C

The Journal of Immunology

A B7.1-Antibody Fusion Protein Retains Antibody Specificity and Ability to Activate Via the T Cell Costimulatory Pathway

Pia M. Challita-Eid, Manuel L. Penichet, Seung-Uon Shin, Tina Poles, Nima Mosammaparast, Kutubuddin Mahmood, Dennis J. Slamon, Sherie L. Morrison and Joseph D. Rosenblatt

J. Immunol. 1998;160;3419-3426
http://www.jimmunol.org/cgi/content/full/160/7/3419

The Journal of Immunology is published twice each month by The American Association of Immunologists, Inc., 9650 Rockville Pike, Bethesda, MD 20814-3994.

Print ISSN: 0022-1767 Online ISSN: 1550-6606.

A B7.1-Antibody Fusion Protein Retains Antibody Specificity and Ability to Activate Via the T Cell Costimulatory Pathway[1]

Pia M. Challita-Eid,* Manuel L. Penichet,‡ Seung-Uon Shin,‡¶ Tina Poles,* Nima Mosammaparast,* Kutubuddin Mahmood,† Dennis J. Slamon,§ Sherie L. Morrison,‡ and Joseph D. Rosenblatt[2]*†

We describe the construction and characterization of an Ab fusion protein specific for the tumor-associated Ag HER2/*neu* linked to sequences encoding the extracellular domain of the B7.1 T cell costimulatory ligand. The Ab domain of the fusion molecule will specifically target HER2/*neu*-expressing tumor cells, while the B7.1 domain is designed to activate a specific immune response. We show that the B7.1 fusion Ab retained ability to selectively bind to the HER2/*neu* Ag and to the CTLA4/CD28 counter-receptors for B7.1. Specific T cell activation was observed when the B7.1 Ab fusion protein was bound to HER2/*neu*-expressing cells. The use of the B7.1 Ab fusion protein may overcome limitations of gene transfer and/or standard Ab therapy and represents a novel approach to the eradication of minimal residual disease. *The Journal of Immunology,* **1998, 160: 3419–3426.**

T cell activation and proliferation require two signals from APCs. The first signal is Ag specific and mediated by recognition of antigenic peptides presented in the context of MHC-I or II by the TCR. A second or costimulatory signal can be provided via binding of a costimulatory ligand of the B7 family on the APC to the CD28 counter-receptor present on T cells. The B7 family includes several Ig-like molecules, including B7.1 and B7.2. Provision of signal 1 without signal 2 may lead to a state of immune tolerance (1). B7.1 gene transfer into nonimmunogenic tumor cells has been shown to elicit a T cell-mediated immune response not only against transfected ($B7^+$) but also against parental nontransfected tumor cells (2–8). Since T cell activation requires both B7.1 activation and TCR engagement, only cells with TCRs that recognize antigenic determinants on tumor cells should be activated (9). B7.1 gene transfer requires either ex vivo manipulation of tumor cells, which is technically difficult, or in vivo delivery via gene therapy vectors, which would not specifically target systemic tumor deposits. As an alternative approach we propose to target B7.1 to tumor cells via an Ab fusion protein with specificity for a tumor-associated surface Ag. The B7.1 costimulatory molecule localized at the tumor site by the Ab should aid in the activation of a systemic antitumor immune response.

The HER2/*neu* oncogene has been found to be amplified ($>5^+$ copies) and/or overexpressed in as many as 30% of human breast cancers, 10 to 30% of ovarian cancers, and a subset of lung and other cancers (10–13). Humanized anti-HER2/*neu* Ab has been demonstrated to be an effective therapeutic agent in several phase I and II clinical trials (14, 15). A phase II trial showed response in over 11% of patients and has led to ongoing phase III trials (15). These studies demonstrate the feasibility of targeting metastatic breast cancer through the HER2/*neu* Ag.

In this report we describe the construction and characterization of an Ab fusion protein in which the T cell costimulatory ligand B7.1 is fused to an anti-HER2/*neu* IgG3 Ab (B7.her2.IgG3) at the amino terminus of the heavy chain. We show that this fusion protein retains both the ability to recognize the tumor-associated Ag HER2/*neu* and the T cell costimulatory function of B7.1.

Materials and Methods

Cell lines and reagents

CHO, EL4, SKBR3, Sp2/0, and P3X63-Ag.653 cells were available in the laboratory or obtained from American Type Cell Collection (Rockville, MD). EL4, Sp2/0, and P3X63Ag8.563 cells were cultured in Iscove's medium supplemented with 5% FBS and L-glutamine, penicillin, and streptomycin (GPS).[3] SKBR3 cells were grown in RPMI 1640 medium containing 10% FBS and GPS. CHO cells were maintained in DMEM supplemented with 10% FBS and GPS. CHO/CD28 and CHO/B7 cells as well as the CD28Ig and B7Ig soluble proteins were provided by Dr. P. Linsley (Bristol-Myers-Squibb Pharmaceutical Research Institute, Seattle, WA). CHO/CD28 and CHO/B7 cells were grown in the same medium as CHO cells supplied with 0.2 mM proline and 1 μM methotrexate. CHO cells transfected with the HER2/*neu* cDNA were maintained under selection with 0.5 mg/ml of Geneticin (Life Technologies, Gaithersburg, MD). Soluble CTLA4Ig was purified from a hybridoma obtained from Dr. J. Allison (University of California, Berkeley, CA) using standard protein A column purification methods.

Expression vectors

HER2/neu retroviral vector and gene delivery. The plasmid encoding the human HER2/neu cDNA (clone 0483 generously provided by Genentech, Inc., San Francisco, CA) was digested with *Hin*dIII, filled in using Klenow polymerase, digested with *Xho*I, and cloned into the *Xho*I and filled-in *Bam*HI sites of the retroviral vector LXSN (16). The resulting plasmid was transfected into the PA317 packaging cell line using Lipofectin reagent (Life Technologies) and cells selected in 0.5 mg/ml Geneticin. Culture supernatant from the vector-producing PA317 cells was harvested, filtered through 0.45-μm pore size filters, and used to transduce CHO cells to derive CHO/Her2 cells.

*Hematology-Oncology Unit, University of Rochester Cancer Center, and †Department of Microbiology and Immunology, University of Rochester, Rochester, NY 14642; ‡Department of Microbiology and Molecular Genetics, Molecular Biology Institute, and §Division of Hematology/Oncology, Department of Medicine, University of California, Los Angeles, CA 90095; and ¶Institute of Environment and Life Science, Hallym University, Kangwon-Do, Korea

Received for publication July 23, 1997. Accepted for publication December 4, 1997.

The costs of publication of this article were defrayed in part by the payment of page charges. This article must therefore be hereby marked *advertisement* in accordance with 18 U.S.C. Section 1734 solely to indicate this fact.

[1] This work was supported by National Cancer Institute Grants EDT76502 and CA59326, the Revlon Foundation, and the Sally Edelman and Harry Gardner Cancer Research Foundation.

[2] Address correspondence and reprint requests to Dr. Joseph D. Rosenblatt, University of Rochester Cancer Center, 601 Elmwood Ave., Box 704, Rochester, NY 14642. E-mail address: Joe_Rosenblatt@urmc.rochester.edu

[3] Abbreviations used in this paper: GPS, L-glutamine, penicillin, and streptomycin; Ser, serine; Gly, glycine; PE, phycoerythrin; CHO, Chinese hamster ovary.

0022-1767/98/$02.00

Anti-HER2/neu κ light chain expression vector. The light chain V domain of the humanized humAb4D5-8 Ab was amplified from the plasmid pAK19 (17) (provided by Dr. P. Carter, Genentech) and fused to the 3′-end of human κ leader sequence by overlapping PCR. The primers used in the first cycle of amplification are: primer a, 5′-GGGGATATCCACCATGG(A/G)ATG(C/G)AGCTG(T/G)GT(C/A)AT(G/C)CTCTT-3′ and b, 5′-GACTGGGTCATCTGGATGTCGGAGTGGACACCTGTGGAG-3′ for the leader sequence using a plasmid encoding human κ light chain sequences as template DNA; and c, 5′-CTCCACAGGTGTCCACTCCGACATCCAGATGACCCAGT-3′ and d, 5′-GCTTGTCGACTTACGTTTGATCTCCACCTTGG-3′ for the V_L sequences using pAK19 as template DNA. The resultant PCR products were mixed and used as template for the amplification with primers a and d. The final PCR product of 470 bp was digested with *Eco*RV and *Sal*I and cloned into the human κ light chain expression vector previously described (18).

Anti-HER2/neu heavy chain expression vector. The strategy used to clone the heavy chain variable domain (V_H) from pAK19 is similar to the V_L cloning strategy. The primers used for amplification are: primer a, 5′-GGGGATATCCACCATGG(A/G)ATG(C/G)AGCTG(T/G)GT(C/A)AT(G/C)CTCTT-3′; b, 5′-GACTCCACCAGCTGAACCTCGGAGTGGACACCTGTGGAG-3′; c, 5′-CTCCACAGGTGTCCACTCCGAGGTTCAGCTGGTGGAGT-3′; and d, 5′-TTGGTGCTAGCCGAGGAGACGGTGACCAG-3′. The final 500-bp PCR product encoding the leader fused to the V_H sequences of anti-HER2/*neu* was cloned as an *Eco*RV/*Nhe*I fragment into the human IgG3 mammalian expression vector previously described (18).

Anti-HER2/neu B7.her2.IgG3 fusion heavy chain expression vector. The extracellular domain of the human B7.1 including the leader sequences was amplified using primers 5′-GGCATAAGCTTGATATCTGAACCATGGGC-3′ and 5′-GCGCGGTTAACCGTTATCAGGAAAATGC-3′ and cloned as a HindIII/*Hpa*I fragment at the 5′ end of the $(Ser\text{-}Gly^4)^3$ linker sequences into a pUC19-flex plasmid. The V_H domain of the humanized humAb4D5-8 Ab was amplified by PCR from the plasmid pAK19 using primers 5′-GGCGGCGGATCCGAGGTTCAGCTGGTG-3′ and 5′-TTGGTGCTAGCCGAGGAGACGGTGACCAG-3′, digested with *Bam*HI and *Hpa*I, and cloned at the 3′ end of the B7.1 and flexible linker sequences. The resulting insert encoding the B7.1-linker-V_H sequences was isolated as an *Eco*RV/*Nhe*I fragment and cloned into the expression vector for the IgG3 heavy chain (18).

Recombinant Ab expression, immunoprecipitation, and purification

Purified recombinant anti-HER2/*neu* Ab alone is referred to in the manuscript as her2.IgG3, and the anti-HER2/*neu* Ab fused to B7.1 is referred to as B7.her2.IgG3. Transfection, expression, and purification of the recombinant Abs were performed as described previously (19). Briefly, nonsecreting Sp2/0 or P3X63-Ag.653 myeloma cells were transfected with 10 μg of each of the anti-HER2/*neu* light chain and heavy chain expression vectors by electroporation. Transfected cells were plated at 10,000 cells/well in 96-well U-bottom tissue culture plates. The next day, selection in 0.5 mM histidinol (Sigma Chemical Co., St. Louis, MO) was initiated and maintained for 10 to 14 days. Wells were screened for Ab secretion by human IgG-specific ELISA as previously described, and positive wells were expanded. To determine the size of the secreted recombinant Abs, supernatants from cells grown overnight in medium containing [^{35}S]methionine were immunoprecipitated with goat anti-human IgG (Zymed Laboratories, Inc., San Francisco, CA) and staphylococcal protein A (IgGSorb, The Enzyme Center, Malden, MA). Precipitated Abs were analyzed on SDS-polyacrylamide gels in either the presence or the absence of reducing agents. For purification of her2.IgG3 and B7.her2.IgG3 Abs, Ab secreting Sp2/0 clones were expanded in roller bottles in Hybridoma Serum-Free Medium (Life Technologies), and 2 to 4 l of cell-free medium was collected. Culture supernatants were passed through a GammaBind protein G column (Pharmacia Biotech, Inc., Piscataway, NJ), and the column was washed with 10 ml of PBS. The protein was successively eluted with a total of 10 ml of 0.1 M glycine at pH 4.0, 2.5, and 2.0, and the eluate was neutralized immediately with 2 M Tris-HCl, pH 8.0. The eluted fractions were dialyzed and concentrated using Centricon filters with a molecular mass cut-off of 30,000 Da (Amicon, Inc., Beverly, MA).

Flow cytometry studies

Cells were detached by treatment with 0.5 mM EDTA, washed, and incubated with recombinant her2.IgG3 or B7.her2.IgG3 antibodies for 1 to 2 h at 4°C, then washed and stained with FITC-conjugated anti-human IgG (Sigma) or PE-conjugated anti-human B7.1 (Becton Dickinson, San Jose, CA) and analyzed by flow cytometry.

Affinity analysis

The affinity of B7.her2.IgG3 fusion protein for the Ag was compared with that of the parental her2.IgG3 Abusing the IAsys Optical Biosensor from Fisons Applied Sensor Technology (Paramus, NJ). Soluble HER2/*neu* Ag (ECD, provided by Genentech) was immobilized on a sensitized microcuvette according to the manufacturer's instructions. Her2.IgG3 or B7.her2.IgG3, at different concentrations in PBS with 0.05% Tween-20, was added to the cuvette, and association and dissociation were measured. Rate constants were calculated using the FASTfit software (supplied with the IAsys System) as previously described (20).

T cell proliferation assays

Human PBMC were isolated from normal donor blood using standard Ficoll-Hypaque density centrifugation. Human T cell enrichment columns (R&D Systems, Minneapolis, MN) were used for T cell purification according to the manufacturer's instructions. Purified T cells were plated in flat-bottom 96-well tissue culture plates at 1×10^5 cells/well in RPMI supplemented with 5% FBS. Irradiated (5000 rad) CHO, CHO/Her2 or CHO/B7 cells were added at 2×10^4 cells/well in the presence of 0, 1, 5, or 10 μg/ml recombinant her2.IgG3 or B7.her2.IgG3 and 10 ng/ml PMA (Sigma). Plates were incubated at 37°C for 3 days, pulsed with 0.5 μCi/well of [^{3}H]thymidine for 16 to 18 h, and harvested, and [^{3}H]thymidine incorporation was measured.

Results

Design and expression of the recombinant Abs

The expression vectors for the human IgG3 heavy and κ light chains were previously described (18). The variable domains of the anti-HER2/*neu* Ab were amplified by PCR from the plasmid pAK19 (provided by P. Carter, Genentech) (17) and cloned into the corresponding heavy or light chain expression vectors to derive her2.IgG3. To construct a fusion Ab between her2.IgG3 and B7.1 (referred to as B7.her2.IgG3), the extracellular domain of human B7.1 was cloned at the 5′ end of the heavy chain variable region of her2.IgG3 (Fig. 1*A*). A flexible $(Ser\text{-}Gly^4)^3$ linker was provided at the fusion site of the recombinant fusion protein to facilitate correct folding of both Ab and B7.1 domains. We elected to express B7.1 at the amino terminus of the heavy chain because B7.1 fused to the carboxyl terminus of the C_H3 domain showed decreased affinity for CD28 (data not shown). These results are consistent with a critical role for the amino terminus of B7.1 in mediating its biologic activity (21). The light chain and either the her2.IgG3 or B7.her2.IgG3 heavy chain expression vectors were cotransfected into Sp2/0 myeloma cells, and stable transfectants secreting soluble proteins were identified by ELISA.

To determine the molecular mass and assembly of the transfected proteins, cells were grown overnight in [^{35}S]methionine, and the secreted proteins were immunoprecipitated and analyzed by SDS-PAGE. In the absence of reducing agents, her2.IgG3 migrates with an apparent molecular mass of 170 kDa, while B7.her2.IgG3 is about 250 kDa (Fig. 1*B*, *lanes 1* and *2*, respectively). Following treatment with 2-ME, light chains of 25 kDa were seen for both proteins, while her2.IgG3 had a heavy chain of approximately 60 kDa, and B7.her2.IgG3 had a heavy chain of approximately 100 kDa (Fig. 1*B*, *lanes 3* and *4*, respectively). Therefore, proteins of the expected molecular mass were produced, and the fusion of the extracellular domain of B7.1 to the her2.IgG3 heavy chain did not appear to alter the secretion of the fully assembled H_2L_2 form of the Ab.

Ag binding

We tested the ability of recombinant her2.IgG3 and B7.her2.IgG3 to bind to the HER2/*neu* antigenic target by flow cytometry (Fig. 2). CHO cells stably expressing the HER2/*neu* Ag (CHO/Her2) derived by retroviral-mediated gene transfer and nontransduced CHO cells were incubated with either her2.IgG3 or B7.her2.IgG3. Binding was assayed by staining with either FITC-conjugated anti-

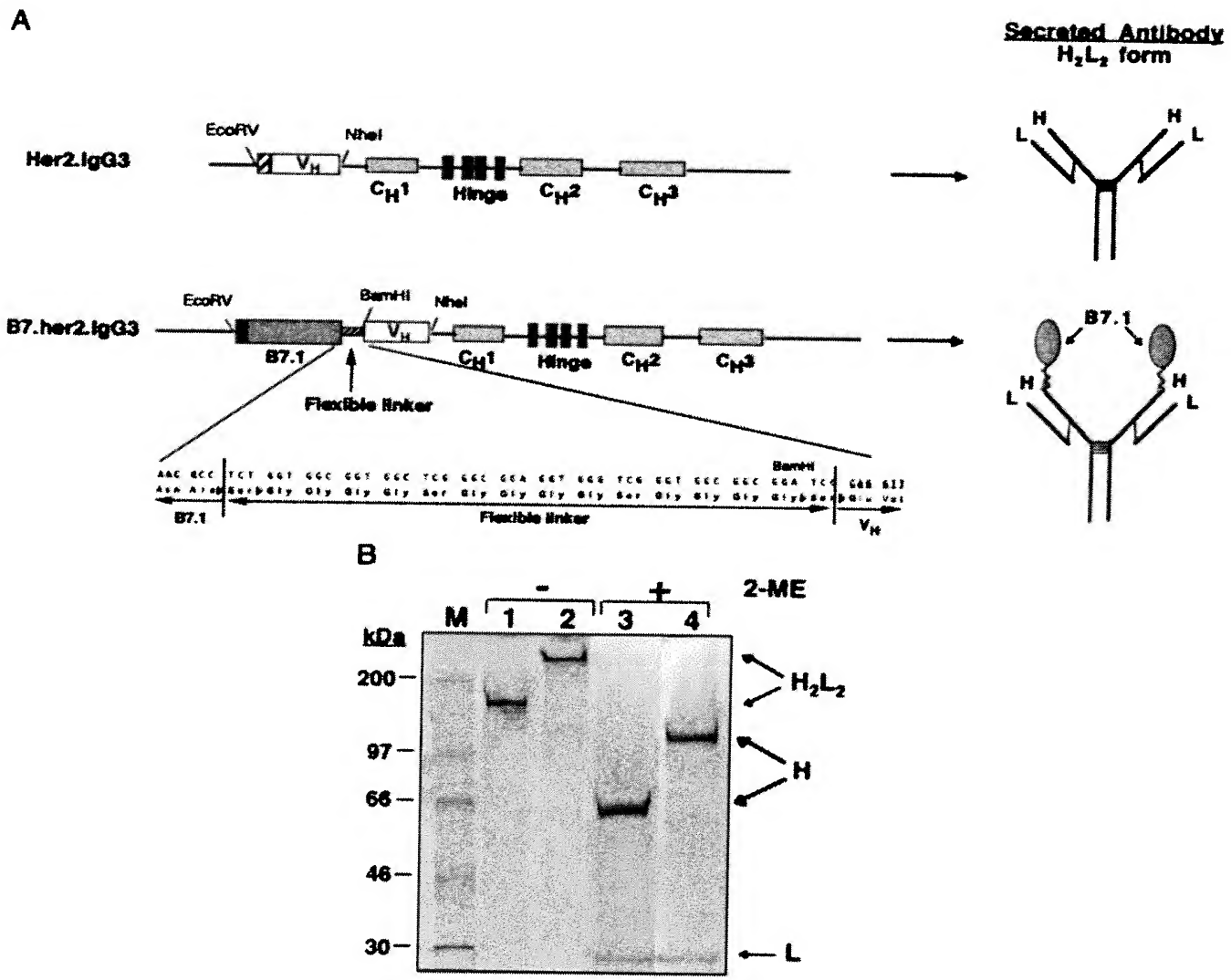

FIGURE 1. *A*, Structure of her2.IgG3 and B7.her2.IgG3 molecules. The heavy and light chain variable regions of humanized humAb4D5 anti-HER2/*neu* were cloned between the *Eco*RV sites and *Nhe*I sites of the mammalian expression vector for human IgG3 previously described (18). For the construction of B7.her2.IgG3, the B7.1 leader and extracellular domain were joined to the $(Ser\text{-}Gly^4)^3$ linker sequences that had been fused to the amino-terminal heavy chain variable sequences of the her2.IgG3 Ab. A schematic diagram of the secreted H_2L_2 forms of control her2.IgG3 and B7.her2.IgG3 is also shown. *B*, SDS-PAGE analysis of the recombinant anti-HER2/*neu* Abs. Cell lines expressing her2.IgG3 (*lanes 1* and *3*) or B7.her2.IgG3 (*lanes 2* and *4*) were labeled by overnight growth in medium containing [^{35}S]methionine. Supernatants from labeled cells were immunoprecipitated with goat anti-human IgG and protein A, and precipitated proteins were analyzed by SDS-PAGE in the absence (*lanes 1* and *2*) or presence (*lanes 3* and *4*) of 2-ME.

human IgG or PE-conjugated anti-human B7.1 Abs followed by flow cytometry. Both her2.IgG3 (Fig. 2, *A* and *B*) and B7.her2.IgG3 (Fig. 2, *D* and *E*) bound specifically to CHO/Her2 and not to parental CHO cells. Therefore, fusion of the extracellular domain of B7.1 to a complete her2.IgG3 Ab resulted in a fusion Ab capable of specifically recognizing the HER2/*neu* Ag through the Ab domain. CHO/Her2 cells incubated with B7.her2.IgG3 also stained positively with anti-human B7.1, indicating that binding of B7.her2.IgG3 to the Ag through its Ab domain did not interfere with Ab recognition of the B7.1 fusion domain (Fig. 2*F*).

The affinities of the her2.IgG3 and B7.her2.IgG3 Abs for the HER2/*neu* Ag were compared using the IAsys biosensor (Fig. 3). Her2.IgG3 or B7.her2.IgG3, at 1×10^{-7} M, was added to a cuvette with soluble HER2/*neu* Ag ECD immobilized on its surface, and the association and dissociation were measured as the samples were added and washed from the cuvette. The calculated affinity of 1.7×10^{-7} M for B7.her2.IgG3 was decreased about 2.5-fold compared with the affinity of 7×10^{-8} M obtained for the parental her2.IgG3. The modest decrease in affinity primarily reflected a reduction in the dissociation constant of B7.her2.IgG3.

B7.1 binding studies

The ability of the B7.1 domain in the B7.her2.IgG3 fusion protein to bind to its receptors CTLA4 and CD28 was studied by two different methods. Soluble CTLA4Ig and CD28Ig immobilized on nitrocellulose membrane were incubated with either her2.IgG3 or B7.her2.IgG3 (Fig. 4*A*). We observed strong binding of B7.her2.IgG3 to CTLA4Ig, but no binding of her2.IgG3. B7.her2.IgG3 also bound CD28Ig, although with a lesser affinity than to CTLA4Ig. This was expected, since the reported affinity of B7.1 for CTLA4 is 20-fold higher than that for CD28 (22). In another experiment, we used CHO cells stably expressing CD28 to detect B7.her2.IgG3 binding (Fig. 4*B*). Parental CHO or CHO/

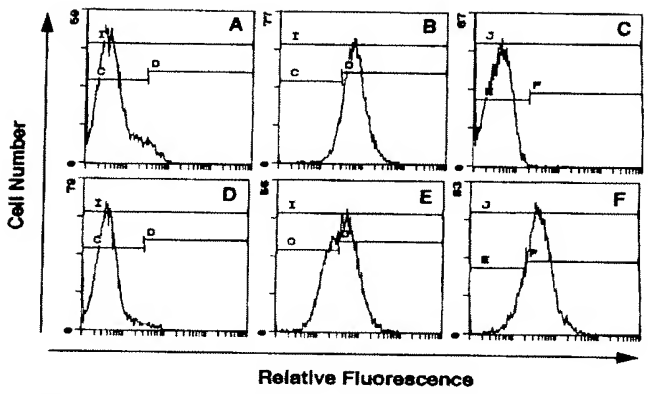

FIGURE 2. Flow cytometry to detect binding of her2.IgG3 or B7.her2.IgG3 to cell surface-expressed HER2/*neu* Ag. Parental CHO (*A* and *D*) or CHO/Her2 (*B*, *C*, *E*, and *F*) cells were incubated with 10 μg/ml of either her2.IgG3 (*A–C*) or B7.her2.IgG3 (*D–F*) at 4°C for 2 h. The cells were washed and stained with either FITC-conjugated anti-human IgG (*A*, *B*, *D*, and *E*) or PE-conjugated anti-human B7.1 (*C* and *F*) at 4°C for 30 min. The cells were then analyzed by flow cytometry. This experiment was repeated six times, and similar results were observed each time.

CD28 cells were incubated with either B7Ig (a gift from Dr. P. Linsley) or B7.her2.IgG3 and washed, and binding was detected by staining with FITC-conjugated anti-human IgG followed by flow cytometry. Specific binding of B7.her2.IgG3 and B7Ig to CD28 present on CHO-CD28$^+$ cells, but not to control CHO cells, was observed.

*Stability of the anti-HER2/*neu *recombinant Abs on the cell surface*

Since recruitment and activation of tumor-specific T cells would depend on the presence of B7.1 on the tumor cell surface, we characterized the stability of B7.her2.IgG3 bound to the HER2/*neu* Ag expressed on the cell membrane. SKBR3 cells from a human breast cancer cell line known to express high levels of HER2/*neu* were incubated with 10 μg/ml of either her2.IgG3 or B7.her2.IgG3 at 4°C to allow maximum binding. The cells were then washed and incubated at 37°C in culture medium. At different times (0, 1, 3, or 24 h), an aliquot of cells was taken and stained with FITC-conjugated anti-human IgG and analyzed by flow cytometry. The results obtained at 0 and 24 h are shown in Figure 5*A*. The mean fluorescence measured at different times was compared with that at

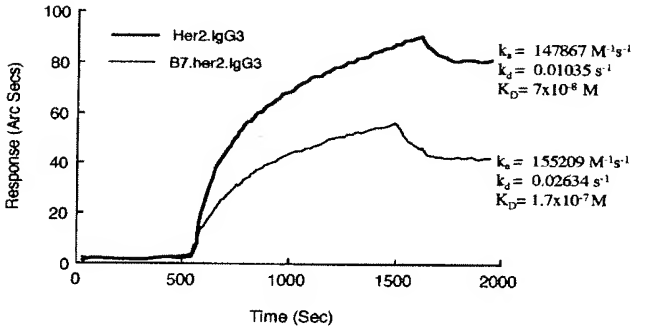

FIGURE 3. Affinity of her2.IgG3 and B7.her2.IgG3 for HER2/*neu* determined using the IAsys biosensor. Binding of her2.IgG3 or B7.her2.IgG3 to a HER2/*neu* extracellular domain-coated microcuvette was assayed as described in *Materials and Methods*, and k_d and k_a were calculated using the Fastfit program. The affinity constant K_d was calculated as k_d/k_a.

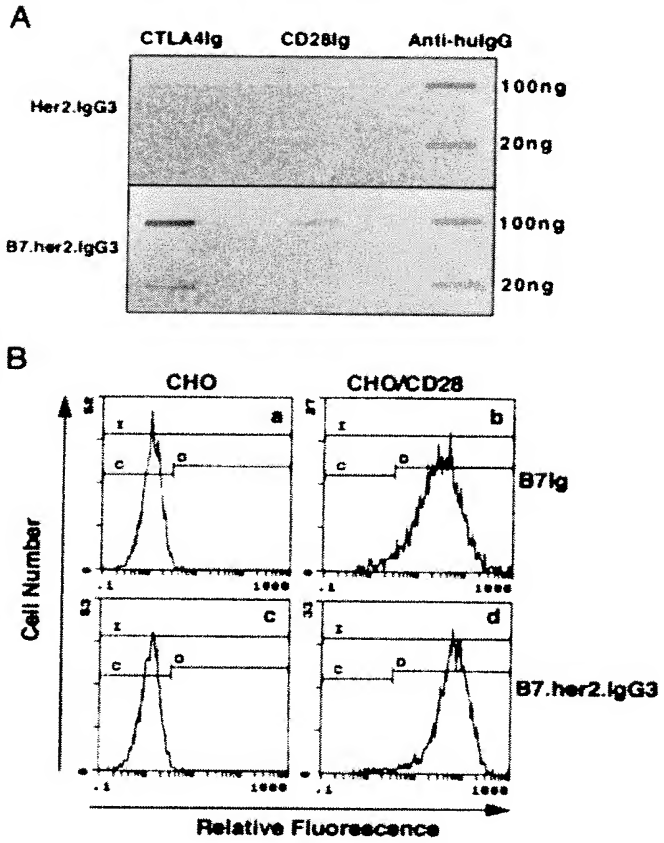

FIGURE 4. Binding of B7.1 to its counter-receptors CD28 and CTLA4 determined by slot blot (*A*) or flow cytometric (*B*) cells. *A*, One hundred or twenty nanograms of CTLA4Ig or CD28Ig immobilized on a nitrocellulose membrane was incubated with either purified her2.IgG3 or B7.her2.IgG3 followed by alkaline phosphatase-conjugated anti-human κ. The blots were then developed with 5-bromo-4-chloro-3-indolyl-phosphate/nitro blue tetrazolium chloride substrate. *B*, Parental CHO (*a* and *c*) or CHO/CD28 cells (*b* and *d*) were incubated with soluble human B7.1 in the form of B7Ig (*a* and *b*) or with B7.her2.IgG3 fusion protein (*c* and *d*). The cells were then washed, incubated with FITC-labeled anti-human IgG, and analyzed by flow cytometry.

time zero, when maximum binding was observed. The time course of Ab binding, calculated as a percentage of the maximum mean fluorescence, is illustrated in Figure 5*B*. We observed a gradual decline in Ab cell surface staining intensity with time. Significant staining (42% of staining at time zero) was still detected at 24 h for both her2.IgG3 and B7.her2.IgG3.

Proliferation assays

To test for the functional ability of the B7.her2.IgG3 molecule to signal via CD28, we performed a syngeneic T cell proliferation assay using human peripheral blood T cells (Fig. 6). CHO/Her2 or control CHO cells were irradiated and incubated in the presence or the absence of either her2.IgG3 or B7.her2.IgG3 and peripheral blood-enriched T cells. PMA at 10 ng/ml was added to the cultures to provide signal 1, which was necessary for proliferation. Addition of B7.her2.IgG3 to CHO/Her2 cells resulted in a dose-dependent increase in T cell proliferation as assayed by [^{3}H]thymidine incorporation. Results from two different donors from two experiments are presented. Levels of T cell proliferation obtained with 10 μg/ml B7.her2.IgG3 approached the levels obtained through stable expression of human B7.1 in CHO cells by gene transfer

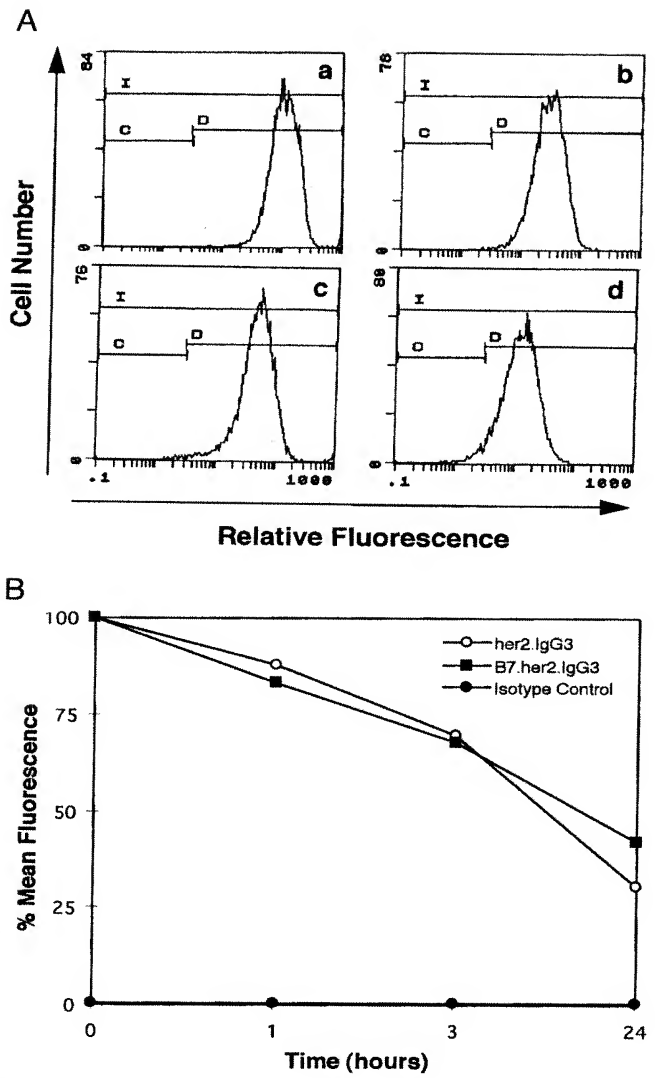

FIGURE 5. Stability of recombinant anti-HER2/*neu* Abs on the surface of Ag-expressing breast cancer cells. SKBR3 cells were incubated at 4°C with her2.IgG3 (*a* and *c*) or with B7.her2.IgG3 (*b* and *d*), and the amount of Ab bound was determined by immunofluorescence. The cells were washed and incubated at 37°C, and aliquots were removed at 0, 1, 3, or 24 h, stained with FITC-conjugated anti-human IgG, and analyzed by flow cytometry. In *A*, we show flow cytometry results at time zero (*a* and *b*) and 24 h after incubation at 37°C (*c* and *d*). In *B*, mean fluorescence is calculated as a percentage of the maximum mean fluorescence observed at time zero. The experiment was repeated three times with similar results.

(CHO/B7). Proliferation was absent in the presence of parental CHO cells or with control her2.IgG3. The significantly lower levels of proliferation observed when B7.her2.IgG3 were incubated with CHO cells suggests that binding of B7.her2.IgG3 to the cell surface via the HER2/*neu* Ag is necessary for optimal T cell costimulation. Visual inspection of the coculture plates showed formation of large foci of proliferating T cells in response to control CHO/B7 cells or in response to incubation with CHO/Her2 cells in the presence of B7.her2.IgG3. Photographs of the cocultures are included in Figure 6*B*. The presence of proliferating T cell colonies directly correlated with the level of proliferation detected by [^{3}H]thymidine incorporation.

Discussion

We describe the construction and characterization of a fusion Ab in which the extracellular domain of the B7.1 costimulatory molecule was fused by genetic engineering to the amino terminus of the heavy chain of an anti-HER2/*neu* Ab. We opted to use the IgG3 backbone for the Ab molecule, since the extended hinge region of IgG3 would be expected to provide greater flexibility in folding to accommodate the presence of B7.1 in the fusion Ab. IgG3 also exhibits Fc-mediated functions, such as complement activation and Fcγ binding (23). We chose the B7.1 costimulatory ligand in preference to B7.2, as Gajewski et al. and other investigators have suggested that B7.1-transduced tumors more successfully induce CTL activity and protect against parental tumor challenge more effectively than tumors transduced with B7.2 (24–27). Although conflicting results with respect to Th1 vs Th2 differentiation have been reported using B7.1 and B7.2, results from several experimental systems suggest that B7.1 costimulation tends to favor differentiation along the Th1 pathway (1, 28–30). Therefore, we chose to link B7.1, rather than B7.2, to an antitumor Ab in an effort to preferentially stimulate a Th1-mediated immune response.

Our results indicate that B7.1 can be effectively linked to the amino terminus of the heavy chain of an anti-HER2/*neu* Ab, with retention of both Ab specificity and the B7.1 interaction with CD28. Binding to HER2/*neu* was demonstrated by flow cytometry as well as IAsys biosensor studies, albeit at a lower affinity than that observed for the control her2.IgG3. Possible reasons for the observed decrease in affinity could be steric hindrance between the anti-HER2/*neu* variable and the B7.1 domains or a change in the kinetics of Ag binding due to the increased size of B7.her2.IgG3. Similarly, specificity of B7.1 for both CTLA4 and CD28 was demonstrated by the ability of B7.her2.IgG3 to bind soluble CTLA4Ig and CD28Ig as well as CD28 expressed on the surface of target cells. Of note, in preliminary attempts to derive a fusion Ab, we constructed an anti-dansyl Ab fusion in which the B7.1 coding sequences were fused to the carboxyl end of the heavy chain C_H3 domain. We did not observe binding of this B7.1 fusion Ab to CD28 expressed on the surface of CHO/CD28 cells or to soluble CD28Ig, suggesting that fusion through the B7.1 amino terminus may disrupt the B7.1/CD28 interaction. This may be due to masking of the amino terminal sequences of B7.1, which are known to be in close proximity to the CD28/CTLA4 binding site (21). Whether fusion via a flexible linker will restore binding of B7.1 to CD28 is currently under investigation. At present, however, we would favor fusion of B7.1 sequences to the amino-terminal heavy chain sequences for suitable B7.1/CD28 interaction. A similar requirement for fusion at the amino terminus of the Ab to maintain activity was observed for nerve growth factor (31). Since the Fc domain remains intact in B7.her2.IgG3, binding to Fc receptors may induce Ag-dependent cellular cytotoxicity or otherwise affect B7.1 function. If this is a problem, further manipulation of the constant region could be performed to eliminate FcR binding sites.

We also sought to address whether anti-HER2/*neu* Abs would remain on the surface of Ag-presenting breast cancer cells. Our results indicated that approximately 40% of surface-bound B7.her2.IgG3 was detectable by flow cytometry for up to 24 h following initial incubation with human SKBR3 breast cancer cells. This suggests that stable presentation of the B7.1 costimulatory ligand on the tumor cell surface may be feasible, and that loss of presentation due to internalization or rapid antigenic shedding via HER2/*neu* binding may not be a significant problem (32).

The management of minimal residual disease is a central problem in breast cancer and other solid tumors. Despite the use of

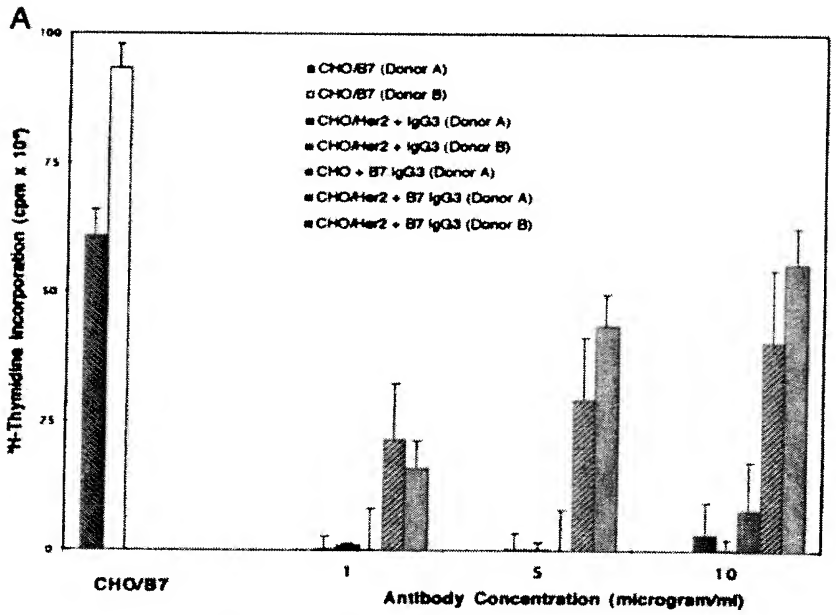

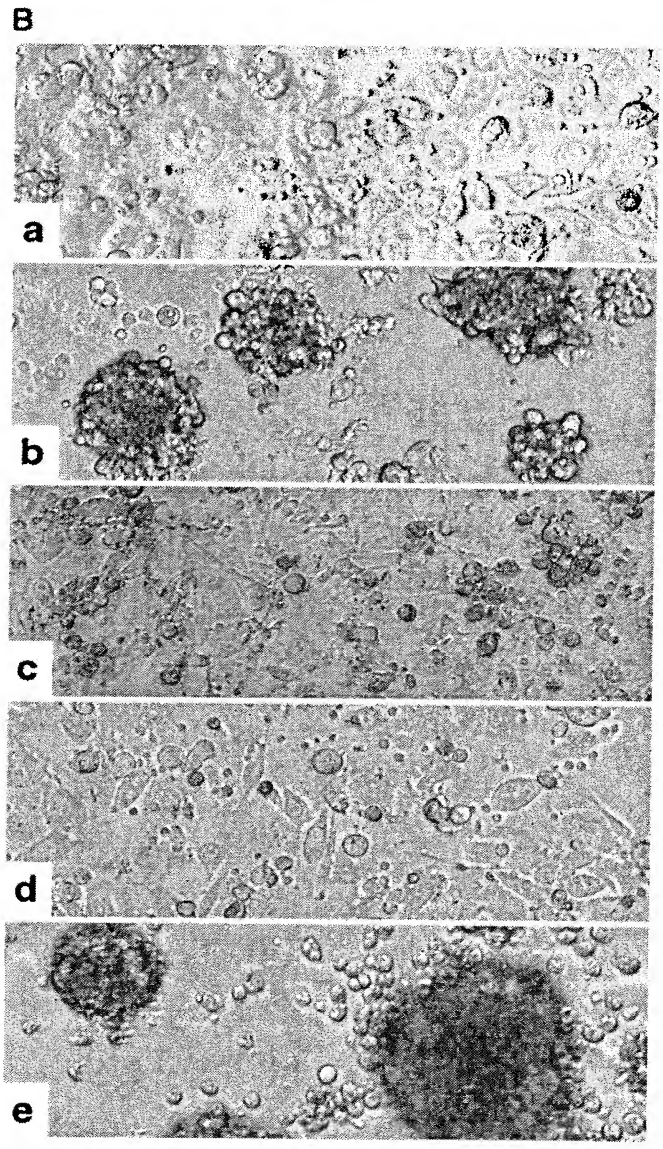

FIGURE 6. In vitro T cell proliferation assay. Peripheral blood T cells isolated from blood of normal donors A and B were plated in 96-well plates in the presence of irradiated CHO or CHO/Her2 cells, PMA (10 ng/ml), and increasing concentrations of either her2.IgG3 or B7.her2.IgG3. The cocultures were incubated at 37°C for 3 days and labeled with [^{3}H]thymidine for the final 16 to 18 h. *A*, Proliferation was measured by harvesting the cells onto glass filters and assessing radioactivity by liquid scintillation counting. The results shown represent the average of triplicate cultures, and error bars denote the SE. Results from two separate experiments using two separate donors, donor A and donor B, are shown. The experiment was repeated five times using a total of three different T cell donors with similar results. *B*, Photographs are shown following 3 days of human T cell incubation in the presence of *a*) CHO/Her2 cells and 10 μg/ml her2.IgG3, *b*) CHO/Her2 and 10 μg/ml B7.her2.IgG3, *c*) CHO cells and 10 μg/ml B7.her2.IgG3, *d*) CHO/Her2 in the absence of Ab, or *e*) CHO/B7 cells stably expressing human B7.1 by gene transfer.

increased dose intensity of chemotherapy or autologous bone marrow transplantation, relapse remains a critical problem (33–36). Chemotherapeutic strategies are necessarily limited by various toxicities. Additional modalities that can achieve further cytoreduction are needed. Although various clinical trials of mAbs, Ab-based conjugates, and/or radioantibodies have been performed, the results of these trials have highlighted obstacles to successful Ab-based therapy of human malignancy. Abs generally are not directly cytotoxic due to poor fixation of complement and/or inadequate activation of Ab-dependent cytotoxicity. Effective use of Abs for delivering cytotoxic agents (e.g., conjugates such as Ab-ricin, or radiolabeled Ab strategies) requires delivery to a majority of, if not all, tumor cells (37). An alternative approach is to elicit an active systemic immune response against tumor cells. Delivery of cytokines has been shown to induce an antitumor T cell response. Although gene transfer has most commonly been used to achieve increased cytokine levels at the site of the tumor, recent studies performed using an Ab-IL-2 fusion protein suggest that Abs can be used for delivering cytokines to tumors. The Ab-cytokine fusion protein retains both Ab specificity and cytokine activity and appears to be more effective than either used alone or in combination, but not covalently linked (38–43). However, fusion of B7.1 rather than cytokine should result in activation of T cells with TCRs that specifically recognize tumor determinants rather than the nonspecific activation expected of a fused cytokine.

In assays for T cell costimulation in vitro, we show that effective stimulation of human T cells was achieved only if B7.her2.IgG3 was bound to a HER2/*neu* target, and limited or no stimulation was observed using target cells that did not express HER2/*neu* Ag. This suggests that the B7.her2.IgG3 fusion protein in soluble form may not be able to effectively provide a costimulatory signal to preactivated T cells, and that the anti-HER2/*neu* Ab domain in the B7.her2.IgG3 fusion protein provided specificity for the T cell costimulation. This property of B7.her2.IgG3 would allow enhanced specificity of the immune response. Similar results have been reported using fusion of the B7.2 costimulatory ligand to a single chain Ab (44). However, a single chain Ab produced in yeast cells may have considerably different glycosylation and antigenicity as well as different pharmacokinetics in vivo compared with the humanized B7.her2.IgG3 we have produced. The relative specificity and type of response achieved with B7.her2.IgG3 fusion compared with the B7.2 single chain fusion remain to be determined. It also remains to be determined whether the specificity and response achieved with B7.1 fusions will differ from those observed using bispecific antitumor/anti-CD28 Ab (45). However, genetically engineered Ab fusion proteins should present fewer problems in manufacture and purification than the described bispecific Abs, which are difficult to purify to homogeneity.

In summary, we have produced an anti-HER2/*neu* IgG fusion protein encoding the extracellular domain of the B7.1 costimulatory ligand. This protein retains targeting specificity via the HER2/*neu* Ag as well as ability to deliver a T cell costimulatory signal. The strategy offers several theoretical advantages. While expression of HER2/*neu* may be heterogeneous, targeting via HER2/*neu* may activate T cells with specificity against other unidentified tumor-associated Ags, resulting in destruction of both HER2/*neu*-positive and nonexpressing cells. Therefore, the Ab fusion protein may allow targeting of micrometastatic disease with relative specificity and would not itself have to bind to all tumor cells to elicit an effective response. The data presented suggest that tumor-specific Abs fused with costimulatory ligands may be a useful method for delivering a costimulatory signal for the purpose of cancer immunotherapy.

Acknowledgments

The authors thank Dr. P. Carter (Genentech, Inc.) for providing sequences of the humanized humAb4D5 Ab, and Dr. V. Planelles for carefully reviewing the manuscript.

References

1. Guinan, E. C., J. G. Gribben, V. A. Boussiotis, G. J. Freeman, and L. M. Nadler. 1994. Pivotal role of the B7:CD28 pathway in transplantation tolerance and tumor immunity. *Blood 84:3261.*
2. Chen, L., S. Ashe, W. A. Brady, I. Hellstrom, K. E. Hellstrom, J. A. Ledbetter, P. McGowan, and P. S. Linsley. 1992. Costimulation of antitumor immunity by the B7 counterreceptor for the T lymphocyte molecules CD28 and CTLA-4. *Cell 71:1093.*
3. Chen, L., P. McGowan, S. Ashe, J. Johnston, Y. Li, I. Hellstrom, and K. E. Hellstrom. 1994. Tumor immunogenicity determines the effect of B7 costimulation on T cell-mediated tumor immunity. *J. Exp. Med. 179:523.*
4. Li, Y., P. McGowan, I. Hellstrom, K. E. Hellstrom, and L. Chen. 1994. Costimulation of tumor-reactive $CD4^+$ and $CD8^+$ T lymphocytes by B7, a natural ligand for CD28, can be used to treat established mouse melanoma. *J. Immunol. 153:421.*
5. Dohring, C., L. Angman, G. Spagnoli, and A. Lanzavecchia. 1994. T-helper- and accessory cell-independent cytotoxic responses to human tumor cells transfected with a B7 retroviral vector. *Int. J. Cancer 57:754.*
6. Marti, W. R., P. Zajac, G. Spagnoli, M. Heberer, and D. Oertli. 1997. Nonreplicating recombinant vaccinia virus encoding human B-7 molecules elicits effective costimulation of naive and memory $CD4^+$ T lymphocytes in vitro. *Cell. Immunol. 179:146.*
7. Hodge, J. W., J. P. McLaughlin, S. I. Abrams, W. L. Shupert, J. Schlom, and J. A. Kantor. 1995. Admixture of a recombinant vaccinia virus containing the gene for the costimulatory molecule B7 and a recombinant vaccinia virus containing a tumor-associated antigen gene results in enhanced specific T-cell responses and antitumor immunity. *Cancer Res. 55:3598.*
8. Hodge, J. W., S. Abrams, J. Schlom, and J. A. Kantor. 1994. Induction of antitumor immunity by recombinant vaccinia viruses expressing B7-1 or B7-2 costimulatory molecules. *Cancer Res. 54:5552.*
9. Linsley, P. S., W. Brady, L. Grosmaire, A. Aruffo, N. K. Damle, and J. A. Ledbetter. 1991. Binding of the B cell activation antigen B7 to CD28 costimulates T cell proliferation and interleukin 2 mRNA accumulation. *J. Exp. Med. 173:721.*
10. Slamon, D. J., G. M. Clark, S. G. Wong, W. J. Levin, A. Ullrich, and W. L. McGuire. 1987. Human breast cancer: correlation of relapse and survival with amplification of the HER-2/neu oncogene. *Science 235:177.*
11. Slamon, D. J. 1987. Proto-oncogenes and human cancers. *N. Engl. J. Med. 317:955.*
12. Bacus, S. S., J. W. Bacus, D. J. Slamon, and M. F. Press. 1990. HER-2/*neu* oncogene expression and DNA ploidy analysis in breast cancer. *Arch. Pathol. Lab. Med. 114:164.*
13. Natali, P. G., M. R. Nicotra, A. Bigotti, I. Venturo, D. J. Slamon, B. M. Fendly, and A. Ullrich. 1990. Expression of the p185 encoded by HER2 oncogene in normal and transformed human tissues. *Int. J. Cancer 45:457.*
14. Pegram, M., A. Lipton, R. Pietras, D. Hayes, B. Weber, J. Baselga, D. Tripathy, T. Twadell, J. Glaspy, and D. Slamon. 1995. Phase II study of intravenous recombinant humanized anti-p185 HER-2 monoclonal antibody (rhuMAb HER-2) plus cisplatin in patients with HER2/*neu* overexpressing metastatic breast cancer. *Proc. Am. Soc. Clin. Oncol. 14:106.*
15. Baselga, J., D. Tripathy, J. Mendelsohn, S. Baughman, C. C. Benz, L. Dantis, N. T. Sklarin, A. D. Seidman, C. A. Hudis, J. Moore, P. P. Rosen, T. Twaddell, I. C. Henderson, and L. Norton. 1996. Phase II study of weekly intravenous recombinant humanized anti-p185HER2 monoclonal antibody in patients with HER2/*neu*-overexpressing metastatic breast cancer. *J. Clin. Oncol. 14:737.*
16. Miller, D. A., and G. J. Rosman. 1989. Improved retroviral vectors for gene transfer and expression. *Biotechniques 7:980.*
17. Carter, P., R. F. Kelley, M. L. Rodrigues, B. Snedecor, M. Covarrubias, M. D. Velligan, W. L. Wong, A. M. Rowland, C. E. Kotts, M. E. Carver, M. Yang, J. H. Bourell, M. Shepard, and D. Henner. 1992. High level *Escherichia coli* expression and production of a bivalent humanized antibody fragment. *Biotechnology 10:163.*
18. Coloma, M. J., A. Hastings, L. A. Wims, and S. L. Morrison. 1992. Novel vectors for the expression of antibody molecules using variable regions generated by polymerase chain reaction. *J. Immunol. Methods 152:89.*
19. Shin, S. U., and S. L. Morrison. 1990. Expression and characterization of an antibody binding specificity joined to insulin-like growth factor 1: potential applications for cellular targeting. *Proc. Natl. Acad. Sci. USA 87:5322.*
20. Coloma, M. J., and S. L. Morrison. 1997. Design and production of novel tetravalent bispecific antibodies. *Nat. Biotechnol. 15:159.*
21. Guo, Y., Y. Wu, M. Zhao, X. P. Kong, and Y. Liu. 1995. Mutational analysis and an alternatively spliced product of B7 defines its CD28/CTLA4-binding site on immunoglobulin C-like domain. *J. Exp. Med. 181:1345.*
22. Linsley, P. S., W. Brady, M. Urnes, L. S. Grosmaire, N. K. Damle, and J. A. Ledbetter. 1991. CTLA-4 is a second receptor for the B cell activation antigen B7. *J. Exp. Med. 174:561.*
23. Morrison, S. L. 1992. In vitro antibodies: strategies for production and application. *Annu. Rev. Immunol. 10:239.*

24. Matulonis, U., C. Dosiou, G. Freeman, C. Lamont, P. Mauch, L. M. Nadler, and J. D. Griffin. 1996. B7-1 is superior to B7-2 costimulation in the induction and maintenance of T cell-mediated antileukemia immunity: further evidence that B7-1 and B7-2 are functionally distinct. *J. Immunol. 156:1126.*
25. Gajewski, T. F., F. Fallarino, C. Uyttenhove, and T. Boon. 1996. Tumor rejection requires a CTLA4 ligand provided by the host or expressed on the tumor: superiority of B7-1 over B7-2 for active tumor immunization. *J. Immunol. 156:2909.*
26. Gajewski, T. F. 1996. B7-1 but not B7-2 efficiently costimulates $CD8^+$ T lymphocytes in the P815 tumor system in vitro. *J. Immunol. 156:465.*
27. Chamberlain, R. S., M. W. Carroll, V. Bronte, P. Hwu, S. Warren, J. C. Yang, M. Nishimura, B. Moss, S. A. Rosenberg, and N. P. Restifo. 1996. Costimulation enhances the active immunotherapy effect of recombinant anticancer vaccines. *Cancer Res. 56:2832.*
28. Freeman, G. J., V. A. Boussiotis, A. Anumanthan, G. M. Bernstein, X. Y. Ke, P. D. Rennert, G. S. Gray, J. G. Gribben, and L. M. Nadler. 1995. B7-1 and B7-2 do not deliver identical costimulatory signals, since B7-2 but not B7-1 preferentially costimulates the initial production of IL-4. *Immunity 2:523.*
29. Greenfield, E. A., E. Howard, T. Paradis, K. Nguyen, F. Benazzo, P. McLean, P. Hollsberg, G. Davis, D. A. Hafler, A. H. Sharpe, G. J. Freeman, and V. K. Kuchroo. 1997. B7.2 expressed by T cells does not induce CD28-mediated costimulatory activity but retains CTLA4 binding: implications for induction of antitumor immunity to T cell tumors. *J. Immunol. 158:2025.*
30. Kuchroo, V. K., M. P. Das, J. A. Brown, A. M. Ranger, S. S. Zamvil, R. A. Sobel, H. L. Weiner, N. Nabavi, and L. H. Glimcher. 1995. B7-1 and B7-2 costimulatory molecules activate differentially the Th1/Th2 developmental pathways: application to autoimmune disease therapy. *Cell 80:707.*
31. McGrath, J. P., X. Cao, A. Schutz, P. Lynch, T. Ebendal, M. J. Coloma, S. L. Morrison, and S. D. Putney. 1997. Bifunctional fusion between nerve growth factor and a transferrin receptor antibody. *J. Neurosci. Res. 47:123.*
32. Tagliabue, E., F. Centis, M. Campiglio, A. Mastroianni, S. Martignone, R. Pellegrini, P. Casalini, C. Lanzi, S. Menard, and M. I. Colnaghi. 1991. Selection of monoclonal antibodies which induce internalization and phosphorylation of p185HER2 and growth inhibition of cells with HER2/*neu* gene amplification. *Int. J. Cancer 47:933.*
33. Harris, L., and S. M. Swain. 1996. The role of primary chemotherapy in early breast cancer. *Semin. Oncol. 23:31.*
34. Sledge, G. W., Jr. 1996. Adjuvant therapy for early stage breast cancer. *Semin. Oncol. 23:51.*
35. Seidman, A. D. 1996. Chemotherapy for advanced breast cancer: a current perspective. *Semin. Oncol. 23:55.*
36. Bearman, S. I., E. J. Shpall, R. B. Jones, P. J. Cagnoni, and M. Ross. 1996. High-dose chemotherapy with autologous hematopoietic progenitor cell support for metastatic and high-risk primary breast cancer. *Semin. Oncol. 23:60.*
37. Rodrigues, M. L., L. G. Presta, C. E. Kotts, C. Wirth, J. Mordenti, G. Osaka, W. L. Wong, A. Nuijens, B. Blackburn, and P. Carter. 1995. Development of a humanized disulfide-stabilized anti-p185HER2 Fv-β-lactamase fusion protein for activation of a cephalosporin doxorubicin prodrug. *Cancer Res. 55:63.*
38. Becker, J. C., N. Varki, S. D. Gillies, K. Furukawa, and R. A. Reisfeld. 1996. Long-lived and transferable tumor immunity in mice after targeted interleukin-2 therapy. *J. Clin. Invest. 98:2801.*
39. Becker, J. C., J. D. Pancook, S. D. Gillies, K. Furukawa, and R. A. Reisfeld. 1996. T cell-mediated eradication of murine metastatic melanoma induced by targeted interleukin 2 therapy. *J. Exp. Med. 183:2361.*
40. Becker, J. C., N. Varki, S. D. Gillies, K. Furukawa, and R. A. Reisfeld. 1996. An antibody-interleukin 2 fusion protein overcomes tumor heterogeneity by induction of a cellular immune response. *Proc. Natl. Acad. Sci. USA 93:7826.*
41. Sabzevari, H., S. D. Gillies, B. M. Mueller, J. D. Pancook, and R. A. Reisfeld. 1994. A recombinant antibody-interleukin 2 fusion protein suppresses growth of hepatic human neuroblastoma metastases in severe combined immunodeficiency mice. *Proc. Natl. Acad. Sci. USA 91:9626.*
42. Harvill, E. T., J. M. Fleming, and S. L. Morrison. 1996. In vivo properties of an IgG3-IL-2 fusion protein: a general strategy for immune potentiation. *J. Immunol. 157:3165.*
43. Harvill, E. T., and S. L. Morrison. 1996. An IgG3-IL-2 fusion protein has higher affinity than hrIL-2 for the IL-2R α subunit: real time measurement of ligand binding. *Mol. Immunol. 33:1007.*
44. Gerstmayer, B., U. Altenschmidt, M. Hoffmann, and W. Wels. 1997. Costimulation of T cell proliferation by a chimeric B7-2 antibody fusion protein specifically targeted to cells expressing the *erbB2* proto-oncogene. *J. Immunol. 158: 4584.*
45. Guo, Y. J., X. Y. Che, F. Shen, T. P. Xie, J. Ma, X. N. Wang, S. G. Wu, D. D. Anthony, and M. C. Wu. 1997. Effective tumor vaccines generated by in vitro modification of tumor cells with cytokines and bispecific monoclonal antibodies. *Nat. Med. 3:451.*

EXHIBIT D

blood 1997 89: 2089-2097

A Superantigen-Antibody Fusion Protein for T-Cell Immunotherapy of Human B-Lineage Malignancies

Cecilia Gidlöf, Mikael Dohlsten, Peter Lando, Terje Kalland, Christer Sundström and Thomas H. Tötterman

Blood (print ISSN 0006-4971, online ISSN 1528-0020), is published semimonthly by the American Society of Hematology, 1900 M St, NW, Suite 200, Washington DC 20036.

A Superantigen-Antibody Fusion Protein for T-Cell Immunotherapy of Human B-Lineage Malignancies

By Cecilia Gidlöf, Mikael Dohlsten, Peter Lando, Terje Kalland, Christer Sundström, and Thomas H. Tötterman

The bacterial superantigen staphylococcal enterotoxin A (SEA) is an efficient activator of cytotoxic T cells when presented on major histocompatibility complex (MHC) class II molecules of target cells. Our previous studies showed that such SEA-directed T cells efficiently lysed chronic B-lymphocytic leukemia (B-CLL) cells. Next, we made a mutated SEA–protein A (SEAm-PA) fusion protein with more than 1,000-fold reduced binding affinity for MHC class II compared with native SEA. The fusion protein was successfully used to direct T cells to B-CLL cells coated with different B lineage–directed monoclonal antibodies (MoAbs). In this communication, we constructed a recombinant anti-CD19-Fab-SEAm fusion protein. The MHC class II binding capacity of the SEA part was drastically reduced by a D227A point mutation, whereas the T-cell activation properties were retained. The Fab part of the fusion protein displayed a binding affinity for CD19$^+$ cells in the nanomolar range. The anti-CD19-Fab-SEAm molecule mediated effective, specific, rapid, and perforin-like T-cell lysis of B-CLL cells at low effector to target cell ratios. Normal CD19$^+$ B cells were sensitive to lysis, whereas CD34$^+$ progenitor cells and monocytes/macrophages were resistant. A panel of CD19$^+$ B-cell lines representing different B-cell developmental stages were efficiently lysed, and the sensitivity correlated with surface ICAM-1 expression. The anti-CD19-Fab-SEAm fusion protein mediated highly effective killing of tumor biopsy cells representing several types of B-cell non-Hodgkin's lymphoma (B-NHL). Humanized severe combined immune deficiency (SCID) mice carrying Daudi lymphoma cells were used as an in vivo therapy model for evaluation of the anti-CD19-Fab-SEAm fusion protein. Greater than 90% reduction in tumor weight was recorded in anti-CD19-Fab-SEAm–treated animals compared with control animals receiving an irrelevant Fab-SEAm fusion protein. The present results indicate that MoAb-targeted superantigens (SAgs) may represent a promising approach for T-cell–based therapy of CD19$^+$ B-cell malignancies.

NON-HODGKIN'S LYMPHOMAS of the B-cell type (B-NHLs) represent a large and growing proportion of malignant neoplasms exhibiting great heterogeneity with respect to histology, immunophenotype, and clinical behavior. At present, about one third of the patients with high-grade disease are cured by high-dose chemoradiotherapy followed or not by stem cell rescue, whereas few, if any, cases with low-grade malignancy are permanently cured.[1] Immunotherapy using naked monoclonal antibodies (MoAbs) has largely been unsuccessful,[2] whereas toxin- and isotope-conjugated pan-B-cell MoAbs followed by stem cell rescue may produce encouraging results.[3-8] Tumor vaccines based on patient-specific Ig idiotypes are presently being attempted and have so far provided proof of the principle.[9-11]

Staphylococcal enterotoxins A (SEA), B, C, D, E, and H are termed superantigens (SAgs) because of their capacity to stimulate a large proportion of T cells expressing particular T-cell receptor Vβ sequences.[12] The SAg molecule binds outside the peptide binding cleft of the major histocompatibility complex (MHC) class II molecule with high affinity, and is presented to T cells as an unprocessed protein.[13,14] Both CD4$^+$ and CD8$^+$ T cells respond to staphylococcal enterotoxins by proliferation, production of cytokines such as interleukin-2, interferon gamma, and tumor necrosis factor α (TNFα), and generation of strong T-cell cytotoxic capacity.[15-17] SAgs have the ability to direct T-cell cytotoxicity against HLA-DR–positive (HLA-DR$^+$) cells such as B cells, dendritic cells, and monocytes.[18]

SAg-directed T cells can lyse a variety of HLA-DR$^+$ tumor target cells, whereas targets lacking the SAg receptor HLA-DR are resistant. We recently demonstrated that SEA-directed T cells kill primary chronic B-lymphocytic leukemia (B-CLL) cells in vitro, and sensitivity to lysis was dependent on HLA-DR, ICAM-1 (CD54), CD18, and CD72 surface molecules.[19] We next demonstrated that the introduction of a point mutation in the SEA molecule reduced its HLA class II binding capacity more than 1,000-fold. Mutated SEA (SEAm) was then fused to protein A and used to screen for MoAbs capable of directing SAg-reactive T cells to leukemic cells.[20] This fusion protein was 100-fold more potent in lysing B-CLL target cells coated with certain B-cell–specific/associated mAbs in comparison to uncoated HLA class II–positive (HLA class II$^+$) B-CLL cells. The most promising antibody specificity turned out to be CD19.

In the present communication, we constructed a recombinant fusion protein between the Fab fragment of an anti-CD19 mAb and a SEA D227A mutant for preclinical in vitro studies of cytotoxic T-cell therapy for human B-cell malignancies. We also tested the potential in vivo antitumor effects of this fusion protein in severe combined immune deficiency (SCID) mice carrying Daudi lymphoma cells and human peripheral blood mononuclear cells as effectors.

MATERIALS AND METHODS

Construction of SEAm. The SEA gene was cloned by polymerase chain reaction (PCR) from the *Staphylococcus aureus* strain ATCC 8095 (obtained from American Type Culture Collection, Rockville, MD). The nucleotide sequence was found to be identical

From the Department of Clinical Immunology, University Hospital, Uppsala; the Pharmacia-Upjohn Research Center, Lund; the Department of Tumor Immunology, Wallenberg Laboratory, University of Lund, Lund; and the Department of Pathology, University Hospital, Uppsala, Sweden.

Submitted July 1, 1996; accepted October 28, 1996.

Supported by grants from the Swedish Cancer Society, the Lion's Cancer Fund at the University Hospital, and the Leo Research Fund.

Address reprint requests to Thomas H. Tötterman, MD, PhD, Department of Clinical Immunology, University Hospital, S-751 85 Uppsala, Sweden.

The publication costs of this article were defrayed in part by page charge payment. This article must therefore be hereby marked "advertisement" in accordance with 18 U.S.C. section 1734 solely to indicate this fact.

0006-4971/97/8906-0022$3.00/0

to the published sequence.[21] Alanine substitution mutagenesis combined with the SEA crystal structure identified D227 as an essential amino acid in the C-terminal major HLA class II binding site.[22] In SEAm, the mutation D227A was introduced by PCR by changing the Asp codon GAT into GCT (Ala). A diagnostic *Spe*I site was introduced at codons 232 to 233 by changing codon 232 from ACA to ACT. Binding studies with HLA class II^+ cells demonstrated a k_d of 10^{-8} mol/L for recombinant native SEA, whereas the k_d for SEAm was estimated to be more than 10^{-5} mol/L.[22]

Cloning of the Fv part of anti-CD19 (CLB-B4/1) and expression in Escherichia coli. The Fv-encoding portions of the mAb CLB-B4/1 (anti-CD19 IgG/k) were cloned from the CLB hybridoma (kindly provided by Drs C. Melief, R.F. Tiebout, and A.M. Kruisbeek, Leiden, The Netherlands) using previously described methodology.[23] Briefly, cDNA was made from the mRNA and coding regions of the entire variable domains, and parts of the signal sequences and the constant domains of the heavy and light chains were amplified by PCR. The oligonucleotides 5′-CAATTTTCT-TGTCCACCTTGGTGC-3′ and 5′-ACTAGTCGACATGGIATG-GAGCIGGATCTTTmTCTT-3′ were used for the heavy chain, resulting in a 563-bp fragment, and the oligonucleotides 5′-ACTAGTCGACATGGATTTICAGGTGCAGATTwTCAGCTTC-3′ and 5′-GCGCCGTCTAGAATTAACACTCATTCCTGTTGAA-3′ were used for the light chain, yielding a 717-bp fragment. For each chain, three separate clones were sequenced and found to be identical. DNA fragments suitable for insertion into the expression vector were obtained in a second PCR step. To assemble a Fab-expression plasmid, the variable regions of CLB-B4/1 mAb were fused to sequences coding for the constant regions of the murine IgG1/k antibody C242.[24] A region coding for the SEA D227A gene was fused after the heavy chain.

The expression plasmid used contained the kanamycin resistance gene and a Lac promoter inducible with isopropyl-βD-thiogalactopyranoside (IPTG). In the fermenter, anti-CD19-Fab-SEA D227A was produced in *E coli* at protein levels exceeding 100 mg/L, which was comparable to similar Fab-SAg constructs previously expressed in our laboratory.[23] The anti-CD19-Fab-SEAm protein was purified with a protein G–based affinity chromatography and ion-exchange chromatography as described. The recombinant product demonstrated a molecular weight of about 82 kD on sodium dodecyl sulfate–polyacrylamide gel electrophoresis (SDS-PAGE).

Iodination of anti-CD19-Fab-SEAm and cell binding assay. The anti-CD19-Fab-SEAm protein was ^{125}I-labeled and used in a cell-binding assay with Daudi B-lymphoma cells.[23,24] The dissociation constant (Kd) and the number of binding sites were determined by Scatchard analyses.

Other reagents. Recombinant SEA was produced as previously described.[22] Anti-CD19 (CLB-anti-CD19) IgG mAb was a gift from Dr C. Melief (Leiden, The Netherlands). A control fusion protein (C215-Fab-SEAm) was constructed and purified to homogeneity as described previously.[23] mAbs against the Apo-1/Fas antigen (CD95) were purchased from Immunotech (Marseille, France) and were as follows: ZB4 (blocking of apoptosis), CH-11 (induction of apoptosis), and UB2 (FITC-conjugated $F(ab)_2$ fragment for staining procedures). FITC-conjugated MoAbs against ICAM-1 (CD54) and LFA-1 (CD11a) were obtained from Immunotech. Anti-CD22 (RFB4) was a gift from Professor G. Janossy (London, UK), and anti-CD24 (SWA11) was kindly provided by Dr U. Zwangermeister Witke (Zürich, Switzerland). Anti-PBC MoAb (reactive with a mitochondrial respiratory enzyme, PDH-E2) used as an irrelevant control was kindly provided by Dr A. Björkland (Department of Clinical Immunology, University of Uppsala). FITC- or PE-conjugated MoAbs used in two-color FACS analysis were as follows: anti-HLA-DR-FITC, anti-CD20-FITC, anti-CD3-FITC, anti-CD34-PE, and anti-CD16-PE from Becton Dickinson (Mountain View, CA) and anti-CD19-FITC, anti-CD19-PE, anti-CD4-PE, anti-CD8-PE, and anti-CD5-PE MoAbs from Ortho Diagnostic Systems (Raritan, NJ). Rabbit $F(ab)_2$ antimouse Ig-FITC (RAM-FITC) and rabbit anti-mouse Ig (RAM) were obtained from Dakopatts (Glostrup, Denmark). Recombinant interleukin-2 and ^{51}Cr were from Amersham (Buckingham, UK). 12-*O*-tetradecanoyl phorbol 13-acetate (TPA), EGTA, propidium iodide (PI), and 2-aminoethylisothiouronium bromide hydrobromide (AET) were purchased from Sigma (St Louis, MO). RPMI 1640 (Flow Laboratories, Glasgow, Scotland) supplemented with 10% fetal calf serum, 1 mmol/L nonessential amino acids, 0.1 mmol/L sodium pyruvate (both from GIBCO, Middlesex, UK), 100 U/mL penicillin, 100 μg/mL streptomycin, 10 mmol/L HEPES, 2 mmol/L L-glutamine, and 5×10^{-5} mol/L β-mercaptoethanol (Sigma) was used as complete medium.

Cell lines. Human peripheral blood mononuclear cells were isolated from a normal healthy subject by routine density centrifugation. A SEA-reactive T-cell line, SEA-T, was established by stimulation of these cells with SEA (1 ng/mL). The cell line was kept for weeks by repeated restimulation with SEA-coated, irradiated (^{137}Cs, 4,000 rad) BSM B-lymphoblastoid cells and recombinant interleukin-2 (20 U/mL) in complete medium and then freeze-stored. These cells were thawed 1 to 2 weeks before use as effector T cells in the in vitro assays described later. The T-cell line was more than 98% $CD3^+$, 80% to 90% $CD8^+$, and 10% to 20% $CD4^+$. Other cell lines were grown in log phase in complete medium at 37°C and 5% CO_2 and were as follows: BSM (Epstein-Barr virus [EBV]-transformed lymphoblast); Raji, a HLA-DR–negative Raji mutant cell line RJ225, and Daudi (all Burkitt's lymphomas); NALM-1, NALM-16, NALL-1, and KM3 (acute lymphoblastic leukemias of pre-B type); U698 and MN60 (lymphoblastic lymphomas of B type); U715A and PL (follicle center cell lymphomas); and LP1 (myeloma).

Leukemia/lymphoma patient cells. Blood samples from six patients with untreated classic B-CLL (95% to 99% monoclonal $CD19^+$ $CD5^+$ cells) were Ficoll-separated (Pharmacia, Uppsala, Sweden) and freeze-stored in liquid nitrogen. Cells from three other B-CLL patients were used fresh in the FACS cytotoxicity assay. Cells from B-NHL patients were prepared from diagnostic lymph nodes using scissors plus steel mesh and kept in liquid nitrogen. The diagnoses (according to the Kiel classification[25]) were as follows: lymphoblastic lymphoma of B type (LB; one patient), centroblastic lymphoma (CB; three patients), centroblastic-centrocytic lymphoma (CB-CC; two patients), hairy cell leukemia (HCL; three patients), and immunocytic lymphoma (IC; three patients).

Highly purified $CD34^+$ progenitor cells. $CD34^+$ enriched progenitor cells were obtained from five patients with multiple myeloma. Progenitor cells were mobilized with the combination of cyclophosphamide (4 g/m^2) plus rh-GSF (lenograstim, 5 μg/kg) and subsequently harvested by leukapheresis.[26] $CD34^+$ progenitor cells were isolated from the leukapheresis product with Ceprate SC technology (CellPro, Bothell, WA). The purity of the enriched fraction was 92% to 95%. Cells were kept in liquid nitrogen if not used fresh in the assays. All patients were from a multicentric phase III trial studying the efficacy of tumor depletion from the peripheral stem cell harvest by $CD34^+$ enrichment. The study was approved by the local ethics committee.

Nonmalignant B cells. To obtain normal B cells (95% $CD19^+$), tonsils were minced, T-cell–depleted by E-rosetting, and stored in liquid nitrogen until use.

Monocytes/macrophages. Normal donor blood was purified in four steps to generate a pure monocyte/macrophage ($CD14^+$) cell population: (1) blood was routinely Ficoll-separated, (2) mononuclear cells were E-rosetted to eliminate T cells and natural killer cells, (3) cells were Percoll-separated (Pharmacia), and (4) magnetic beads were used together with MoAbs against CD19 and CD3 to

reduce contaminating B and/or T cells. Greater than 95% of the remaining cells were $CD14^+$.

Short-term cell cultures. Freeze-stored B-CLL cells were thawed and cultured for 3 days with or without TPA (1.6×10^{-7} mol/L) in complete medium and used as targets in the assays. B-CLL cells separated from fresh blood were cultured overnight and used as targets in the FACS-cytotoxicity assay.

B-NHL cells, $CD34^+$ progenitor cells, and $CD19^+$ tonsil cells were thawed and incubated overnight in complete medium before use. Purified monocytes/macrophages were similarly kept in medium overnight before use.

^{51}Cr-release assay. Cytotoxicity was measured in a standard 4-hour ^{51}Cr-release assay and expressed as follows: % specific lysis = 100 × (experimental − background cpm/maximal background cpm). Target cells were labeled for 2 hours with ^{51}Cr (250 μCi/1 × 10^6 cells). The cells were then washed twice and seeded in triplicate in v-bottomed microtiter plates at a concentration of 2.5×10^3 cells per well. SEA, anti-CD19-Fab-SEAm, or control fusion protein was added directly to the assay. Indicated numbers of effector cells were added in 0.2 mL complete medium. The plates were incubated at 37°C and 5% CO_2, supernatants were collected, and the released ^{51}Cr was measured in a gamma counter (LKB-Wallac 1282; Stockholm, Sweden). Spontaneous release was estimated by incubation of target cells in medium alone, and maximum release by resuspending the wells with 0.1% Tween 20. Spontaneous release was typically less than 30% of maximum release.

FACS-cytotoxicity assay. Target and effector cells were seeded in flat-bottomed microtiter plates (50,000 to 100,000 target cells per well depending on B-cell content adjusted to an E:T cell ratio of 20:1) and incubated at 37°C and 5% CO_2 with anti-CD19-Fab-SEAm or control fusion protein for 4 hours. Cells were then stained with an antibody cocktail consisting of anti-CD19,20,22,24, washed, and stained with the secondary antibody RAM-FITC. After a second wash, cells were stained with propidium iodide (PI) immediately before analysis in a fluorescence microscope or a FACScan flow cytometer (Becton Dickinson). FACS data from cells stained green (B cells) were collected and analyzed with the Lysis II software (Becton Dickinson). The number of B cells was correlated with a fixed total number of cells counted (500,000 cells). Double-stained cells were considered dead. B-cell viability remained high (75% to 90%) if cells were kept for 4 hours in medium alone or medium plus fusion protein without effector T cells.

Flow cytometric analysis of cell phenotype. Cell phenotype was determined by FACS analysis as described elsewhere.[19] Appropriate isotypic control MoAbs were used to estimate the level of nonspecific surface binding.

SCID mice. Two- to 3-month-old female SCID mice (C.B-17) were obtained from Bommice (Ry, Denmark) and kept under pathogen-free conditions. The animals were injected intraperitoneally (IP) with 3×10^5 Daudi lymphoma cells and 5 days later with Ficoll-separated human peripheral blood mononuclear cells.[24] Treatment with anti-CD19-Fab-SEAm or C215-Fab-SEAm control fusion protein was initiated at day 5 and given as four daily intravenous injections (100 μg per injection). Animals were killed after 40 days, and the macroscopically observed tumors in the peritoneal cavity were counted and total tumor mass in each animal was determined as described previously.[27] Immunohistochemistry was used to confirm the presence of tumor cells. Tumors with a weight less than 5 mg were estimated as 2 mg, tumors with a weight greater than 5 mg and less than 10 mg as 7 mg, and tumors larger than 10 mg as the actual weight. All tumors larger than 1 mg were counted. Each treatment cohort contained five to seven mice to permit comparison to other treatment cohorts treated simultaneously with the same batch of effector cells. Statistical significance was determined by the Mann-Whitney *U* test.

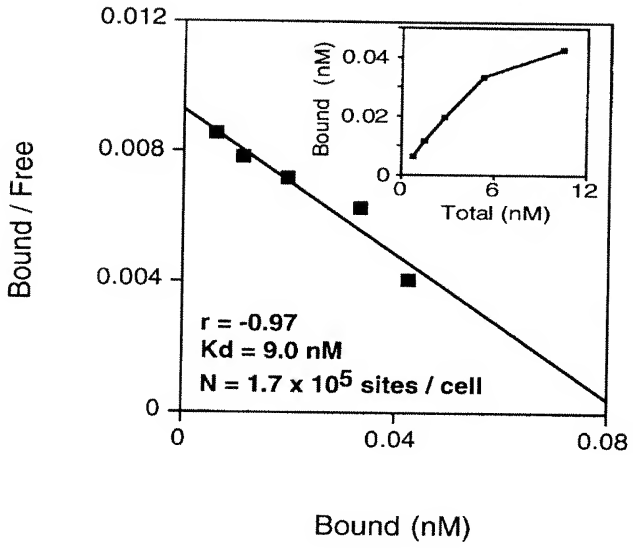

Fig 1. Binding of ^{125}I-labeled anti-CD19-Fab-SEAm fusion protein to Daudi lymphoma cells. Daudi cells (3×10^5/mL) were incubated (1 hour at 22°C) with serially diluted ^{125}I-anti-CD19-Fab-SEAm (0.7 to 300 nmol/L). Cell-bound radioactivity is shown as a Scatchard plot and as a saturation curve (insert) after correction for background binding (B/Fnonspecific = 0.02) in each point. Scatchard analysis showed an apparent K_d of 9.0 nmol/L and approximately 1.7×10^5 sites per cell (R = −.97). Each value is the mean of triplicate samples.

RESULTS

Prokaryotic expression of anti-CD19-Fab-SEAm fusion protein. The variable (V) region of the H chain of the CLB-CD19 antibody cDNA was ligated to the first constant (C) region of a H chain gene fragment from a consensus murine IgG1. This Fd gene fragment was then fused to the SEAm gene and expressed as a bicistronic transcription unit with the gene encoding the V region of the CLB-CD19 κ light chain ligated to the first C region of a consensus κ chain. The pKP865 vector was used for expression of the Fab-SEAm fusion protein in *E coli.* The fusion protein was purified to more than 95% homogeneity as determined by SDS-PAGE and reverse-phase high-performance liquid chromatography (data not shown). Under nonreducing conditions, the protein migrated as an 82-kD band that dissociated into the light chain (26 kD) and Fd-SEAm fusion protein under reducing conditions.

Binding affinity of the fusion protein to the CD19 antigen and MHC class II molecules. The binding affinity of anti-CD19-Fab-SEAm to CD19 and HLA class II molecules was investigated using $CD19^+HLA\text{-}DR^+$ Daudi cells. Scatchard analysis showed an apparent K_d of 10^{-9} mol/L and demonstrated approximately 1.7×10^5 antigen sites per cell (Fig 1). Binding of anti-CD19-Fab-SEAm to $HLA\text{-}DR^+CD19^-$ target cells failed to show a specific binding, and the K_d was estimated to be more than 10^{-5} mol/L (data not shown).

T-cell targeting to MHC class II^+ and class II^- Burkitt cell lines. To investigate residual HLA class II affinity of the anti-CD19-Fab-SEAm fusion protein, we performed cytotoxicity experiments with the SEA-T effector cell line

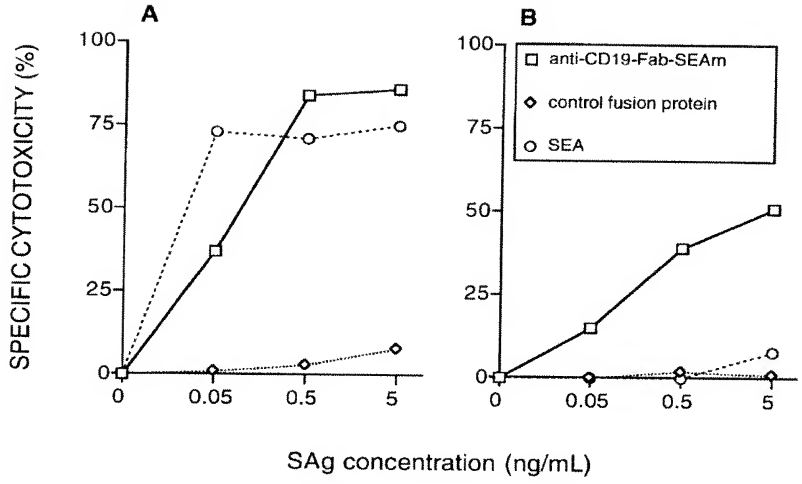

Fig 2. Effects of anti-CD19-Fab-SEAm against 2 CD19⁺ lymphoma cell line targets. T-cell targeting to (A) Raji cells (CD19⁺HLA-DR⁺⁺) and (B) RJ225 cells (CD19⁺HLA-DR^{low}) mediated by anti-CD19-Fab-SEAm fusion protein, native SEA, or C215-Fab-SEAm control fusion protein. Each value is the mean of triplicate samples. The E:T ratio was 40:1, and specific cytotoxicity was measured in a ^{51}Cr-release assay.

against RJ225 (HLA-DR^{low}CD19⁺) and native Raji (DR⁺⁺CD19⁺) target cells (Fig 2). A control fusion protein (C215-Fab-SEAm, directed against human colon cancer cells) or native SEA were used as controls. As expected, Raji but not RJ225 cells were efficiently killed by T cells plus native SEA. The irrelevant control fusion protein containing a D227A mutation in the SEA part mediated minimal background lysis of either target. In contrast, the anti-CD19-Fab-SEAm fusion protein was highly efficient in directing T-cell lysis of both RJ225 and Raji cells at very low concentrations of the protein. The lysis was clearly dose-dependent, and up to 75% cytotoxicity was recorded in the presence of 0.5 to 5.0 ng/mL of the fusion protein. Thus, residual MHC class II–dependent lysis with the anti-CD19-Fab-SEAm fusion protein was low.

Sensitivity of normal B cells, CD34⁺ cells, and monocytes/macrophages in T-cell/anti-CD19-Fab-SEAm fusion protein killing. To examine whether normal CD19⁺ B cells were sensitive to anti-CD19-Fab-SEAm fusion protein–mediated killing, we used B cells purified from tonsil tissue (95% CD19⁺ cells). Significant lysis (60%) of these B cells was seen when using anti-CD19-Fab-SEAm–targeted T cells compared with the control fusion protein (6%) (not shown).

The sensitivity of CD34⁺CD19⁻ progenitor cells (92% to 98% purity) from five myeloma patients was also tested. None of these cell preparations were sensitive to lysis by anti-CD19-Fab-SEAm plus T cells. Two CD34⁺ targets were also used in an indirect cytotoxicity system using mAbs against CD34 or CD19 together with PA-SEAm.[20] The CD34 MoAb mediated efficient lysis, whereas the CD19 MoAb did not (Fig 3).

Monocytes/macrophages (>95% CD14⁺ cells) representing HLA class II⁺ CD19⁻ normal target cells were used in anti-CD19-Fab-SEAm–directed T-cell lysis. Neither the anti-CD19-Fab-SEAm nor the control fusion protein mediated any cytotoxicity. In contrast, native SEA mediated a strong dose-dependent T-cell lysis of monocytes (results not shown).

SAg-mediated lysis of resting and activated B-CLL cells. We reported previously that T-cell lysis of B-CLL targets coated with native SEA or, alternatively, PA-SEAm (SEAm fused with protein A) combined with B-cell–reactive MoAb, was augmented if the target cells were preactivated with TPA.[19,20] Therefore, B-CLL cells from six donors were cultured in the presence or absence of TPA for 3 days and used as targets in the assay. Anti-CD19-Fab-SEAm–targeted T cells lysed resting B-CLL cells as effectively as TPA-activated cells (Fig 4). In comparison, native SEA mediated slightly enhanced killing of TPA-activated B-CLL cells compared with nonactivated B-CLL cells (not shown). The irrelevant fusion protein was inactive against both target cells.

A dose-dependent response to anti-CD19-Fab-SEAm was obvious, with significant lysis already at 0.5 ng/mL of the anti-CD19 fusion protein against nonactivated and TPA-activated cells.

Impact of effector to target cell ratio in anti-CD19-Fab-SEAm–mediated killing of B-CLL cells. The impact of the E:T ratio was studied in cytotoxicity assays with four different B-CLL targets. The anti-CD19-Fab-SEAm fusion protein mediated significant lysis already at a low E:T ratio of 3.75:1, and maximal lysis was seen at an E:T ratio of 15:1. The irrelevant fusion protein mediated low levels of killing at E:T ratios varying from 3.75:1 to 60:1 (not shown).

Killing of CD19⁺ B-cell lines. Thirteen B-cell lines representing different B-cell maturation stages were used as targets in anti-CD19-Fab-SEAm–mediated T-cell killing to evaluate whether lytic sensitivity was restricted to a particular differentiation step. The cell lines were categorized into six different groups: lymphoblasts of pre-B type (NALL-1, NALM-1, NALM-16, and KM3), lymphoblasts of B type (U698 and MN60), EBV-transformed lymphoblasts (BSM), Burkitt's lymphomas (Daudi, Raji, and RJ225), follicle center cell lymphomas (U715A, and PL), and myeloma (LP1). All cell lines were sensitive to anti-CD19-Fab-SEAm–directed T-cell killing, except for the CD19⁻ myeloma cell line LP1. There was an anti-CD19-Fab-SEAm dose-dependent response against all sensitive targets (not shown). The control fusion protein mediated negligible levels of cytotoxicity at 0.5 ng/mL, but at high concentrations (5 ng/mL) some background was seen for cell lines expressing high amounts

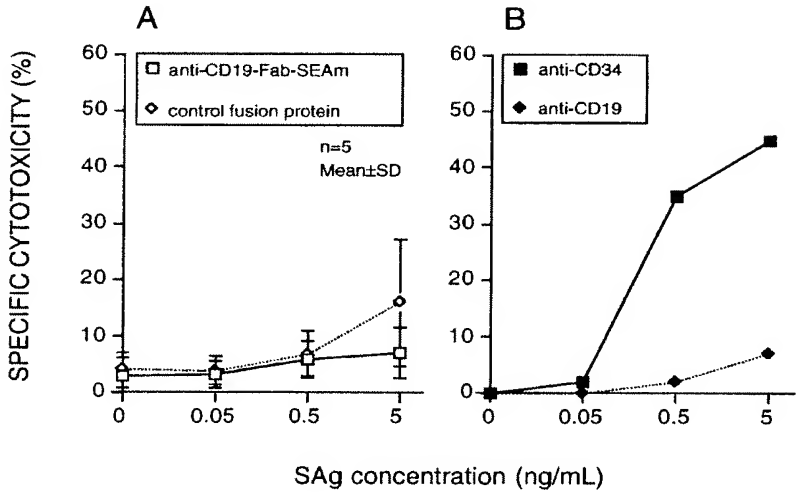

Fig 3. Progenitor cell sensitivity to SAg-directed T-cell killing. Highly purified CD34$^+$ cells were used as targets. (A) Anti-CD19-Fab-SEAm fusion protein or C215-Fab-SEAm control fusion protein. Results are the mean ± SD % cytotoxicity. (B) An indirect system including MoAbs against CD34 or CD19 followed by RAM and PA-SEAm. Each value is the mean of triplicate samples. The E:T ratio was 40:1, and specific cytotoxicity was measured in a ^{51}Cr-release assay.

of HLA-DR and ICAM-1 (not shown). The specific cytotoxicity at an anti-CD19-Fab-SEAm protein concentration of 0.5 ng/mL is shown in Fig 5.

The specific cytotoxicity correlated with the surface expression of ICAM-1 (r = .86) but not with CD19 expression, which was low on all target cells (Fig 6A).

Since surface expression of ICAM-1 seemed to be of major importance for target cell sensitivity to SAg-mediated T-cell cytotoxicity, we wanted to evaluate whether upregulation of ICAM-1 expression could confer increased sensitivity to lysis. For this purpose, we treated target cell lines with TNFα, which has been reported to upregulate ICAM-1 on several cell types. The pre-B-cell lines NALL-1 and NALM-1, which exhibit low ICAM-1 expression (mean fluorescence intensity [MFI], 97 and 25, respectively) and moderate to low sensitivity (30% and 16% specific cytotoxicity) to anti-CD19-Fab-SEAm and T cells, were stimulated with TNFα[28] (1,000 U/mL) for 40 hours and then analyzed for surface ICAM-1 expression. Stimulation resulted in a 1.7- and 4.8-fold increase, respectively (MFI, 167 and 120), in surface ICAM-1 expression, but did not alter CD19 expression. Target cell sensitivity increased moderately for NALL-1 (from 30% to 36%) but drastically for NALM-1 (from 16% to 49%) (Fig 6B). This was not due to an increased fragility of TNF-exposed targets, since the control fusion protein mediated minimal lysis of these cells (0% to 14%, not shown).

Anti-CD19-Fab-SEAm–directed T-cell lysis of B-NHL bi-

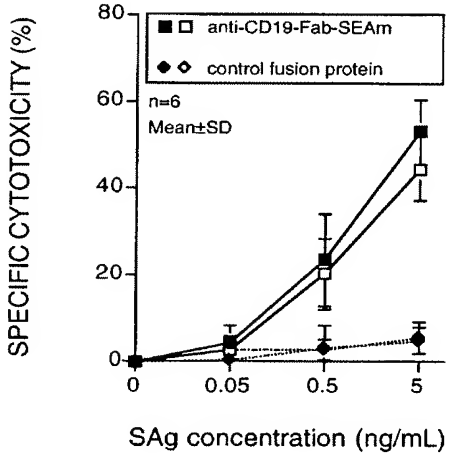

Fig 4. SAg-mediated T-cell killing of B-CLL target cells. Cells from 6 patients with B-CLL were cultured for 3 days with TPA (■, ◆) or in medium alone (□, ◇) and used as targets. Cytotoxic T cells were directed by addition of anti-CD19-Fab-SEAm fusion protein or C215-Fab-SEAm control fusion protein. Results are the mean ± SD. Each value is the mean of triplicate samples. The E:T ratio was 40:1, and specific cytotoxicity was measured in a ^{51}Cr-release assay.

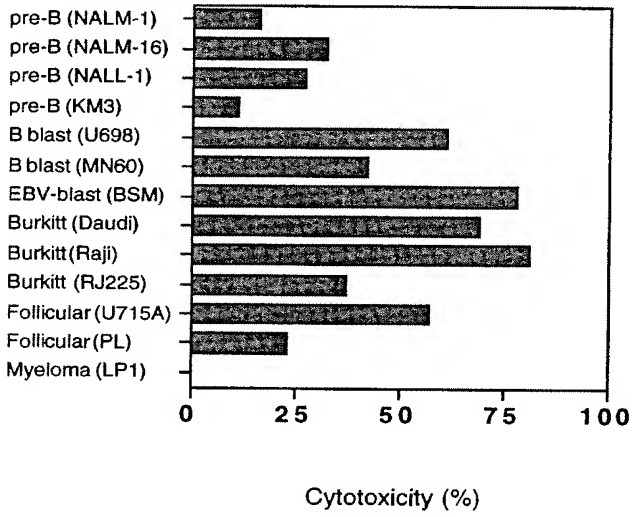

Fig 5. Anti-CD19-Fab-SEAm–directed lysis of 13 different B-cell lines. SAg concentration was 0.5 ng/mL and E:T ratio 40:1. Results are shown as specific cytotoxicity with the anti-CD19-Fab-SEAm fusion protein (minus cytotoxicity with C215-Fab-SEAm control fusion protein) as measured in a ^{51}Cr-release assay. Each value is the mean of triplicate samples.

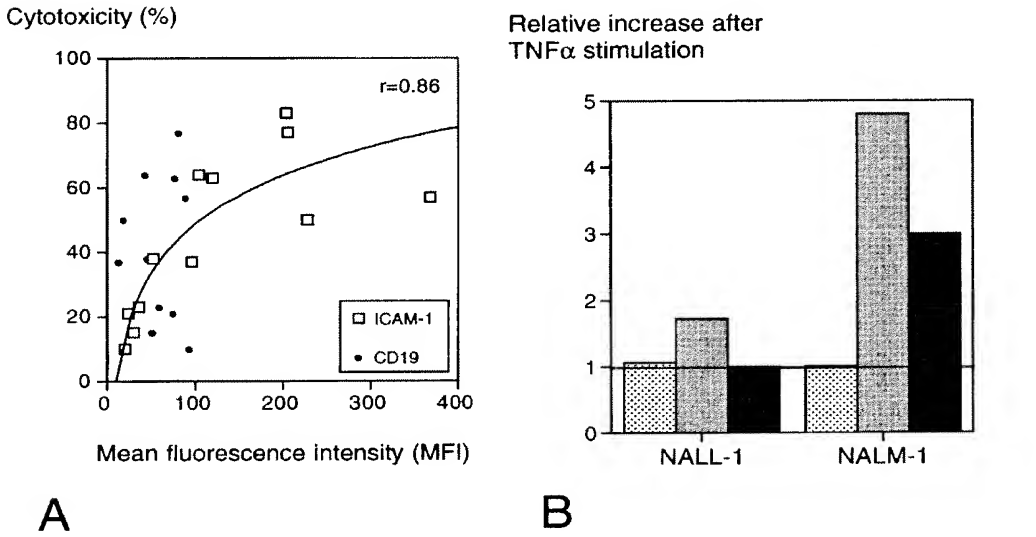

Fig 6. (A) Surface ICAM-1 and CD19 expression of 12 different CD19⁺ B-cell lines (expressed as MFI) correlated with their sensitivity to anti-CD19-Fab-SEAm plus T cells. A logarithmic curve fit is shown for the ICAM-1/cytotoxicity correlation. (B) Effect of TNFα treatment of 2 pre-B-cell lines. Cell surface CD19 and ICAM-1 expression and sensitivity to anti-CD19-Fab-SEAm–mediated T-cell lysis (fusion protein concentration 0.5 ng/mL) is shown. The pre-B-cell lines (NALL-1 and NALM-1) were stimulated with TNFα (1,000 U/mL for 40 hours). Surface antigen expression and sensitivity of nonstimulated cells is presented as 1.0 (horizontal bar) to allow comparison to stimulated cells. Each value is the mean of triplicate samples. ▩, CD19 expression; ▩, ICAM-1 expression; ■, sensitivity to lysis.

opsy cells. Freeze-thawed cells originally prepared from diagnostic lymph nodes obtained from 12 patients with various B-cell lymphomas showed poor uptake of ^{51}Cr in a pilot study. Further, these lymph node preparations consisted of a mixture of clonal B cells and normal T cells. These facts excluded the use of the ^{51}Cr-release assay, and instead we developed a method based on fluorescence-labeled B cells. This flow cytometric method estimated living versus dead target B cells after a 4-hour incubation with effector cells and fusion proteins, and enabled us to investigate the sensitivity of malignant lymph node B cells to anti-CD19-Fab-SEAm–directed cytotoxicity.

All B-NHL targets were sensitive to T cells and anti-CD19-Fab-SEAm compared with the control fusion protein. Twenty-five percent to 80% specific cytotoxicity against malignant B cells was seen (Fig 7) after 4 hours of incubation with effector cells plus anti-CD19-Fab-SEAm fusion protein (0.5 ng/mL).

Freshly separated cells from three patients with B-CLL were incubated in medium overnight and used as targets in the FACS-based assay. These fresh leukemic target cells were extremely sensitive to anti-CD19-Fab-SEAm–mediated cytotoxicity, and more than 97% cytotoxicity was seen in each case (data not shown).

Anti-CD19-Fab-SEAm–based tumor therapy in SCID mice. To evaluate the therapeutic efficacy of the anti-CD19-Fab-SEAm fusion protein in vivo against human B-lymphoma cells, we used a humanized SCID model. SCID mice were injected IP with 3×10^5 Daudi lymphoma cells and were injected 5 days later IP with 3×10^5 human blood mononuclear cells. Anti-CD19-Fab-SEAm therapy was given as four daily intravenous treatments (100 μg per injection) from days 5 to 8. Control animals received PBS or an irrelevant control fusion protein. At day 40, the animals were killed and the number of tumors and the total tumor weight IP estimated. A significant antitumor effect was seen in the anti-CD19-Fab-SEAm–treated animals compared with con-

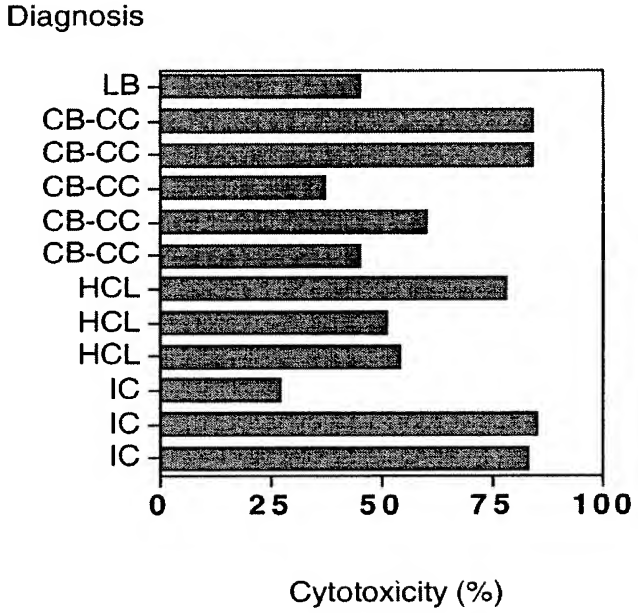

Fig 7. T-cell plus SAg killing of malignant B cells from 12 patients with B-NHL. Target cell viability was determined by FACS analysis after a 4-hour incubation with anti-CD19-Fab-SEAm plus T cells. SAg concentration was 0.5 ng/mL, and results are shown as % dead cells after incubation with anti-CD19-Fab-SEAm minus % dead cells after incubation with the C215-Fab-SEAm control fusion protein.

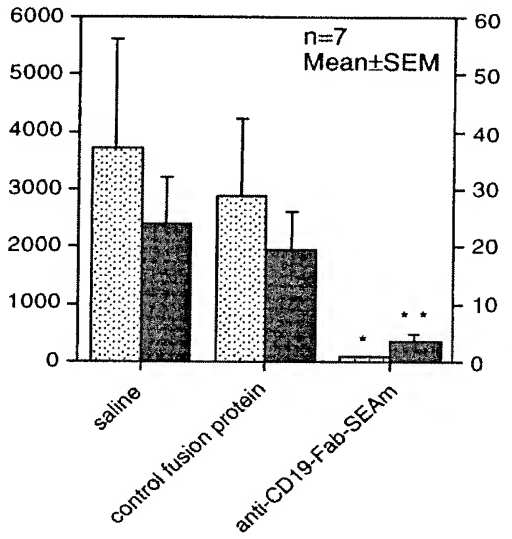

Fig 8. Fab-SAg treatment of humanized SCID mice carrying B-lymphoma cells reduces tumor growth. SCID mice (7 animals per group) were injected IP with 3 × 10^5 Daudi B-lymphoma cells. Five days later, mice were injected IP with 3 × 10^5 normal human peripheral blood mononuclear cells. On days 5 to 8, mice were treated with daily intravenous injections (100 μg per injection) of anti-CD19-Fab-SEAm. Control animals received saline (PBS) or C215-Fab-SEAm control fusion protein, which does not bind to B-lymphoma cells. At day 40, the animals were killed and the (■) number of tumors and (⊠) total tumor weight (mg) were determined IP. Statistical evaluation was performed using the Mann-Whitney *U* test, where fusion protein–treated animals were compared with PBS-treated animals ($P < .01$, *$P < .05$). One of 2 experiments producing similar results is shown as the mean ± SEM.**

trol animals receiving effector cells only or effector cells combined with the irrelevant Fab-SEAm fusion protein. Anti-CD19-Fab-SEAm treatment resulted in greater than 90% reduction of the total tumor weight ($P < .05$) and a drastic decrease in the number of macroscopically detectable tumors ($P < .01$) (Fig 8).

DISCUSSION

In the present study, we extended our previous results with SAg-mediated T-cell lysis of B-CLL cells[19,20] to construct a direct SAg-antibody fusion protein between an anti-CD19-Fab and a SEAm. The choice of a mAb directed against CD19 appeared justified, since CD19 is considered a strictly B-lineage–specific antigen that is expressed on the cell surface of the whole B-cell differentiation range starting with the IgH rearrangement up to plasmablasts. This would potentially enable T-cell therapy for a wide range of human B-cell malignancies. The anti-CD19-Fab-SEAm fusion protein showed high-affinity binding in the nanomolar range to the CD19 antigen. The mutated Fab-SEAm protein exhibited a 1,000-fold lower binding affinity for HLA class II compared with nonmutated SAg. This should favor CD19 antigen-specific targeting compared with interactions with HLA-DR^+CD19^- normal cells including monocytes, dendritic cells, and activated endothelial cells. It is anticipated that higher amounts of the mutated protein as compared with the wild-type protein could be administered in vivo before systemic immune activation and toxic side effects due to HLA-DR binding would occur.[23]

Our present in vitro studies with B-CLL cells as targets showed that such cells were efficiently lysed by low numbers of T cells and anti-CD19-Fab-SEAm. Lysis was rapid, specific, and mediated by surface CD19, but apparently not by MHC class II molecules. Importantly, with this fusion protein, no preactivation of the target cells was needed to increase their sensitivity, in contrast to our experience using other SAg constructs.[19,20] Normal $CD19^+$ B cells were also sensitive for SAg-directed T-cell killing, whereas $CD34^+$ progenitor cells and $CD14^+$ monocytes/macrophages were resistant. In vivo, an anti-CD19-Fab-SEAm protein would potentially eradicate all $CD19^+$ B-lineage cells, including normal counterparts. However, current clinical transplant regimens including high-dose chemoradiotherapy followed by pan-B-cell–purged or, alternatively, $CD34^+$ cell–enriched autografts effectively deplete the B-cell range with surprisingly little effect on posttransplant infection rates. Importantly, sparing of T-cell plus SAg-resistant $CD34^+$ precursor cells should allow full regeneration of the B-cell compartment.

We extended the target cell range to include B-NHL biopsy cells representing several histologies, as well as a full range of established B-cell lines. All $CD19^+$ cells and tumor biopsy cells were sensitive to T-cell/SAg–mediated lysis. The sensitivity of target cells was positively correlated with surface ICAM-1 expression but not with surface CD19 density. CD19 is required for anti-CD19-Fab-SEAm–mediated lysis, because only $CD19^+$ target cells are lysed, but most likely very low levels of CD19 are sufficient for maximal cytotoxicity. This is consistent with the high potency of targeted SEA and recent views that only a few MHC/peptide complexes are required to activate T cells. The target cell surface expression of CD19 was found to be uniform on all cells examined. The expression was low (<100 MFI) compared with that of other B-cell surface markers like CD24 and CD40. CD19 expression did not change when cells were stimulated in vitro. Properties such as antigen shedding or internalization may play a role in antibody-directed killing, and these factors need to be investigated further. A role for ICAM-1 in SAg-induced cytotoxicity was supported by our previous studies using HLA-DR single and HLA-DR/ICAM-1 double transfectants.[29] Stimulation of B-cell line target cells with TNFα led to a parallel increase in surface expression of ICAM-1 and target cell sensitivity to T-cell/anti-CD19-Fab-SEAm–mediated lysis. SEA is a potent inducer of TNFα in vitro[16] and in vivo,[17] suggesting that endogenously produced TNFα may enhance SAg-based lysis of neoplastic B cells in a therapeutic setting.

Freshly separated leukemia cells were extremely sensitive to anti-CD19-Fab-SEAm and T cells. The fact that many of the target cells in this study were obtained from patients displaying multiresistance to cytostatic drugs makes Fab-SEAm–mediated T-cell killing of B-cell tumor cells a potentially attractive adjuvant to conventional debulking therapy. The concept of Fab-SEA–based T-cell immunotherapy for

lymphomas/leukemias is attractive also in other aspects: first, leukemic cells are easily accessible for mAb/T-cell targeting compared with solid tumors; second, B-lymphoma tissue frequently contains large numbers of T cells, which could mediate a local cytotoxic response without a requirement of effector cell homing into the tumor tissue; and third, the expression of surface ICAM-1 molecules by the proliferative tumor cell compartment in lymph nodes is higher than in blood,[30,31] which might favor eradication of the clonogenic cells.

We have investigated the mechanisms of target cell lysis in T-cell/anti-CD19-Fab-SEAm fusion protein–mediated killing. Preliminary data indicate that lysis in the short-term 4-hour assay seems to be perforin-mediated, since the chelator EGTA, which binds Ca^{2+} needed for cytotoxic granulae release, totally abolished lysis. The addition of Fas-blocking antibodies did not alter SAg/T-cell lysis, and neither was there any correlation between target cell surface Fas expression and sensitivity for lysis (data not shown). SAg-triggered T cells release large amounts of TNFα, which is known to be toxic to several tumor types. However, we showed previously that high concentrations of TNFα had no adverse effect on B-CLL cells.[19] SEA-induced cytotoxic T cells (CTL) appear rapidly in mice treated with a single injection of SEA[17] or Fab-SEA.[32] However, perforin knockout mice generate only marginal SEA-dependent CTL activity (J. Hansson, M. Dohlsten, unpublished observation, June 1996). Therefore, it remains likely that release of perforin/granzyme-containing granulae is important in SAg-dependent T-cell–mediated lysis of B-lineage tumor cells in vitro.

In vivo studies of the anti-CD19-Fab-SEAm fusion protein were performed in humanized SCID mice with IP growing Daudi cells. The growth of Daudi cells in SCID mice has previously been evaluated by Ghetie et al,[33] who found disseminated IP growth, including engagement of the mesenteric lymph nodes. Tumor metastases in the liver and kidney were detected only at late stages. A similar disseminated growth pattern IP was seen after 3 to 4 weeks also in our study. At this time point, the tumor load in our model was mainly confined to the IP cavity. Because IP infusion of human peripheral blood mononuclear cells allows persistence of human lymphocytes in the peritoneal cavity for several weeks but only a marginal presence of these cells extraperitoneally (data not shown), the study setting was focused on evaluating antitumor effects against IP tumor growth. Treatment was initiated 5 days after tumor inoculation. Treated animals showed a dramatic reduction of tumor size and number compared with control animals. Further studies using syngeneic but "humanized" in vivo animal models are under development in our laboratory including hCD19cDNA-transfected murine B-cell leukemia cells and the use of hCD19 transgenic mice.

MoAb-targeted SAgs have been used to direct cytotoxic T cells to other types of human malignant cells in vitro. These studies include the use of MoAbs against CD7 and CD38 for lysis of acute T-lymphoblastic leukemia cell lines,[34] anti–ganglioside GD_2 human/mouse chimeric MoAb for lysis of human neuroectodermal tumor lines,[35] and C242 MoAb against human colon carcinoma.[24] Taken together, these results suggest that MoAb-targeted SAg may have a general applicability for a large variety of tumor types. Our present results with anti-CD19-Fab-SEAm argue for a further clinical development of targeted SAgs for T-cell immunotherapy of human B-lymphocyte–lineage malignancies.

ACKNOWLEDGMENT

We thank Professor C. Melief, Leiden, The Netherlands, for the kind gift of the anti-CD19 producer hybridoma. We also thank Dr L. Abrahmsén, Pharmacia Bioscience Centre, Stockholm, Sweden, for help with the construction of fusion proteins, and Dr M. Bengtsson, University Hospital, Uppsala, Sweden, for help with the progenitor cell purification.

REFERENCES

1. Aisenberg AC: Coherent view of non-Hodgkin's lymphoma. J Clin Oncol 13:2656, 1995

2. Dillman RO: Antibodies as cytotoxic therapy. J Clin Oncol 12:1497, 1994

3. Sausville EA, Headlee D, Stetler-Stevenson M, Jaffe ES, Solomon D, Figg WD, Herdt J, Kopp WC, Rager H, Steinberg SM, Ghetie V, Schindler J, Uhr J, Wittes RE, Vitetta ES: Continuous infusion of the anti-CD22 immunotoxin IgG-RFB4-SMPT-dgA in patients with B-cell lymphoma: A phase I study. Blood 85:3457, 1995

4. Amlot PL, Stone MJ, Cunningham D, Fay J, Newman J, Collins R, May R, McCarthy M, Richardson J, Ghetie V, Ramilo O, Thorpe PE, Uhr JW, Vitetta ES: A phase I study of an anti-CD22–deglycosylated ricin A chain immunotoxin in the treatment of B-cell lymphomas resistant to conventional therapy. Blood 82:2624, 1993

5. Grossbard ML, Gribben JG, Freedman AS, Lambert JM, Kinsella J, Rabinowe SN, Eliseo L, Taylor JA, Blättler WA, Epstein CL, Nadler LM: Adjuvant immunotoxin therapy with anti-B4–blocked ricin after autologous bone marrow transplantation for patients with B-cell non-Hodgkin's lymphoma. Blood 81:2263, 1993

6. Uckun FM, Evans WE, Forsyth CJ, Waddick KG, Ahlgren L, Chelstrom LM, Burkhardt A, Bolen J, Myers DE: Biotherapy of B-cell precursor leukemia by targeting genistein to CD19-associated tyrosine kinases. Science 267:886, 1995

7. Press OW, Eary JF, Appelbaum FR, Martin PJ, Nelp WB, Glenn S, Fisher DR, Porter B, Matthews DC, Gooley T, Bernstein ID: Phase II trial of 131I-B1 (anti-CD20) antibody therapy with autologous stem cell transplantation for relapsed B cell lymphomas. Lancet 346:336, 1995

8. Kaminski MS, Zasadny KR, Francis IR, Milik AW, Ross CW, Moon SD, Crawford SM, Burgess JM, Petry NA, Butchko GM, Glenn SD, Wahl RL: Radioimmunotherapy of B-cell lymphoma with [^{131}I]anti-B1 (anti-CD20) antibody. N Engl J Med 329:459, 1993

9. Kwak LW, Campbell MJ, Czerwinski DK, Hart S, Miller RA, Levy R: Induction of immune responses in patients with B-cell lymphoma against the surface-immunoglobulin idiotype expressed by their tumors. N Engl J Med 327:1209, 1992

10. Tao M-H, Levy R: Idiotype/granulocyte-macrophage colony-stimulating factor fusion protein as a vaccin for B-cell lymphoma. Nature 362:755, 1993

11. Hsu FJ, Benike C, Fagnoni F, Liles TM, Czerwinski D, Taidi B, Engleman EG, Levy R: Vaccination of patients with B-cell lymphoma using autologous antigen-pulsed dendritic cells. Nat Med 2:52, 1996

12. Marrack P, Kappler J: The staphylococcal enterotoxins and their relatives. Science 248:705, 1990

13. Fischer H, Dohlsten M, Lindvall M, Sjögren HO, Carlsson

R: Binding of staphylococcal enterotoxin A to HLA-DR on B cell lines. J Immunol 142:3151, 1989

14. Mollick JA, Cook RG, Rich RR: Class II MHC molecules are specific receptors for staphylococcal enterotoxin A. Science 244:817, 1989

15. Dohlsten M, Hedlund G, Sjögren H-O, Carlsson R: Two subsets of human $CD4^+$ T helper cells differing in kinetics and capacities to produce interleukin 2 and interferon-gamma can be defined by the Leu-18 and UCHL1 monoclonal antibodies. Eur J Immunol 18:1173, 1988

16. Fischer H, Dohlsten M, Andersson U, Hedlund G, Ericsson P-O, Hansson J, Sjögren HO: Production of TNF-α and TNF-β by staphylococcal enterotoxin A activated human T cells. J Immunol 144:4663, 1990

17. Dohlsten M, Lando PA, Hedlund G, Trowsdale J, Kalland T: Targeting of human cytotoxic T lymphocytes to MHC class II–expressing cells by staphylococcal enterotoxins. Immunology 71:96, 1990

18. Hedlund G, Dohlsten M, Lando PA, Kalland T: Staphylococcal enterotoxins direct and trigger CTL killing of autologous HLA-DR^+ mononuclear leukocytes and freshly prepared leukemia cells. Cell Immunol 129:426, 1990

19. Wallgren A-C, Festin R, Gidlöf C, Dohlsten M, Kalland T, Tötterman TH: Efficient killing of chronic B-lymphocytic leukemia cells by superantigen-directed T cells. Blood 82:1230, 1993

20. Gidlöf C, Dohlsten M, Kalland T, Tötterman TH: Antibodies are capable of directing superantigen-mediated T-cell killing of chronic B lymphocytic leukemia cells. Leukemia 9:1534, 1995

21. Betley MJ, Mekalanos JJ: Nucleotide sequence of the type A staphylococcal enterotoxin gene. J Bacteriol 170:34, 1988

22. Abrahmsen L, Dohlsten M, Segren S, Björk P, Jonsson E, Kalland T: Characterization of two distinct MHC class II binding sites in the superantigen staphylococcal enterotoxin A. EMBO J 14:2978, 1995

23. Dohlsten M, Abrahmsen L, Björk P, Lando PA, Hedlund G, Forsberg G, Brodin T, Gascoigne NRJ, Förberg C, Lind P, Kalland T: Monoclonal antibody-superantigen fusion proteins: Tumor specific agents for T cell based tumor therapy. Proc Natl Acad Sci USA 91:8945, 1994

24. Dohlsten M, Lando PA, Björk P, Abrahmsen L, Ohlsson L, Lind P, Kalland T: Immunotherapy of human colon cancer by antibody-targeted superantigens. Cancer Immunol Immunother 41:162, 1995

25. Lennert K, Feller A: Histopathology of Non-Hodgkin's Lymphomas (ed 2). New York, NY, Springer-Verlag, 1992

26. Brugger W, Bross KJ, Glatt M, Weber F, Mertelsmann R, Kanz L: Mobilization of tumor cells and hematopoietic progenitor cells into peripheral blood of patients with solid tumors. Blood 83:636, 1994

27. Lando PA, Dohlsten M, Ohlsson L, Kalland T: Tumor-reactive superantigens suppress tumor growth in humanized SCID mice. Int J Cancer 62:466, 1995

28. Triozzi PL, Eicher DM, Smoot J, Rinehart JJ: Modulation of leukemic cell sensitivity to lymphokine-activated killer cytolysis: Role of intercellular adhesion molecule-1. Exp Hematol 20:1072, 1992

29. Dohlsten M, Hedlund G, Lando PA, Trowsdale J, Altmann D, Patarroyo M, Fischer H, Kalland T: Role of the adhesion molecule ICAM-1 (CD54) in staphylococcal enterotoxin–mediated cytotoxicity. Eur J Immunol 21:131, 1991

30. Stauder R, Greil R, Schulz TF, Thaler J, Gattringer C, Radaskiewicz T, Dierich MP, Huber H: Expression of leucocyte function–associated antigen-1 and 7F7-antigen, an adhesion molecule related to intercellular adhesion molecule-1 (ICAM-1) in non-Hodgkin lymphomas and leukaemias: Possible influence on growth pattern and leukaemic behaviour. Clin Exp Immunol 77:234, 1989

31. Horst E, Radaszkiewicz T, Hooftman-den Otter A, Pieters R, van Dongen JJM, Meijer CJLM, Pals ST: Expression of the leucocyte integrin LFA-1 (CD11a/CD18) and its ligand ICAM-1 (CD54) in lymphoid malignancies is related to lineage derivation and stage of differentiation but not to tumor grade. Leukemia 5:848, 1991

32. Rosendahl A, Hansson J, Sundstedt A, Kalland T, Dohlsten M: Immune response during tumor therapy with antibody-superantigen fusion proteins. Int J Cancer 67:1, 1996

33. Ghetie MA, Richardson J, Tucker T, Jones D, Uhr JW, Vitetta ES: Disseminated or localized growth of a human B-cell tumor (Daudi) in SCID mice. Int J Cancer 45:481, 1990

34. Ihle J, Holzer U, Krull F, Dohlsten M, Kalland T, Niethammer D, Dannecker GE: Antibody-targeted superantigens induce lysis of major histocompatibility complex class II–negative T-cell leukemia lines. Cancer Res 55:623, 1995

35. Holzer U, Bethge W, Krull F, Ihle J, Handgretinger R, Reisfeld RA, Dohlsten M, Kalland T, Niethammer D, Dannecker GE: Superantigen-staphylococcal-enterotoxin-A–dependent and antibody-targeted lysis of GD2-positive neuroblastoma cells. Cancer Immunol Immunother 41:129, 1995

EXHIBIT E

[CANCER RESEARCH 56, 4998–5004, November 1, 1996]

A Chimeric Lym-1/Interleukin 2 Fusion Protein for Increasing Tumor Vascular Permeability and Enhancing Antibody Uptake[1]

Peisheng Hu, Jason L. Hornick, Michelle S. Glasky, Aoyun Yun, Mary N. Milkie, Leslie A. Khawli, Peter M. Anderson, and Alan L. Epstein[2]

Department of Pathology, University of Southern California School of Medicine, Los Angeles, California 90033 [P. H., J. L. H., M. S. G., A. Y., M. N. M., L. A. K., A. L. E.], and Section of Pediatric Hematology/Oncology, Mayo Clinic, Rochester, Minnesota [P. M. A.]

ABSTRACT

A murine antihuman B-cell monoclonal antibody, Lym-1, has shown considerable promise for the treatment of human malignant lymphomas. To enhance its clinical potential, a genetically engineered fusion protein consisting of a chimeric Lym-1 (chLym-1) and interleukin 2 (IL-2) was tested for mediating cytotoxicity, increasing vasopermeability, and enhancing antibody uptake in human malignant lymphomas. The chLym-1/IL-2 fusion protein, which was expressed initially in a baculovirus system and more recently in the glutamine synthetase gene amplification system, was shown to be processed and assembled into a normal immunoglobulin monomer with two IL-2 molecules per antibody. It was found to be equivalent to the chLym-1 antibody in antigen-binding specificity and relative affinity. In addition, it maintains IL-2 cytokine activity as demonstrated by support of T-cell proliferation. Moreover, in antibody-dependent cellular cytotoxicity assays against Raji target cells, chLym-1/IL-2 had approximately 2-fold and 4-fold higher cytotoxicity than chLym-1 and murine Lym-1, respectively. Used as a pretreatment, chLym-1/IL-2 enhances the uptake of chLym-1 at the tumor site by altering the permeability of tumor vessels producing tumor:normal organ ratios of 420:1 for blood and 1708:1 for muscle at 3 days. The *in vitro* and *in vivo* activities of chLym-1/IL-2, therefore, suggest that this genetically engineered antibody fusion protein may represent a new immunotherapeutic reagent for the treatment of human malignant lymphomas.

INTRODUCTION

Several major obstacles have been identified that limit the amount of MAb[3] that binds to tumor. These include antigenic heterogeneity, circulating free antigen, antigenic modulation, lack of tumor specificity, and low tumor uptake (1–4). Dosimetric calculations obtained from clinical studies in humans have shown that only ~0.01-0.1% of the injected antibody dose actually binds and accumulates in the tumor despite the use of high avidity MAbs to tumor antigens (5–8). It has long been known that two key parameters that control the uptake of macromolecules in tumors are blood flow and vascular permeability (9–12). On the basis of this information, we formulated the hypothesis that MAbs might be used as carriers of vasoactive and proinflammatory peptides to alter the blood flow and/or permeability of tumor vessels without affecting these parameters in normal tissues. This approach is unique in that it is aimed at altering the physiology of tumor vessels to enhance the tumor uptake of MAbs. Our previous studies indicated that one vasoactive agent, IL-2, is a highly potent inducer of vasopermeability and a promising reagent for this approach (13, 14). IL-2 is a potent biological mediator of the immune system, and it occupies a central role in the augmentation of cell-mediated immune responses. Its major functions include the proliferation of T lymphocytes (15) and the generation of nonspecific tumor killing by activated macrophages, LAK cells, and tumor-infiltrating lymphocytes (16). In addition to its cytokine activity, IL-2 has been shown to induce vascular permeability when administered systemically by causing the efflux of intravascular fluids to the extravascular spaces (capillary leak syndrome; Refs. 17–20). In a previous study (14), our laboratory used a chemically produced Lym-1/IL-2 vasoconjugate as a pretreatment to increase uptake of a radiolabeled MAb tracer by 3–4-fold with no concomitant increase in uptake in normal organs. This was the first report of an immunoconjugate that specifically enhances tumor localization of blood-borne macromolecules. The mechanism of action of this immunoconjugate was attributed specifically to an increase in tumor vascular permeability.

These findings have important implications for the use of MAbs in the radioimmunodetection and therapy of cancer. In addition, IL-2 immunoconjugate pretreatment may potentially be used to improve the delivery of other biologically important molecules to tumor sites. The Lym-1/IL-2 immunoconjugate generated by chemical coupling methods was found, however, to be devoid of IL-2 cytokine activity with respect to T-cell proliferation and LAK cell generation. Thus, it appears that LAK cell generation is not a prerequisite for the vascular permeability changes. From the outset, it was believed that a completely functional IL-2 moiety would produce optimal vasopermeability effects at the tumor site compared to a chemically conjugated moiety. It was with these factors in mind that a fusion protein was constructed with chLym-1 and IL-2 to generate a vasopermeability- and cytokine-active chLym-1/IL-2, which can be used for treatment of the human malignant lymphomas.

MATERIALS AND METHODS

Reagents

Iodine-125 was obtained as sodium iodide in 0.1N sodium hydroxide, and chromium-51 was obtained as $Na_2{}^{51}CrO_4$ in normal saline (pH 8–10) from DuPont New England Nuclear (North Billerica, MA). Centricon concentrators were supplied by Amicon (Danvers, MA). Sephadex, buffer salts, and other reagents such as chloramine T, sodium metabisulfite, hydrogen peroxide, and 2,2′-azino-bis(3-ethylbenzthiazoline-6-sulfonic acid) were purchased from Sigma Chemical Co. (St. Louis, MO).

The transfer vectors pBacPAK1 and pAcUW31, *Bsu36 I*-digested BacPAK6 viral DNA, and wild-type *Autographa californica* nuclear polyhedrosis virus (AcNPV, E2 strain) were obtained from Clontech Laboratories (Palo Alto, CA). Grace's insect cell culture medium, gentamicin, and fungizone were purchased from Life Technologies (Gaithersburg, MD). Low melting gel agarose was obtained from FMC Bioproducts (Rockland, ME). Restriction endonucleases, T4 ligase, and other molecular biology reagents were purchased from New England Biolabs (Beverly, MA) or Boehringer Mannheim (Indianapolis, IN). Both BALB/c and athymic nude mice were purchased from Harlan-Sprague-Dawley (Indianapolis, IN).

Received 5/21/96; accepted 9/3/96.

The costs of publication of this article were defrayed in part by the payment of page charges. This article must therefore be hereby marked *advertisement* in accordance with 18 U.S.C. Section 1734 solely to indicate this fact.

[1] This work was supported in part by Grant 2 RO1 CA47334 from the National Cancer Institute (to A. L. E.), the Children's Cancer Research Fund (to P. M. A.), and NIH PO1 CA21737 Marrow Transplant Project Grant (to P. M. A.).

[2] To whom requests for reprints should be addressed, at the Department of Pathology, University of Southern California School of Medicine, 2011 Zonal Avenue, HMR 211, Los Angeles, CA 90033.

[3] The abbreviations used are: MAb, monoclonal antibody; IL-2, interleukin 2; LAK, lymphokine-activated killer; chLym-1, chimeric Lym-1; muLym-1, murine Lym-1; Sf9, *Spodoptera frugiperda*; BV, baculovirus; ADCC, antibody-dependent cellular cytotoxicity; CMC, complement-mediated cytotoxicity; IEF, isoelectric focusing; pI, isoelectric point.

Antibodies and Cell Lines

chLym-1 (IgG1κ) was constructed and expressed as described previously (21). MAb muLym-1 (IgG_{2a}) directed against a variant of the HLA-Dr antigen expressed in human B-cell lymphomas and muLym-2 directed against a different B-cell epitope (22) were obtained from Techniclone International, Inc. (Tustin, CA). The murine B72.3 MAb directed against the TAG-72 antigen expressed on colorectal carcinoma cells (23) was obtained from Cytogen Corp. (Princeton, NJ). muLym-1 $F(ab')_2$ fragments and biotinylated muLym-1 were prepared as described previously (24, 25). muLym-1 anti-idiotype MAb 1A7 was produced and purified as described previously (21). ^{125}I-labeled MAbs were prepared as described previously (21).

The Raji cell line, derived from an African Burkitt's lymphoma, was used to determine specific binding of Lym-1-derived antibodies (22). Raji cells were grown in RPMI 1640 (Irvine Scientific, Irvine, CA) supplemented with 10% fetal bovine serum (Hyclone Laboratories, Logan, UT), L-glutamine, penicillin G (100 units/ml), and streptomycin (100 μg/ml).

Sf9 (Clontech) and High Five (Invitrogen, San Diego, CA) cells were grown in EX-CELL 400 serum-free medium (JRH Biosciences) with fungizone (2.5 g/liter) at room temperature in an orbital shaker. Viral stocks were produced by infecting attached cell cultures at a low multiplicity of infection and harvesting 2–4 days after infection.

Construction and Expression of chLym-1/IL-2 Fusion Protein

Construction of the expression vector was carried out using standard techniques. A BV transfer vector for chLym-1, pBVchLym-1 (21), was used as the parent vector. This vector carries the cDNA sequences for the human-mouse chLym-1 heavy chain under the control of the polyhedrin promoter and light chain under the control of the p10 promoter. Two oligonucleotides, 5′-GGAACTACT-GGTGGCGGTGGCGCTAGCGCACCTACTTCAAGTTCTACA-3′ and 5′-GTATCTACTAGTTCAAGTTAGTGTTGAGATGATGCT-3′, were used to amplify the human *IL-2* gene from a plasmid template obtained from the American Type Culture Collection (clone 67618; Rockville, MD). The PCR fragment was inserted into the *Spe*I site of pBVchLym-1, resulting in the BV transfer vector pBVchLym-1/IL-2, encoding the chimeric light chain, and a fusion protein consisting of the chLym-1 heavy chain with human IL-2 at its COOH terminus. Expression of chLym-1/IL-2 was carried out as described previously (21). Briefly, purified pBVchLym-1/IL-2 was cotransfected into Sf9 cells with linear viral DNA BacPAK6 (*Bsu36 I*-digested; Clontech) using Lipofectin (Life Technologies) according to the manufacturer's protocol. Five days after cotransfection, the virus-containing supernatant medium was collected, serially diluted, and used to infect fresh monolayers of Sf9 cells. Three days after infection, 0.01% neutral red was added in the agarose overlay during plaque identification to assist in the visualization of recombinant virus. Several well-isolated plaques were selected, and small-scale infections with these putative recombinant viruses were performed to amplify the viruses. The recombinant BVs were identified by Western blot and ELISA for producing chimeric antibody.

Fusion Protein Purification

chLym-1/IL-2 was purified from the infected High Five cell culture medium by protein A affinity chromatography as described previously (21). Protein concentration of purified chLym-1/IL-2 preparations was determined spectrophotometrically. Purity of chLym-1/IL-2 was examined by SDS-PAGE of samples in reducing gels according to the method of Laemmli (26).

Immunoassays

ELISA for chLym-1/IL-2. Identification of chLym-1/IL-2-containing supernatants was initially carried out by indirect ELISA with muLym-1 anti-idiotype antibody 1A7 essentially as described previously (21). Purified chLym-1 was used as the positive control, and wild-type BV supernatant was used as the negative control.

ELISA for IL-2. For the detection of the IL-2 portion of chLym-1/IL-2, plates were coated with MAb 1A7, incubated with chLym-1/IL-2, chLym-1, or wild-type BV supernatant, as above. Rabbit antihuman IL-2 was used as the secondary antibody (BioSource International, Camarillo, CA), followed by horseradish peroxidase-conjugated goat anti-rabbit immunoglobulin. The antibody binding was developed and detected as described previously (21).

Raji Cell Competition RIA. The antigen-binding activity of chLym-1/IL-2 was determined by a competition RIA for binding to live Raji lymphoma cells. For these studies, 2×10^6 washed Raji cells were aliquoted to individual tubes and incubated with 20 ng of ^{125}I-labeled muLym-1 and increasing serial dilutions of cold muLym-1, chLym-1/IL-2, or an irrelevant MAb (muLym-2). The cells and MAbs were incubated for 1 h at room temperature with constant mixing. After incubation, the cells were washed twice, and the cell pellet-associated radioactivity was measured in a gamma counter. Maximal binding was determined from tubes containing no cold antibodies.

IL-2 Bioassay

Biological activity of chLym-1/IL-2 preparations was determined by a standard IL-2-dependent T-cell proliferation assay (27). Two IL-2 standards were used. Carrier-free IL-2 was obtained from Hoffmann-La Roche, Inc. (Nutley, NJ). Roche IL-2 stock (7.4 mg/ml, specific activity $\sim 45 \times 10^6$ IU/ml) was diluted to yield a stock solution containing 1×10^6 Biological Response Modifier Program units/ml (3×10^6 IU/ml). IL-2 was additionally obtained from Cetus (Emeryville, CA) at a specific activity of 18×10^6 IU/ml and diluted with water according to the manufacturer's instructions. The growth of the IL-2-dependent murine T-cell line, CTLL-2, was used to determine the amount of IL-2 bioactivity in a sample. Briefly, serially diluted samples and standards were incubated with 4×10^5 CTLL-2 cells in triplicate for 15 h at 37°C in 96-well flat-bottom microtiter plates. The cells were then pulsed with 0.5 μCi of [^{3}H]thymidine for 6 h, and the samples were harvested and counted.

Cytotoxicity Assays

ADCC was performed using the chromium release method described previously (21). Briefly, Raji cells were labeled for 2 h at 37°C with 250 μCi $Na_2{}^{51}CrO_4$ in RPMI 1640. The cells were subsequently washed and added to 96-well V-bottomed microtiter plates. Different antibody preparations (chLym-1/IL-2, chLym-1, muLym-1, or muB72.3) were added in triplicate to individual wells at various antibody concentrations (10–0.001 μg/ml). Fresh peripheral blood mononuclear effector cells from healthy human donors were immediately added at various effector:target cell ratios to the assay plates. The plates were incubated for 4 h at 37°C and centrifuged. Supernatants were then harvested, and the radioactivity was measured in a gamma counter. Maximum release was obtained by lysing the Raji cells with 10% SDS. Spontaneous release was detected in the wells that contained only target cells without antibody. The percentage of specific lysis or cytotoxicity was calculated as:

$$\% \text{ specific lysis} = \frac{\text{Experimental release} - \text{spontaneous release}}{\text{Maximal release} - \text{spontaneous release}} \times 100$$

CMC was determined using an assay similar to that described above for ADCC, except that instead of effector cells, complement was added to the labeled Raji cells. Fresh human serum was used as a source of complement. Serum was added to each well, and the cells were incubated at 37°C for 4 h in the presence of different antibody preparations at various concentrations. Supernatants were harvested and counted. The percentage of specific lysis or cytotoxicity was calculated as for ADCC. ANOVA was used for statistical analysis of these data.

IEF of Purified MAbs

pIs were determined by IEF in a Bio-Rad model 111 Mini IEF cell through a pH gradient constructed with a mixture of BioLyte ampholytes (Bio-Rad) at concentrations of 1.2% 3/10 ampholyte and 0.8% 5/8 ampholyte according to protocols provided by Bio-Rad. Purified antibodies were applied directly to the gel, and IEF was carried out under constant voltage. IEF standards (Bio-Rad) were included in each run to determine the pI of the samples. IEF gels were fixed and stained with Coomassie blue R-250 and dried overnight.

Determination of Antibody Avidity

To determine the avidity constant (K_a) of chLym-1/IL-2, a live cell RIA was performed using a directly labeled antibody preparation by the method of Frankel and Gerhard (28). Each experimental variable was run in duplicate. Washed Raji cell suspensions containing 10^6 cells/ml were added to test tubes, and the cells were incubated with 10–110 ng of ^{125}I-labeled chLym-1/IL-2 in

200 μl of PBS for 1 h at room temperature with constant shaking. The cells were then washed three times with PBS containing 1% BSA to remove unbound antibody and counted in a gamma counter. The amount of bound antibody was then determined by the remaining cell-bound radioactivity (cpm) in each test tube and the specific activity (cpm/ng) of the radiolabeled MAb. Scatchard plot analysis was used to obtain the slope of the data. From the slope, the equilibrium, or avidity constant K_a, was calculated by the equation $K = -(\text{slope}/n)$, where n is the valence of the antibody (2 for IgG).

Pharmacokinetic and Biodistribution Studies

Six-week-old non-tumor-bearing BALB/c mice were used to determine pharmacokinetic clearance of chLym-1 and chLym-1/IL-2. Different groups of BALB/c mice ($n = 5$) were given i.p. injections of radiolabeled MAbs (30–40 μCi/mouse). The whole-body activity at injection and at selected times thereafter was measured with a CRC-7 microdosimeter (Capintec Inc., Pittsburgh, PA). The data were analyzed, and half-lives were determined using the RSTRIP pharmacokinetic program (MicroMath, Inc., Salt Lake City, UT).

To determine tissue biodistribution of chLym-1/IL-2, female athymic nude mice (BALB/c background) were obtained at approximately 6 weeks of age. The mice were irradiated with 400 rads from a cesium source and 3 days later were injected with a 0.2-ml inoculum consisting of 4×10^7 Raji cells and 4×10^6 human fetal lung fibroblast feeder cells s.c. in the left thigh. The tumors were grown for 12–18 days until they reached ~1 cm in diameter. Within each group of mice ($n = 5$), individual mice were injected i.v. with a 0.2-ml inoculum containing 100 μCi/10 μg of ^{125}I-labeled chLym-1/IL-2. All animals were sacrificed by sodium pentobarbital overdose at 24 and 72 h postinjection, and various organs, blood, and tumor were removed and weighed. The samples were then counted in a gamma counter. For each mouse, data were expressed as tumor:organ ratio (cpm per gram tumor/cpm per gram organ) and percent injected dose/gram (%ID/g). From these data, the mean and SD were calculated for each group.

Enhancement of Vascular Permeability

To demonstrate that pretreatment with chLym-1/IL-2 leads to increased vascular permeability at the tumor site and increased uptake of macromolecules, the following studies were undertaken. Raji tumor-bearing mice generated as above were injected i.v. with 50 μg of chLym-1/IL-2 followed 3 h later by a 0.2-ml inoculum containing 100 μCi/10 μg of ^{125}I-labeled chLym-1 or ^{125}I-labeled mouse albumin. Twenty-four (mouse albumin) or 72 (chLym-1) hr later, biodistribution studies were performed as above. Student's t test was used for statistical analysis of these data.

RESULTS

Construction, Expression, and Purification of chLym-1/IL-2. The human γ1 sequence of the chLym-1 heavy chain was mutated by PCR using primers to generate a unique *Spe*I restriction endonuclease site immediately before the γ1 stop codon. A PCR fragment containing the human *IL-2* gene preceded by a five amino acid linker was then inserted into the *Spe*I site, resulting in a Lym-1 V_H/human γ1/human *IL-2* fusion gene (Fig. 1). The fusion gene was digested with *Bgl*II and *Bam*HI and cloned into the *Bam*HI site of the BV transfer vector containing the *chLym-1* light chain gene to generate the complete vector pBVchLym-1/IL-2. The fusion genes were expressed in High Five insect cells, and the protein product was purified from the supernatant by protein A affinity chromatography. The chLym-1/IL-2 expressed in this system was correctly processed and assembled into the expected immunoglobulin monomer as demonstrated by SDS-PAGE in reducing gels with the observation of two well-defined bands at 25 and 66 kDa, corresponding to the molecular weights of immunoglobulin light chain and heavy chain plus human IL-2 (Fig. 2). IEF of chLym-1/IL-2 gave a pI of 8.4, whereas chLym-1 focused into a single band of pI 8.7 (data not shown).

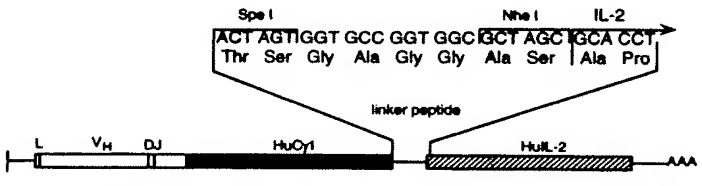

Fig. 1. Schematic diagram depicting the linker between the human γ1 and human *IL-2* genes in the chLym-1 heavy chain/*IL-2* fusion gene.

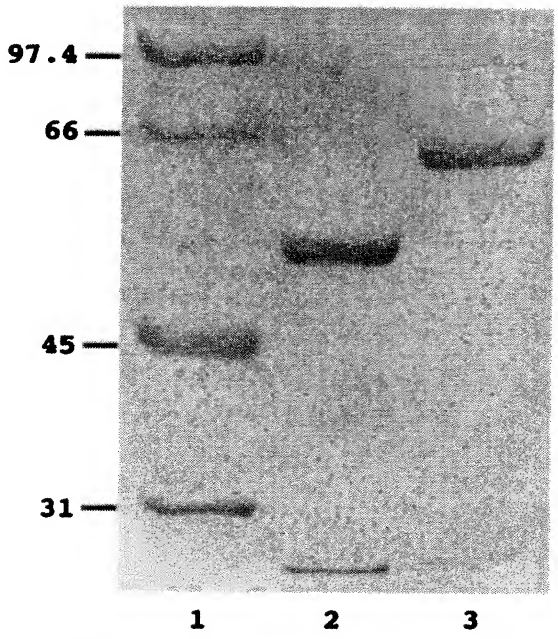

Fig. 2. Electrophoretic identification of chLym-1/IL-2. Coomassie blue-stained reducing SDS-PAGE gel of purified chLym-1 (*Lane 2*) and chLym-1/IL-2 (*Lane 3*). *Lane 1* contains molecular weight standards (kDa).

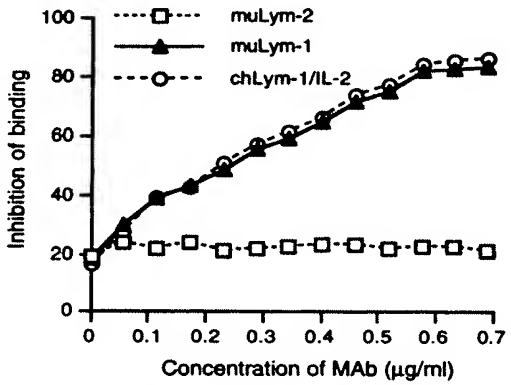

Fig. 3. Competition binding assay with muLym-1 and chLym-1/IL-2. Purified MAbs were assayed for their ability to inhibit binding of ^{125}I-labeled muLym-1 to Raji lymphoma cells. muLym-1 and Lym-2 served as positive and negative controls, respectively.

Immunobiochemical Analysis. Purified chLym-1/IL-2 was evaluated for its immunoreactivity with the target antigen of muLym-1 by assaying its binding to antigen-bearing Raji lymphoma cells. In a RIA, increasing concentrations of chLym-1/IL-2, muLym-1, or an irrelevant MAb (muLym-2) were evaluated for their ability to inhibit binding of ^{125}I-labeled muLym-1 to Raji cells (Fig. 3). muLym-2 was unable to compete with ^{125}I-labeled muLym-1, but cold chLym-1/IL-2 and muLym-1 were able to inhibit 100% of the ^{125}I-labeled muLym-1 binding to Raji cells. These studies confirm that chLym-1/IL-2 maintains the immunoreactivity of muLym-1.

Avidity binding studies were conducted in which ^{125}I-labeled

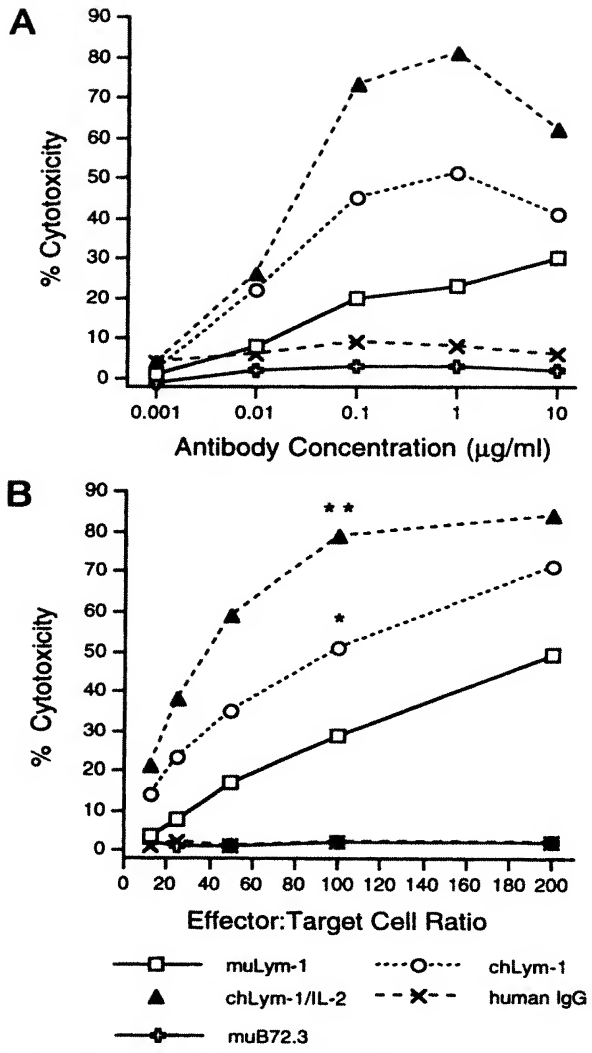

Fig. 4. ADCC activity of chLym-1/IL-2. MAbs were cultured with ^{51}Cr-labeled Raji target cells and human peripheral blood mononuclear cell effectors at varying concentrations of MAb and E:T ratios as indicated. *A*, E:T ratio was held constant at 100:1, and the MAb concentration was increased from 0.001 to 10 μg/ml. *B*, the MAb concentration was held constant at 1 μg/ml, and the E:T ratio was increased from 10:1 to 200:1. At all ratios: *, significant increase over muLym-1 ($P < 0.001$); **, significant increase over chLym-1 ($P = 0.001$). Human IgG and murine B72.3 served as negative controls.

chLym-1/IL-2 or chLym-1 was incubated with live Raji cells, and the percentage of bound radioactivity was used to calculate the avidity constant K_a as described in "Materials and Methods." chLym-1/IL-2 and chLym-1 had similar binding constants of 3.26×10^8 M^{-1} and 3.92×10^8 M^{-1}, respectively.

Cytotoxicity Studies. chLym-1/IL-2 and chLym-1 were evaluated for their ability to mediate ADCC and CMC in standard ^{51}Cr release assays against Raji target cells. chLym-1/IL-2 mediated approximately 2-fold higher ADCC than chLym-1 at the maximal MAb concentration of 1 μg/ml when the effector:target cell ratio was held constant at 100:1 (Fig. 4*a*). When the antibody concentration was held constant at 1 μg/ml and the effector:target cell ratio varied, maximal cytotoxicity of 85% was obtained at a ratio of 200:1 (Fig. 4*b*). chLym-1/IL-2 was also evaluated for its ability to induce CMC, and it induced 67% cytotoxicity at a MAb concentration of 1 μg/ml, approximately the same as that induced by chLym-1 (Fig. 5).

IL-2 Bioactivity of chLym-1/IL-2. Because our initial hypothesis was that a genetically engineered fusion protein would maintain biological activity of the IL-2 moiety, we assayed the ability of chLym-1/IL-2 to support IL-2-dependent T-cell proliferation. A bioassay with the IL-2-dependent CTLL-2 line was performed; chLym-1/IL-2 was assayed, along with IL-2 standards (Fig. 6). On a molar basis, chLym-1/IL-2 had an average of 25% of the activity required to produce 50% maximum proliferation of the IL-2-dependent cell line compared to recombinant IL-2 standards. At higher concentrations (*e.g.*, >1 nM), maximum proliferation was achieved as evidenced by the plateau of the incorporation of [^{3}H]thymidine into DNA.

***In Vivo* Pharmacokinetic and Tumor Binding Studies.** Whole-body clearance studies were performed to establish pharmacokinetic differences between chLym-1/IL-2 and chLym-1. Normal non-tumor-bearing mice were injected with ^{125}I-labeled chLym-1/IL-2, and the whole-body activity was determined at various time points by placing the mice in a microdosimeter. chLym-1/IL-2 cleared very fast and had a whole-body half-life of 11 h (Fig. 7). By comparison, the whole-body half-lives of chLym-1 and muLym-1 were 20 and 99 h, respectively. The faster clearance of chLym-1/IL-2 was apparent when its tumor uptake was assayed by biodistribution in tumor-bearing nude mice (Table 1). Compared to chLym-1, the overall uptake of chLym-1/IL-2 was significantly lower *in vivo* (2.74 ± 0.16% and 2.82 ± 0.18% *versus* 4.34 ± 0.73% and 4.95 ± 0.32% ID/g at 24 h

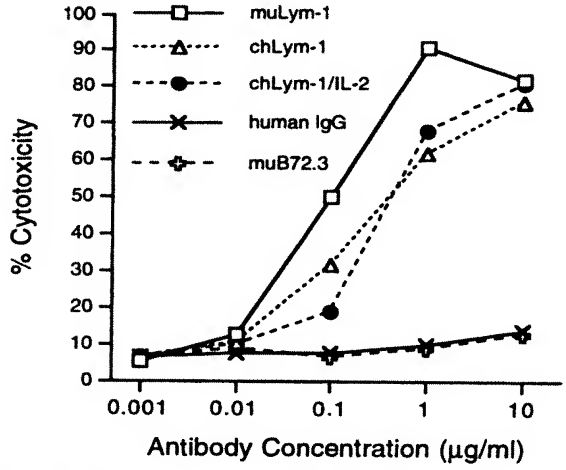

Fig. 5. CMC activity of chLym-1/IL-2. MAbs were cultured with ^{51}Cr-labeled Raji target cells and fresh human serum as a complement source at varying MAb concentrations as indicated. Human IgG and murine B72.3 served as negative controls.

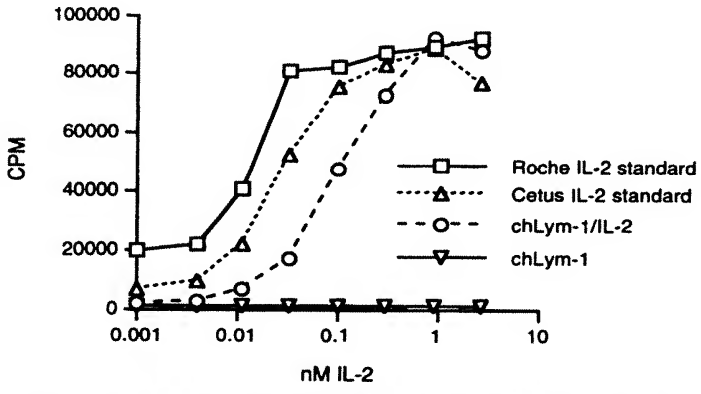

Fig. 6. Biological activity of chLym-1/IL-2 as determined by the ability to support the proliferation of CTLL-2 cells. Serial dilutions of samples and recombinant IL-2 standards were incubated with 4×10^5 CTLL-2 cells in triplicate for 15 h at 37°C. The cells were pulsed with 0.5 μCi of [^{3}H]thymidine for 6 h, and the samples were harvested and counted.

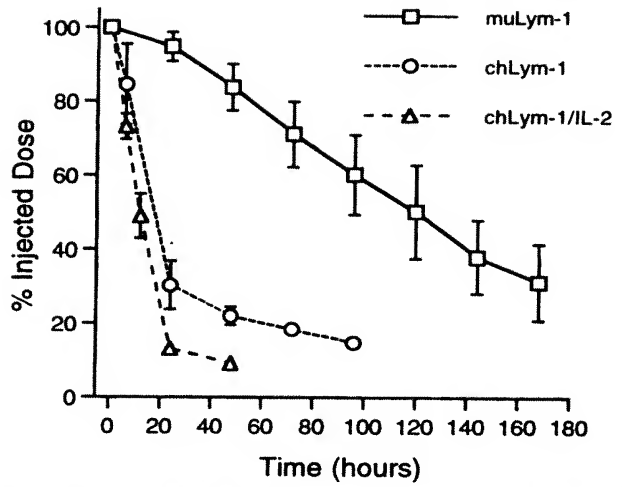

Fig. 7. Whole-body pharmacokinetic clearance of muLym-1, chLym-1, and chLym-1/IL-2 in non-tumor-bearing mice. *Bars*, SD.

($P = 0.001$) and 72 h ($P < 0.0001$), respectively; the data for chLym-1 have been published previously (21)). Tumor:organ ratios, indications of normal organ uptake, were considerably higher, however, with chLym-1/IL-2. Tumor:blood ratios, normally the lowest of all organs (indicating high uptake in blood), were 18:1 and 420:1 at 72 h for chLym-1 and chLym-1/IL-2, respectively. This lower normal organ uptake for chLym-1/IL-2 indicates that very little of this reagent is binding to normal tissues, where toxicity caused by the IL-2 moiety can occur.

Enhancement of Vasopermeability at the Tumor Site. chLym-1/IL-2 was assayed for its ability to induce vasopermeability at the tumor site and increase uptake of radiolabeled mouse albumin and chLym-1. Raji lymphoma-bearing nude mice were injected with 50 μg of chLym-1/IL-2 or chLym-1 and 3 h later injected with ^{125}I-labeled mouse albumin. The mice were sacrificed 24 h later, and biodistribution analysis was performed. In this study, pretreatment with the vasoactive fusion protein increased the tumor uptake of radiolabeled mouse albumin 2.5-fold (Table 2).

In a second study, Raji lymphoma-bearing nude mice were injected with 50 μg of chLym-1/IL-2 fusion protein, followed 3 h later with ^{125}I-labeled chLym-1. The control mice received ^{125}I-labeled chLym-1 without pretreatment. Biodistribution analysis was performed after 3 days for both groups. The results of this study were consistent with those seen with the muLym-1/IL-2 chemical conjugate (Table 3), although the magnitude of the enhancement was less. Uptake of chLym-1 was increased from 4.95 ± 0.32% with no pretreatment to 6.53 ± 0.29% after chLym-1/IL-2 pretreatment, a 32% increase in tumor uptake of radiolabeled antibody ($P < 0.0001$). As shown below, even more dramatic increases were noted in the tumor:organ ratios by chLym-1/IL-2 pretreatment with values now more than 1000:1 in some organs.

DISCUSSION

In this study, a genetically engineered fusion protein consisting of the chimeric MAb Lym-1 and IL-2 has been generated that retains both tumor targeting and cytokine activities. The insect BV expression system was used to facilitate the rapid generation and characterization of the fusion protein because recombinant proteins can be attained much more quickly in this system than in a mammalian expression system. Moreover, the production of recombinant proteins in insect cells allows for correct processing, folding, and glycosylation (29). However, because the BV produces a lytic infection that kills the infected cells after a short period of time and therefore results in relatively low expression levels (5–10 μg/ml), it is not well suited for large-scale production. To produce high levels of chLym-1/IL-2 for clinical evaluation, the glutamine synthetase gene amplification system is being used for expression from myeloma cells (30). This mammalian expression system can enable large-scale expression levels up to 500 μg/ml.

Biochemical analysis of the chLym-1/IL-2 fusion protein demonstrates the presence of two IL-2 moieties per antibody molecule as evidenced by the increase in molecular weight over native chLym-1 (Fig. 2). The IL-2 moiety is present at the COOH terminus of the immunoglobulin heavy chain following a short peptide linker that enables proper folding of the IL-2. Extensive analysis of the fusion protein shows that the antibody binding sites successfully compete with chLym-1 and muLym-1 in Raji binding assays and that there is little change in the affinity binding constant of the fusion protein when compared with native antibody. The functional properties of the IL-2 component of the fusion protein were demonstrated by several methods, including bioassay, ADCC studies, and vascular permeability determinations in tumor-bearing nude mice. The results of these studies demonstrate that the fusion protein retains the proliferation, cytotoxic activation, and vasopermeability activities of IL-2. Specifically, the fusion protein is able to support *in vitro* T-cell proliferation at one-fourth the level of recombinant IL-2 and produces a 2- and 4-fold higher ADCC response when compared to chLym-1 and muLym-1, respectively. Like chLym-1, the fusion protein shows a markedly decreased whole-body half-life compared to muLym-1 due to the presence of human sequences. Despite a whole-body half-life that is 9-fold shorter than muLym-1 (11 h *versus* 99 h), biodistribution analyses

Table 1 *Biodistribution of chLym-1/IL-2 in nude mice bearing Raji lymphoma tumors*

Organ	% Injected dose/gram		Tumor:organ ratio	
	24 h	72 h	24 h	72 h
Blood	0.08 (0.04)[a]	0.03 (0.00)	41.75 (18.58)	110.86 (17.23)
Skin	0.06 (0.03)	0.02 (0.01)	50.72 (15.95)	126.27 (37.32)
Muscle	0.02 (0.02)	0.01 (0.00)	195.22 (94.46)	446.03 (121.54)
Bone	0.06 (0.04)	0.03 (0.01)	63.47 (33.53)	114.60 (32.56)
Heart	0.05 (0.04)	0.01 (0.00)	75.43 (43.43)	239.77 (64.28)
Lung	0.12 (0.07)	0.03 (0.01)	32.42 (22.20)	96.89 (21.90)
Liver	0.16 (0.06)	0.05 (0.03)	18.32 (5.46)	145.03 (200.82)
Spleen	0.07 (0.04)	0.02 (0.01)	50.59 (23.12)	183.49 (95.90)
Pancreas	0.04 (0.04)	0.02 (0.01)	131.91 (82.44)	209.66 (131.23)
Stomach	0.30 (0.47)	0.04 (0.02)	37.88 (27.45)	83.18 (36.62)
Intestine	0.07 (0.08)	0.02 (0.01)	74.05 (42.23)	207.71 (85.19)
Kidney	0.64 (0.19)	0.28 (0.07)	4.54 (1.19)	10.59 (2.04)
Tumor	2.74 (0.16)	2.82 (0.18)		

[a] Mean (SD).

Table 2 *Biodistribution of ^{125}I-labeled mouse albumin 24 h after pretreatment with chLym-1 or genetically engineered chLym-1/IL-2 vasoactive fusion protein*

Pretreatment (3 h)	^{125}I-labeled albumin uptake in tumor
chLym-1	0.90 ± 0.28
chLym-1/IL-2	2.25 ± 0.14[a]

[a] $P < 0.0001$.

demonstrate good tumor uptake of ~3.0% dose/gram, which is maintained from 24 to 72 h postinjection. These data indicate that the radiolabeled antibody is stably retained at the tumor site. Because of this property and the relatively fast clearance of the fusion protein, tumor:normal tissue ratios are high at 72 h in the range of 200:1 for most organs. Finally, the Lym-1/IL-2 fusion protein was shown to be an effective enhancer of radiolabel uptake in tumor when used as a pretreatment. As depicted in Table 3, a 3-h pretreatment of 50 μg of chLym-1/IL-2 produced a 32% increase in the uptake of radiolabeled chLym-1 in the tumor and tumor: normal tissue ratios of more than 1000:1 in some organs at 3 days. In a second experiment, chLym-1/IL-2 was used as a pretreatment for ^{125}I-labeled mouse albumin. Twenty-four-h biodistribution analysis of this study showed that chLym-1/IL-2 induced a 2.5-fold increase in radiolabeled albumin uptake in tumor, indicative of its potent vasopermeability activity. The lower degree of enhancement in uptake compared to pretreatment with the muLym-1 chemical conjugate might be attributed to the rapid clearance of this xenogeneic protein in the mouse. In patients, however, where clearance of the fusion protein would be expected to be slower, the effects of pretreatment with chLym-1/IL-2 would be expected to approach the values seen in the murine model.

In view of these results, it appears that the genetically engineered chLym-1/IL-2 fusion protein can pretarget antigen-positive tumors and induce a localized vasopermeability effect. Used in this way, this fusion protein can enhance the delivery of macromolecules, such as radiolabeled antibodies or drugs, to the tumor without affecting the vasculature of normal tissues and organs. With regard to its mechanism of action, it has been hypothesized that the effects of IL-2 may be due to the induction of a diffusible second messenger, possibly nitric oxide, because inhibitors of this molecule appear to abrogate the vasopermeability effects of IL-2 (31, 32). This would explain why pretargeting of IL-2 to tumor cells is effective despite the fact that it localizes distant from its site of action, *i.e.*, the tumor endothelium. In our previous study (14), we showed that the linkage of IL-2 to an irrelevant antibody had no effect on the permeability of tumor vessels, indicating that the IL-2 moiety must accumulate and be retained at the tumor site before inducing its effect.

There is a great body of literature that describes the therapeutic potential of IL-2 in the treatment of cancer (33, 34). Researchers, however, have only just begun to explore the use of IL-2 in conjunction with MAbs. Previous studies by Gill *et al.* (35) using free IL-2 and muLym-1 and other MAbs (36–39) have demonstrated that the combination of these reagents produces a more potent ADCC reaction both *in vitro* and *in vivo*, causing significant retardation of tumor growth. Moreover, more sophisticated experiments using gene transfer have shown that tumor cells engineered to secrete functional IL-2 selectively inhibit tumor cell growth in susceptible hosts. Tumor models used to demonstrate the effectiveness of this approach include mouse mammary cells (40), mouse neuroblastoma cells (41), mouse thymoma cells (42), mouse Lewis lung carcinoma cells (43), human melanoma (44), and human acute leukemia cells (45). Although these methods are presently impractical in the clinical setting, they do demonstrate the importance of targeting IL-2 to the tumor to obtain optimal therapeutic efficacy while producing minimal toxicity. An alternative approach is the generation of recombinant antibody-IL-2 fusion proteins using the pan-carcinoma MAb L6 (46), the anti-GD2 chimeric MAb ch14.18 (47–49), an antilysozyme single-chain MAb (50), the antihuman epidermal growth factor receptor chimeric MAb ch225 (51), and the anticolon carcinoma TAG-72 single chain MAb (52, 53). As in our experiments, these investigators were able to demonstrate retention of IL-2 cytokine activity, which could be targeted to the tumor in appropriate animal models. As stated by Naramura *et al.* (51), one of the important rationales for producing these fusion proteins is the ability to deliver relatively larger amounts of IL-2 to the tumor site in such a way as to minimize the toxicity seen with systemically administered IL-2. Indeed, the major reason for developing these novel reagents is to harness the cytokine activity of potent immunostimulatory molecules close to their site of action. In our study, we intend to use an additional property of IL-2, *i.e.*, its vasopermeability effects, to increase the amount of therapeutic antibody or drug targeting the tumor. To test the cytokine functionality of the chLym-1/IL-2 fusion protein, studies will have to be conducted in clinical trials because the Lym-1 antigen is not present in animal lymphomas, and an appropriate animal tumor model is therefore not available. Like Gillies *et al.* (47, 48), we believe that antibody fusion proteins represent a new approach for the delivery of potent cytokines to the tumor. As demonstrated by our studies, these reagents may be used additionally to enhance antibody uptake in tumors to improve their therapeutic potential. Moreover, a two-pronged attack represented by the delivery of both a radionuclide and IL-2 may produce better therapeutic responses than treatments using either a radionuclide or the cytokine alone.

Table 3 *Biodistribution of ^{125}I-labeled chLym-1 72 h after pretreatment with genetically engineered chLym-1/IL-2 vasoactive fusion protein*

Organ	% Injected dose/gram		Tumor:organ ratio	
	No pretreatment	Pretreatment	No pretreatment	Pretreatment
Blood	0.36 (0.10)[a]	0.02 (0.01)	14.79 (4.13)	420.36 (253.13)
Skin	0.19 (0.05)	0.03 (0.01)	27.00 (6.79)	364.55 (280.74)
Muscle	0.05 (0.02)	0.01 (0.00)	99.53 (32.45)	1708.30 (1188.18)
Bone	0.08 (0.04)	0.02 (0.01)	67.25 (25.84)	417.33 (176.05)
Heart	0.15 (0.08)	0.01 (0.00)	44.92 (26.25)	932.59 (585.24)
Lung	0.47 (0.46)	0.02 (0.01)	16.40 (8.51)	403.32 (137.84)
Liver	0.14 (0.02)	0.04 (0.01)	36.15 (6.06)	182.84 (75.15)
Spleen	0.16 (0.08)	0.02 (0.01)	37.54 (16.97)	336.59 (199.26)
Pancreas	0.08 (0.02)	0.01 (0.00)	68.06 (19.76)	1143.45 (722.17)
Stomach	0.09 (0.03)	0.02 (0.01)	62.09 (19.53)	473.67 (181.32)
Intestine	0.06 (0.02)	0.01 (0.00)	93.03 (33.58)	837.28 (346.82)
Kidney	0.25 (0.05)	0.13 (0.05)	20.52 (4.36)	55.68 (20.58)
Tumor	4.95 (0.32)	6.53 (0.29)[b]		

[a] Mean (SD).
[b] Significant increase in uptake ($P < 0.0001$).

REFERENCES

1. Goldenberg, D. M. Monoclonal antibodies in cancer detection and therapy. Am. J. Med., *94:* 297–312, 1993.
2. Kemshead, J. T., and Hopkins, K. Uses and limitations of monoclonal antibodies (MoAbs) in the treatment of malignant disease: a review. J. Royal Soc. Med., *86:* 219–224, 1993.
3. Kosmas, C., Linardou, H., and Epenetos, A. A. Advances in monoclonal antibody tumour targeting. J. Drug Target, *1:* 81–91, 1993.
4. Murray, J. L. Factors for improving monoclonal-antibody targeting. Diagn. Oncol., *2:* 234–241, 1992.
5. Goodwin, D. A. Pharmacokinetics and antibodies. J. Nucl. Med., *28:* 1358–1362, 1987.
6. Goldenberg, D. M. Targeting of cancer with radiolabeled antibodies. Prospects for imaging and therapy. Arch. Pathol. Lab. Med., *112:* 580–587, 1988.
7. Dykes, P. W., Bradwell, A. R., Chapman, C. E., and Vaughn, A. T. M. Radioimmunotherapy of cancer: clinical studies and limiting factors. Cancer Treat. Rev., *14:* 87–106, 1987.
8. Carrasquillo, J. A., Bunn, P. A., Keenan, A. M., Reynolds, J. C., Schroft, R. W., Foon, K. A., Su, M-H., Gazdar, A. F., Mulshine, J. L., Oldham, R. K., Perentesis, P., Horowitz, M., Eddy, J., James, P., and Larson, S. M. Radioimmunodetection of cutaneous T-cell lymphoma with ^{111}In-labeled T101 monoclonal antibody. N. Engl. J. Med., *315:* 673–680, 1986.
9. Jain, R. K. Transport of molecules across tumor vasculature. Cancer Metastasis Rev., *6:* 559–593, 1987.
10. Jain, R. K. Determinants of tumor blood flow: a review. Cancer Res., *48:* 2641–2658, 1988.
11. Sands, H. Radioimmunoconjugates. An overview of problems and promises. Antibody Immunoconj. Radiopharm., *1:* 213–226, 1988.
12. Sands, H. Experimental studies of radioimmunodetection of cancer: an overview. Cancer Res., *50* (Suppl.)*:* 809s–813s, 1990.
13. Khawli, L. A., Miller, G. K., and Epstein, A. L. Effect of seven new vasoactive immunoconjugates on the enhancement of monoclonal antibody uptake in tumors. Cancer (Phila.), *73* (Suppl.)*:* 824–831, 1994.
14. LeBerthon, B., Khawli, L. A., Alauddin, M., Miller, G. K., Charak, B. S., Mazumder, A., and Epstein, A. L. Enhanced tumor uptake of macromolecules induced by a novel vasoactive interleukin 2 immunoconjugate. Cancer Res., *51:* 2694–2698, 1991.
15. Morgan, D. A., Ruscetti, F. W., and Gallo, R. Selective *in vitro* growth of T lymphocytes from normal human bone marrows. Science (Washington DC), *193:* 1007–1008, 1976.
16. Grimm, E. A., Mazumder, A., Zhang, H. Z., and Rosenberg, S. A. The lymphokine activated killer phenomenon: lysis of NK resistant fresh solid tumor cells by IL-2 activated autologous human peripheral blood lymphocytes. J. Exp. Med., *155:* 1823–1841, 1982.
17. Rosenstein, M., Ettinghausen, S. E., and Rosenberg, S. A. Extravasation of intravascular fluid mediated by the systemic administration of recombinant interleukin-2. Immunology, *137:* 1735–1742, 1986.
18. Ohkubo, C., Bigos, D., and Jain, R. K. Interleukin 2-induced leukocyte adhesion to the normal and tumor microvasculature endothelium *in vivo* and its inhibition by dextran sulfate: implications for vascular leak syndrome. Cancer Res., *51:* 1561–1563, 1991.
19. Edwards, M. J., Miller, F. N., Sims, D. E., Abney, D. L., Schuschke, D. A., and Corey, T. S. Interleukin 2 acutely induces platelet and neutrophil-endothelial adherence and macromolecular leakage. Cancer Res., *52:* 3425–3431, 1992.
20. Damle, N. K., and Doyle, L. V. IL-2 activated human killer lymphocytes but not their secreted products mediate increase in albumin flux across cultured endothelial monolayers. J. Immunol., *142:* 2660–2669, 1989.
21. Hu, P., Glasky, M. S., Yun, A., Alauddin, M. M., Hornick, J. L., Khawli, L. A., and Epstein, A. L. A human-mouse chimeric Lym-1 monoclonal antibody with specificity for human lymphomas expressed in a baculovirus system. Hum. Antib. Hybrid., *6:* 57–67, 1995.
22. Epstein, A. L., Marder, R. J., Winter, J. N., Stathopoulos, E., Chen, F-M., Parker, J. W., and Taylor, C. R. Two new monoclonal antibodies, Lym-1 and Lym-2, reactive with human B-lymphocytes and derived tumors, with immunodiagnostic and immunotherapeutic potential. Cancer Res., *47:* 830–840, 1987.
23. Colcher, D., Hand, P. H., Nuti, M., and Schlom, J. A spectrum of monoclonal antibodies reactive with human mammary tumor cells. Proc. Natl. Acad. Sci. USA, *78:* 3199–3203, 1981.
24. Chen, F-M., Liu, C-Z., Gaffar, S. A., and Epstein, A. L. Chromatographic methods for large-scale preparation of immunoglobulin G2a monoclonal antibodies Lym-1 and TNT-1 F(ab')$_2$ fragments. J. Chromatogr., *563:* 243–255, 1991.
25. Khawli, L. A., Alauddin, M. M., Miller, G. K., and Epstein, A. L. Improved immunotargeting of tumors with biotinylated monoclonal antibodies and radiolabeled streptavidin. Antibody Immunoconj. Radiopharm., *6:* 13–27, 1993.
26. Laemmli, U. K. Cleavage of structural proteins during the assembly of the head of bacteriophage T4. Nature (Lond.), *227:* 680–685, 1970.
27. Anderson, P. M., Rogosheske, J. R., Ramsay, N. K. C., and Weisdorf, D. J. Biologic activity of interleukin-2 in intravenous admixtures containing antibiotic, morphine sulfate, or total parenteral nutrient solution. Am. J. Hosp. Pharm., *49:* 608–612, 1992.
28. Frankel, M. E., and Gerhard, W. The rapid determination of binding constants for antiviral antibodies by radioimmunoassay. An analysis of the interaction between hybridoma proteins and influenza virus. Mol. Immunol., *16:* 101–106, 1979.
29. O'Reilly, D. R., Miller, L. K., and Luckow, V. A. Baculovirus expression vectors. A laboratory manual, pp. 216–229. New York: Oxford University Press, 1994.
30. Bebbington, C. R., Renner, G., Thomson, S., King, G., Abrams, D., and Yarranton, G. T. High-level expression of a recombinant antibody from myeloma cells using glutamine synthetase as an amplifiable selectable marker. Bio-Technology (NY), *10:* 169–175, 1992.
31. Samlowski, W. E., Yim, C-Y., McGregor, J. R., Kwon, O-D., Gonzales, S., and Hibbs, J. B., Jr. Effectiveness and toxicity of protracted nitric oxide synthesis inhibition during IL-2 treatment of mice. J. Immunother., *18:* 166–178, 1995.
32. Orucevic, A., and Lala, P. K. N^G-nitro-L-arginine methyl ester, an inhibitor of nitric oxide synthesis, ameliorates interleukin-2-induced capillary leak syndrome in healthy mice. J. Immunother., *18:* 210–220, 1996.
33. Marincola, F. M. Interleukin-2. Biol. Ther. Cancer Updates, *4:* 1–16, 1994.
34. Richards, J. M., and Lotze, M. T. IL-2 therapy. Current status and future directions. Contemp. Oncol., 34–42, 1992.
35. Gill, I., Agah, R., Hu, E., and Mazumder, A. Synergistic antitumor effects of interleukin 2 and the monoclonal antibody Lym-1 against human Burkitt lymphoma cells *in vitro* and *in vivo*. Cancer Res., *49:* 5377–5379, 1989.
36. Biddle, W. C., Pancook, J., Goldrosen, M., Han, T., Foon, K. A., and Vaickus, L. Antibody-dependent, cell-mediated cytotoxicity by an anti-Class II murine monoclonal antibody: effects of recombinant interleukin 2 on human effector cell lysis of human B-cell tumors. Cancer Res., *50:* 2991–2996, 1990.
37. Morgan, A. C., Jr., Sullivan, W., Graves, S., and Woodhouse, C. S. Murine monoclonal IgG3 to human colorectal tumor-associated antigens: enhancement of antibody-dependent cell-mediated cytotoxicity by interleukin 2. Cancer Res., *49:* 2773–2776, 1989.
38. Hank, J. A., Robinson, R. R., Surfus, J., Mueller, B. M., Reisfeld, R. A., Cheung, N-K., and Sondel, P. M. Augmentation of antibody-dependent cell-mediated cytotoxicity following *in vivo* therapy with recombinant interleukin 2. Cancer Res., *50:* 5234–5239, 1990.
39. Vuist, W. M. J., Buitenen, M. A. d. R., Hekman, A., Rumke, P., and Melief, C. J. M. Potentiation by interleukin 2 of Burkitt's lymphoma therapy with anti-pan B (anti-CD19) monoclonal antibodies in a mouse xenotransplantation model. Cancer Res., *49:* 3783–3788, 1989.
40. Tsai, S-C. J., Gansbacher, B., Tait, L., Miller, F. R., and Heppner, G. H. Induction of antitumor immunity by interleukin-2 gene-transduced mouse mammary tumor cells *versus* transduced mammary stromal cells. J. Natl. Cancer Inst., *85:* 546–553, 1993.
41. Katsanis, E., Orchard, P. J., Bausero, M. A., Gorden, K. B., McIvor, R. S., and Blazar, B. R. *Interleukin-2* gene transfer into murine neuroblastoma decreases tumorigenicity and enhances systemic immunity causing regression of preestablished retroperitoneal tumors. J. Immunother., *15:* 81–90, 1994.
42. Visseren, M. J. W., Koot, M., van der Voort, E. I. H., Gravestein, L. A., Shoenmakers, H. J., Kast, W. M., Zijlstra, M., and Melief, C. J. M. Production of interleukin-2 by EL-4 tumor cells induces natural killer cell- and T cell-mediated immunity. J. Immunother., *15:* 119–128, 1994.
43. Ohira, T., Ohe, Y., Heike, Y., Podack, E. R., Olsen, K. J., Nishio, K., Nishio, M., Miyahara, Y., Funayama, Y., Ogasawara, H., Arioka, H., Kato, H., and Saijo, N. Gene therapy for Lewis lung carcinoma with tumor necrosis factor and interleukin 2 cDNAs co-transfected subline. Gene Ther., *1:* 269–275, 1994.
44. Uchiyama, A., Hoon, D. S. B., Morisaki, T., Kaneda, Y., Yuzuki, D. H., and Morton, D. L. Transfection of *interleukin 2* gene into human melanoma cells augments cellular immune response. Cancer Res., *53:* 949–952, 1993.
45. Cignetti, A., Guarini, A., Carbone, A., Forni, M., Cronin, K., Forni, G., Gansbacher, B., and Foa, R. Transduction of the *IL2* gene into human acute leukemia cells: induction of tumor rejection without modifying cell proliferation and IL2 receptor expression. J. Natl. Cancer Inst., *86:* 785–791, 1994.
46. Fell, H. P., Gayle, M. A., Grosmaire, L., and Ledbetter, J. A. Genetic construction and characterization of a fusion protein consisting of a chimeric F(ab') with specificity for carcinomas and IL-2. J. Immunol., *146:* 2446–2452, 1991.
47. Gillies, S. D., Reilly, E. B., Lo, K-M., and Reisfeld, R. A. Antibody-targeted interleukin 2 stimulates T-cell killing of autologous tumor cells. Proc. Natl. Acad. Sci. USA, *89:* 1428–1432, 1992.
48. Gillies, S. D., Young, D., Lo, K-M., and Roberts, S. Biological activity and *in vivo* clearance of antitumor antibody/cytokine fusion proteins. Bioconjugate Chem., *4:* 230–235, 1993.
49. Sabzevari, H., Gillies, S. D., Mueller, B. M., Pancook, J. D., and Reisfeld, R. A. A recombinant antibody-interleukin 2 fusion protein suppresses growth of hepatic human neuroblastoma metastases in severe combined immunodeficiency mice. Proc. Natl. Acad. Sci. USA, *91:* 9626–9630, 1994.
50. Savage, P., So, A., Spooner, R. A., and Epenetos, A. A. A recombinant single chain antibody interleukin-2 fusion protein. Br. J. Cancer, *67:* 304–310, 1993.
51. Naramura, M., Gillies, S. D., Mendelsohn, J., Reisfeld, R. A., and Mueller, B. M. Mechanisms of cellular cytotoxicity mediated by a recombinant antibody-IL2 fusion protein against human melanoma cells. Immunol. Lett., *39:* 91–99, 1994.
52. Xiang, J., Liu, E., Moyana, T., and Qi, Y. Single-chain antibody variable region-targeted interleukin-2 stimulates killing of human colorectal carcinoma cells. Immunol. Cell Biol., *72:* 275–285, 1994.
53. Bei, R., Schlom, J., Kashmiri, S. V. S. Baculovirus expression of a functional single-chain immunoglobulin and its IL-2 fusion protein. J. Immunol. Methods, *168:* 245–255, 1995.

EXHIBIT F

Bioconjugate Chem. **1997**, *8*, 510–519

Construction, Expression, and Activities of L49-sFv-β-Lactamase, a Single-Chain Antibody Fusion Protein for Anticancer Prodrug Activation

Nathan O. Siemers, David E. Kerr, Susan Yarnold, Mark R. Stebbins, Vivekananda M. Vrudhula, Ingegerd Hellström, Karl Erik Hellström, and Peter D. Senter*

Bristol-Myers Squibb Pharmaceutical Research Institute, 3005 First Avenue, Seattle, Washington 98121. Received February 11, 1997®

The L49 (IgG_1) monoclonal antibody binds to p97 (melanotransferrin), a tumor-selective antigen that is expressed on human melanomas and carcinomas. A recombinant fusion protein, L49-sFv-bL, that contains the antibody binding regions of L49 fused to the *Enterobacter cloacae* r2-1 β-lactamase (bL) was constructed, expressed, and purified to homogeneity in an *Escherichia coli* soluble expression system. The variable regions of L49 were cloned by reverse transcription–polymerase chain reaction from L49 hybridoma mRNA using signal sequence and constant region primers. Construction of the gene encoding L49-sFv-bL was accomplished by hybridization insertion of V_H, V_L, and sFv linker sequences onto a pET phagemid template containing the bL gene fused to the pelB leader sequence. Optimal soluble expression of L49-sFv-bL in *E. coli* was found to take place at 23 °C with 50 μM isopropyl β-D-thiogalactopyranoside induction and the use of the nonionic detergent Nonidet P-40 for isolation from the bacteria. Construction and expression of a soluble form of the p97 antigen in Chinese hamster ovary cells allowed affinity-based methods for analysis and purification of the fusion protein. Surface plasmon resonance, fluorescent activated cell sorting, and Michaelis–Menten kinetic analyses showed that L49-sFv-bL retained the antigen binding capability of monovalent L49 as well as the enzymatic activity of bL. *In vitro* experiments demonstrated that L49-sFv-bL bound to 3677 melanoma cells expressing the p97 antigen and effected the activation of 7-(4-carboxybutanamido)cephalosporin mustard (CCM), a cephalosporin nitrogen mustard prodrug. On the basis of these results, L49-sFv-bL was injected into nude mice with subcutaneous 3677 tumors, and localization was determined by measuring bL activity. Tumor to blood conjugate ratios of 13 and 150 were obtained 4 and 48 h post conjugate administration, respectively, and the tumor to liver, spleen, and kidney ratios were even higher. A chemically produced L49-Fab′-bL conjugate yielded a much lower tumor to blood ratio (5.6 at 72 h post administration) than L49-sFv-bL. Therapy experiments established that well-tolerated doses of L49-sFv-bL/CCM combinations resulted in cures of 3677 tumors in nude mice. The favorable pharmacokinetic properties of L49-sFv-bL allowed prodrug treatment to be initiated 12 h after the conjugate was administered. Thus, L49-sFv-bL appears to have promising characteristics for site-selective anticancer prodrug activation.

INTRODUCTION

A considerable amount of attention has been directed toward the use of monoclonal antibody–enzyme conjugates in combination with suitable prodrugs for the selective delivery of chemotherapeutic agents to tumors (*1–3*). The monoclonal antibody (mAb[1]) portions of these immunoconjugates recognize tumor-selective antigens and are capable of delivering the enzymes to tumor cell surfaces. Once tumor localization and systemic conjugate clearance have taken place, a prodrug form of a chemotherapeutic agent is administered, which is converted into an active drug by the targeted enzyme. This leads to the selective delivery of anticancer drugs to sites of neoplasia. Pharmacokinetic studies have shown that the intratumoral drug concentrations resulting from mAb–enzyme/prodrug combinations can be significantly greater than that achieved by systemic drug administration (*4–6*). This probably accounts for the observed antitumor activities, which include complete tumor regressions and cures in a number of different models for human cancer (*7–10*).

Our recent research has focused on the use of antibodies against the human p97 (melanotransferrin) tumor antigen for the delivery of β-lactamase (bL) to tumor cells (*10*). This antigen has been found to be overexpressed on a majority of clinical melanoma isolates and is also observed on human carcinomas (*11–14*). Significant antitumor activities have been obtained using the combination of a chemically conjugated anti-p97 Fab′-bL and CCM (*10*), a cephalosporin containing prodrug of PDM (Figure 1). These effects were observed in a melanoma tumor model that was resistant to the activities of PDM.

A critical aspect of this targeting strategy surrounds the ability of the mAb to selectively deliver the enzyme to tumor cells and then clear from the systemic circulation before the prodrug is administered. The pharmacokinetics of the immunoconjugate can be greatly influenced by the nature, valency, and molecular weight of the mAb and also by the way that the enzyme is attached. Typically, mAb–enzyme conjugates are prepared using

* Author to whom correspondence should be addressed.

® Abstract published in *Advance ACS Abstracts,* June 15, 1997.

[1] Abbreviations: bL, β-lactamase; CHO, Chinese hamster ovary; CCM, 7-(4-carboxybutanamido)cephalosporin mustard; FITC, fluorescein isothiocyanate; IMDM, Iscove's Modified Dulbecco's Medium; IPTG, isopropyl β-D-thiogalactopyranoside; mAb, monoclonal antibody; PBS, 10 mM Na_2HPO_4, 1 mM KH_2PO_4, 137 mM NaCl, 2.7 mM KCl, pH 7.4; PCR, polymerase chain reaction; PDM, phenylenediamine mustard; SDS–PAGE, sodium dodecyl sulfate polyacrylamide gel electrophoresis; sp97, soluble p97 antigen; Tris, tris(hydroxymethyl)aminomethane.

S1043-1802(97)00075-X CCC: $14.00

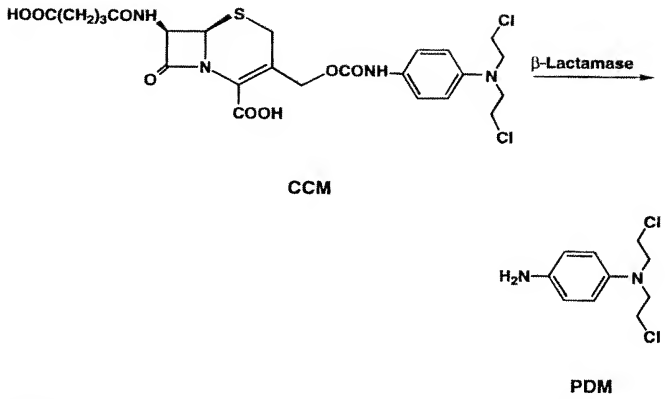

Figure 1. Structures of the cephalosporin mustard prodrug CCM and the parent drug phenylenediamine mustard PDM.

bifunctional cross-linking reagents that react with exposed amino acid residues on the individual proteins. Immunoconjugates produced in this manner are heterogeneous due to the inherent lack of regiospecificity of the cross-linking reagents. In addition, these conjugates are typically isolated in low yields. Although recent papers describe alternative coupling chemistries that can afford higher yields of more homogeneous immunoconjugates (*15*–*17*), these methods still involve chemical modification steps that contribute to product heterogeneity.

Recombinant technology offers an alternative method for producing homogeneous mAb–enzyme fusion proteins that can be designed to have appropriate pharmacokinetic properties for prodrug activation. There have recently been reports of the production, characterization, and activities of recombinant Fab, sFv, and disulfide-stabilized Fv–enzyme fusion proteins (*4*, *18*–*20*). In this paper, we describe the construction, expression, and characteristics of L49-sFv-bL, an antibody β-lactamase fusion protein that binds to the p97 antigen. We also detail the construction and expression of sp97, a soluble form of the p97 antigen that has proven to be useful for conjugate analysis and purification. *In vitro* and *in vivo* experiments are presented that illustrate the ability of L49-sFv-bL to activate the phenylenediamine mustard prodrug CCM on p97 positive human melanoma cells, selectively localize in human tumor xenografts in nude mice, and induce regressions and cures of established tumors when combined with CCM.

MATERIALS AND METHODS

Materials. The *Enterobacter cloacae* P99 bL gene was obtained from the plasmid pNU363 (*21*) and subjected to codon-based mutagenesis at the nucleotides corresponding to amino acids 286–290. The r2-1 bL mutant, which has the sequence TSFGN at positions 286–290, was selected from the resulting library and displayed greater enzymatic activity than the wild type enzyme using cephalosporin doxorubicin as the substrate (*22*). L49-Fab′-bL was prepared as previously described by combining thiol-containing Fab′ fragments of the antibodies with maleimide-substituted bL, forming a thioether link between the two proteins (*23*). CCM (*24*) and PDM (*25*) were prepared as previously described.

Isolation and Characterization of the L49 mAb. The L49-producing hybridoma was developed using standard techniques as previously described for the isolation of other hybridomas (*26*). Balb/C mice were immunized repeatedly with the H2981 (lung carcinoma), CH3 (lung carcinoma), and W56 (melanoma) cell lines, all of which were derived from human tumors. Spleen cells from immunized mice were fused with the cell line P3X63-Ag8.563 (*26*) that was transfected with the neomycin resistance gene. Standard selection and cloning yielded a hybridoma producing the L49 IgG_1 mAb.

Scatchard analysis of L49 binding was performed by radiolabeling the mAb with [^{125}I]Iodogen to a specific activity of 0.3 mCi/mg of protein. 3677 melanoma cells (*10*) in 96-well plates (13 000 cells/well) were incubated with 0.03–10 nM [^{125}I]L49 for 30 min on ice, and then the cells were separated from unbound radioactivity by centrifugation through silicon oil. The tubes were frozen, the cell pellet was cut from the supernatant, and both fractions were counted in a gamma counter. Binding affinity and the number of sites per cell were determined by Scatchard analysis (*27*).

Soluble p97 (sp97). A secreted form of p97 (sp97) was made utilizing PCR-based mutagenesis to introduce a stop codon after cysteine 709 (*14*), three amino acids upstream of the glycophosphatidylinositol anchor domain (*28*, *29*). The 3′ oligonucleotide used in the PCR reaction contained the mutation changing the S710 codon to a stop codon. Coding sequences for 29 amino acids, including the membrane anchor region, were deleted from the carboxyl terminus of wild type p97. Cloning and expression of sp97 were accomplished using a glutamine synthetase gene as an amplifiable marker in CHO cells (*30*). The sp97 gene was cloned into pEE14 (*31*) and transfected into CHO-K1 cells by calcium phosphate coprecipitation. Transformants were initially selected for resistance to 25 μM methionine sulfoximine, and sp97-secreting colonies were selected for amplification at drug concentrations of 100, 250, and 500 μM. The selection and amplification medium used was Glasgow Minimum Essential Medium without L-glutamine, tryptose phosphate broth, or sodium bicarbonate supplemented with 10% dialyzed fetal bovine serum.

A cloned CHO cell line secreting sp97 was cultured in 10 shelf cell factories. Soluble p97 was isolated from the medium on a 96.5 immunoaffinity chromatography column as described previously for the purification of wild type p97 from melanoma cells (*32*). Small amounts of residual contaminants were removed by gel filtration on a Sephacryl S300 HR column (Pharmacia LKB) using PBS as eluant. Solutions containing sp97 were concentrated by ultrafiltration to 1–5 mg/mL, sterilized by passage through a 0.1 μm filter, and stored at 2–8 °C for up to 6 months without noticeable loss of biochemical or biological activity.

Cloning of L49 Variable Regions and sFv Construction. Construction of L49-sFv-bL by hybridization insertion was performed with materials and protocols from the Bio-Rad M13 mutagenesis kit, except for isolation of single-stranded phagemid template (Qiagen M13 kit, M13K07 helper phage). The variable regions of the L49 mAb were cloned from the corresponding hybridoma mRNA by RT-PCR (Perkin-Elmer GeneAmp reagents and Model 9600 thermal cycler), using random hexamer primed reverse transcription reactions and signal sequence and constant region PCR primers (*33*). Construction of L49-sFv-bL began with a single-stranded template of the pET-26b phagemid containing the r2-1 mutant of the *E. cloacae* P99 bL gene (*22*) fused to the pelB leader sequence. Hybridization mutagenesis was used to insert the 218 linker sequence (*34*) (chemically synthesized oligonucleotide, 5′-TTCTGACACTGGCGTGCCCTTGGTAGAGCCTTCGCCAGAGCCCGGTTTGCCAGAGCCGGACGTCGAGCCGGCCATCGCCGGCTG-3′) and full V_H and V_L region sequences (oligonucleotides produced by asymmetric PCR; V_H forward primer, 5′-CCAGCCGGCGATGGCCGAGGTGCAGCTTCAGGAGT-

3′; V_H reverse primer, 5′-AGAGCCGGACGTCGAGCCTGAGGAGACGGTGACAGAGG-3′; V_L forward primer, 5′-AGGCTCTACCAAGGGCGATTTTGTGATGACCCAAAC-3′; V_L reverse primer, 5′-TTCTGACACTGGCGTCCGTTTGATTTCCAGCTTGG-3′) in three consecutive insertion reactions between the pelB leader sequence and bL in a 5′-pelB-V_H-218-V_L-bL-3′ orientation.

Expression, Purification, and Characterization of L49-sFv-bL. L49-sFv-bL was expressed as a soluble protein in *E. coli* strain BL21(λDE3) at 23 °C in 4 L baffled shake flasks. T-broth (1 L) containing 30 μg/mL kanamycin was inoculated with several colonies of freshly transformed BL21(λDE3) cells. The flasks were shaken (200 rpm) at 37 °C until the absorbance at 660 nm reached 0.8, the culture was cooled to 23 °C, and IPTG (50 μM) was added. Incubation at 23 °C with shaking was continued for an additional 16 h, at which time the absorbance at 660 nm was between 8 and 15. The cells were pelleted by centrifugation and resuspended in 30 mM Tris, 2 mM EDTA, and 0.3% (v/v) Nonidet P-40 at pH 8.5 and 4 °C. The mixture was stirred gently for 1 h and repelleted, and the supernatant was decanted and filtered (0.2 μm).

Purification of L49-sFv-bL was accomplished according to a two-step affinity purification. The above supernatant was first applied to a Sepharose column of immobilized sp97 antigen. The column was washed with PBS until the absorbance at 280 nm reached the baseline level, and bound protein was eluted with 50 mM sodium phosphate and 100 mM NaCl at pH 11.2. Fractions containing the bound protein were neutralized with 1:10 v/v of 3 M sodium phosphate, pH 7. This material was then subjected to Sepharose 4B *m*-aminophenylboronic acid affinity chromatography (*35*) using washing and pH 11.2 elution conditions described above. The resulting preparation was dialyzed against PBS, filtered (0.2 μm), and stored at 4 °C (0.1−1.1 mg/mL).

Competition binding experiments were performed as described earlier (*10*, *36*). Immunoassays were performed by coating polystyrene 96-well plates with sp97 (0.1 mL, 2 μg/mL in PBS, overnight, 4 °C). The plates were blocked by adding specimen diluent (Genetic Systems Corp.) for 1 h at 22 °C, and the diluent was then removed. Fresh specimen diluent (0.1 mL) containing serial dilutions of the samples was added. After 1 h at 22 °C, the plates were washed and developed for 15 min at room temperature with 0.1 mL of a nitrocefin solution (*37*) at 0.1 mM in PBS containing 1% dimethylformamide. Absorbance measurements were read in an ELISA plate reader using a 490 nm filter with 630 nm as the reference wavelength.

Surface plasmon resonance experiments were performed on a BIAcore 2000 instrument (Pharmacia) at 25 °C. p97 was immobilized on a research grade CM5 sensor chip (Pharmacia) using the recommeneded *N*-ethyl-*N*′-(dimethylaminopropyl)carbodiimide/*N*-hydroxysuccinimide coupling conditions. Before use, the sensor surface was subjected to several rounds of analyte binding, followed by regeneration to ensure a stable level of derivatization. The mobile phase buffer for immobilization was PBS containing 0.005% P20 surfactant (Pharmacia). For binding studies, 0.2 mg/mL bovine serum albumin was added to the buffer.

***In Vitro* Cytotoxicity.** 3677 melanoma cells were plated into 96-well microtiter plates (10^4 cells/well in 100 μL of IMDM with 10% fetal bovine serum, 60 μg/mL penicillin, and 0.1 mg/mL streptomycin) and allowed to adhere overnight. For blocking experiments, the cells were incubated with unconjugated L49 at 1 μM for 30 min prior to treatment with the L49 conjugates. The cells were treated with L49-sFv-bL or L49 Fab′-bL at 10 nM. After 30 min at 4 °C, the plates were washed three times with antibiotic-free RPMI 1640 medium (Gibco) with 10% fetal bovine serum, and then various concentrations of CCM were added. CCM and PDM were also added to cells treated with medium alone. After 1 h at 37 °C, cells were washed three times with IMDM and incubated for approximately 18 h at 37 °C. The cells were then pulsed for 12 h with [^{3}H]thymidine (1 μCi/well) at 37 °C, detached by freezing at −20 °C and thawing, and harvested onto glass fiber filter mats using a 96-well harvester. Radioactivity was counted using a LKB Wallac β-plate counter.

Conjugate Localization. Subcutaneous 3677 melanoma tumors were established in female athymic nu/nu mice (8−12 weeks old, Harlan Sprague-Dawley, Indianapolis, IN) by transplanting tumors that had been previously passaged as previously described (*10*). Tumor-bearing mice were injected iv with L49-sFv-bL (1 or 4 mg of mAb component/kg) or with L49-Fab′-bL (1.8 mg/kg). At various time intervals, the mice were anesthetized, bled through the orbital plexus, and sacrificed. Tissues were removed and homogenized in PBS containing 15 μg/mL aprotinin (2 mL/g of tissue). To the homogenate was added 50 mM sodium phosphate containing 100 mM NaCl at pH 11.2 (10 mL/g of tissue), and the suspension was mixed. After 20 min at room temperature, 3 M sodium phosphate at pH 7.0 was added (2 mL/g of tissue), and the mixture was mixed and centrifuged.

Quantification of conjugate concentrations was accomplished using a direct enzyme immunoassay. Polystyrene 96-well microtiter plates were coated with an affinity-purified rabbit polyclonal antiserum to wild type *E. cloacae* bL (1 μg/mL) and were then blocked with specimen diluent (Genetic Systems Corp.). Serially diluted tissue extracts or purified samples (L49-sFv-bL as a standard for the fusion protein samples, L49-Fab′-bL as a standard for the L49-Fab′-bL samples) were added to the wells and allowed to bind for 3 h at room temperature. The plates were washed and developed by the addition of 0.1 mL of nitrocefin (*37*) at 0.1 mM in PBS containing 1% dimethylformamide. Absorbance measurements were read in an ELISA plate reader using a 490 nm filter with 630 nm as the reference wavelength.

***In Vivo* Therapy Experiments.** 3677 tumor-bearing mice (subcutaneous implants, six animals/group, average tumor volume 130 mm^3) were injected with L49-sFv-bL (iv, 7−8 days post tumor implant), followed 12-48 h later by CCM using doses of fusion protein and prodrug as indicated under Results. Treatment with L49-sFv-bL + CCM was repeated 1 week later. Animals were monitored 1−2 times/week for body weight, general health, and tumor growth. Tumor volume was estimated using the following formula: longest length × perpendicular dimension^2 ÷ 2. Cures were defined as an established tumor that, after treatment, was not palpable for ≥10 tumor volume doubling delays (≥40 days in the 3677 tumor model). Maximum tolerated doses led to <20% weight loss and no treatment-related deaths and were within 50% of the dose at which such events took place.

RESULTS

Characterization of the L49 MAb. The L49 mAb (IgG_1) binds to the p97 antigen, which has been shown to be present on most human melanomas and many carcinomas (*11*−*13*). Scatchard analysis of the binding of radiolabeled L49 to the 3677 human melanoma cell line indicated that the mAb bound with a dissociation constant of 1.0 nM (Figure 2). At saturation, there were approximately 2.1 × 10^4 molecules of L49 bound/cell.

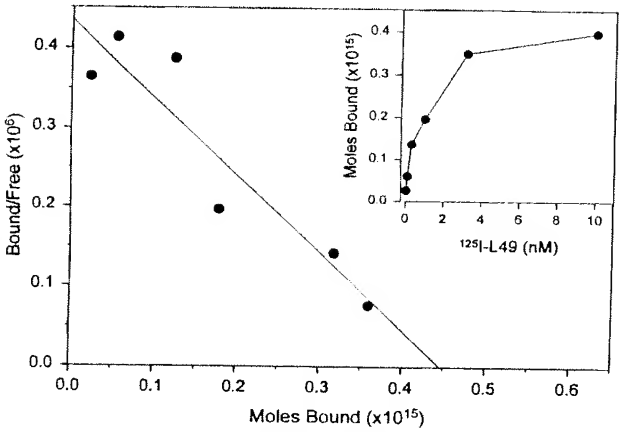

Figure 2. Scatchard analysis of L49 mAb binding to 3677 melanoma cells.

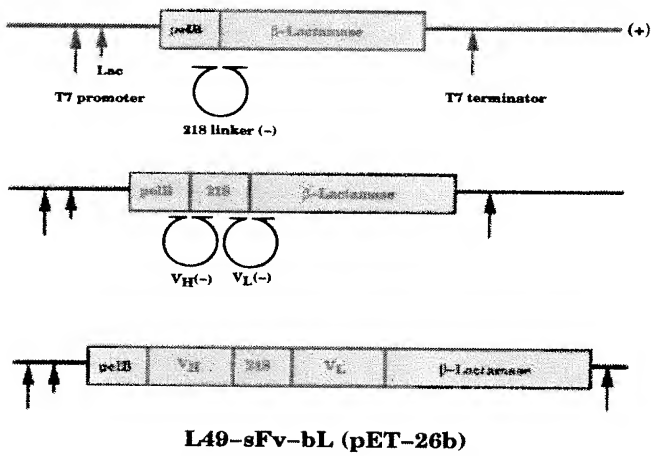

Figure 3. Construction of L49-sFv-bL. Three successive hybridization insertion reactions were used to install the 218 linker, variable heavy, and variable light chain sequences into a pET phagemid containing the r2-1 mutant of the *E. cloacae* bL. Single-stranded (+) phagemid DNA was produced by infection of XL-1 Blue carrying the pET phagemids with M13K07 helper phage. An oligonucleotide coding for the 218 linker sequence (− strand), with complentary regions to the 3′ end of the pelB sequence and the 5′ end of the bL gene was prepared by chemical synthesis. Corresponding V_H and V_L sequences (− strand) were generated by asymmetric PCR.

These values are very similar to those obtained for the 96.5 mAb (*10*), which also binds to p97 but to an epitope different from the one that L49 binds to (unpublished data).

Cloning and Expression of L49-sFv-bL. The variable region genes for the L49 mAb heavy and light chains were cloned from the L49 hybridoma line by reverse transcription PCR of hybridoma mRNA and amplification of the corresponding cDNA. A consensus sequence was determined by examining several clones from independent reverse transcription reactions to reduce the possibility of reverse transcription or PCR-derived errors. The PCR primers used were complementary to the signal sequence and constant region of the mAb. Thus, the entire variable regions were obtained.

L49-sFv-bL was constructed in a stepwise fashion by hybridization insertion of the sFv linker, V_H, and V_L region sequences onto a single-stranded pET phagemid template containing the pelB leader sequence and bL gene (Figure 3). The particular bL gene used coded for a mutant of the *E. cloacae* P99 bL (r2-1) that contained the amino acids TSFGN at positions 286−290. This

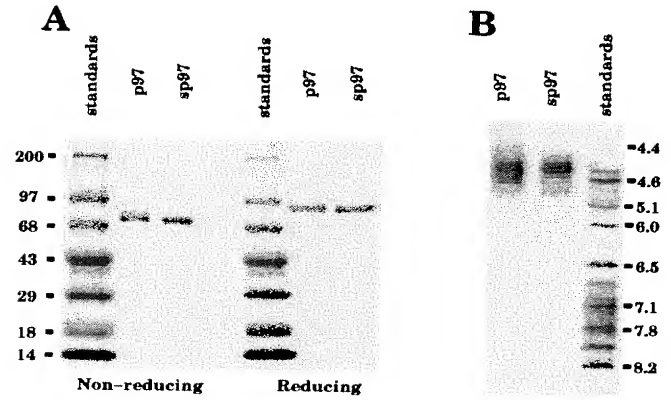

Figure 4. (A) SDS−PAGE (4−20%) and (B) isoelectric focusing analyses (pH 3−10) of recombinant sp97 and wild type p97 antigen.

mutated bL has been shown to have greater activity than the wild type enzyme toward hydrolysis of some cephalosporin prodrugs (*22*). The 218 linker sequence corresponds to amino acids GSTSGSGKPGSGEGSTKG and was used as the sFv linker on the basis of its ability to reduce sFv protein aggregation (*34*). An oligonucleotide coding for the 218 linker (− strand, produced by chemical synthesis) was first annealed to the phagemid template, resulting in a pelB-218-bL construct. V_H and V_L region segments (produced by asymmetric PCR) were then inserted into the intermediate construct in two separate steps to generate the final L49-sFv-bL gene in an pelB-V_H-218-V_L-bL orientation. The pelB leader sequence results in transport of the protein into the periplasmic space of *E. coli*. No additional linker was placed between V_L and the bL enzyme.

To facilitate the isolation and characterization of L49-containing fusion proteins, a soluble form of the p97 antigen was developed. This was made by truncating the p97 gene at a site upstream of the region encoding the membrane-anchoring domain. The soluble antigen (sp97) was expressed in CHO-K1 cells and purified by affinity chromatography. SDS−PAGE analysis of recombinant sp97 indicated that it was slightly lower in molecular weight than p97 (Figure 4A). Isoelectric focusing revealed little difference between p97 and sp97 (Figure 4B), a result that was anticipated, since only a single charged residue is lost in the sp97 construct. The multiple bands observed in the isoelectric focusing gel are due to charge herterogeneity in the expressed proteins.

L49-sFv-bL was expressed in soluble form in an *E. coli* strain that was transformed with the plasmid shown in Figure 3. Quantitation of L49-sFv-bL-containing samples was performed using an immunoassay in which the fusion protein was captured onto microtiter plates that were coated with sp97. The bL enzyme activity was then determined using nitrocefin as a colorimetric indicator (*37*). Thus, only bifunctional fusion protein was measured. Under the transcriptional control of the T7 promoter and lac operon, fusion protein expression could be detected by SDS−PAGE analyses of cell pellets in cultures that were induced with IPTG at concentrations as low as 1.6 μM (Figure 5A). Significant levels of toxicity were observed when the IPTG concentration exceeded 90 μM, resulting in inhibition of cell growth and in the eventual outgrowth of cell populations that did not express fusion protein. Typically, 50 μM IPTG induction was used for large scale experiments, since this led to higher levels of fusion protein expression without significant levels of cytotoxicity. It was also found that expression of L49-sFv-bL was enhanced at lower tem-

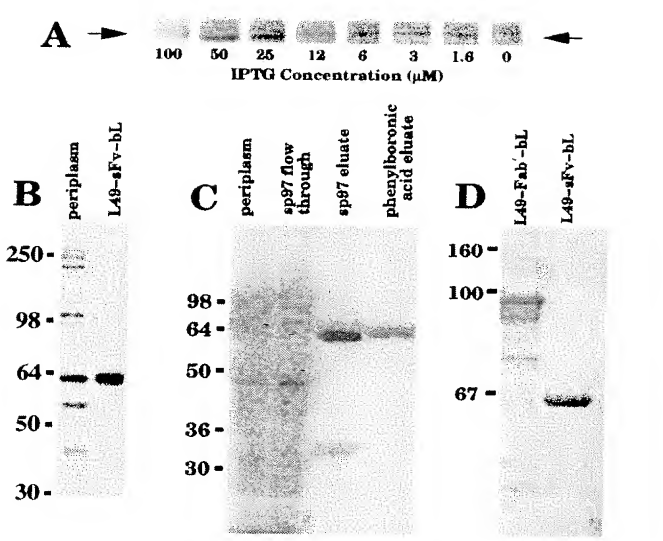

Figure 5. SDS–PAGE analyses of L49-sFv-bL expression and purification. (A) Induction of L49-sFv-bL at various IPTG concentrations (30 °C, total cellular protein, 12% Tris–glycine SDS–PAGE, Coomassie staining, nonreducing conditions). The band corresponding to L49-sFv-bL is indicated with arrows. (B) Western analysis with rabbit polyclonal anti-bL: (lane 1) periplasm; (lane 2) L49-sFv-bL standard (12% Tris–glycine SDS–PAGE, nonreducing conditions). (C) Purification of L49-sFv-bL: (lane 1) periplasm; (lane 2) flow through from the sp97 affinity column; (lane 3) material that eluted from the sp97 column at pH 11; (lane 4) material that bound and eluted off the phenylboronic acid column (12% Tris–glycine SDS–PAGE, Coomassie staining, nonreducing conditions). (D) Comparison of L49-sFv-bL to chemically prepared L49-Fab'-bL: (lane 1) L49-Fab'-bL; (lane 2) L49-sFv-bL (10% Tris–glycine SDS–PAGE, Coomassie staining, nonreducing conditions).

peratures, such that protein yields were higher at 23 or 30 °C compared to 37 °C. Similar results have been noted for the expression of antibody fragments and other recombinant proteins in *E. coli* (*38*).

In shake flask cultures, 80% of active material was present in the periplasm of the bacterial cells, with the remainder present in the culture supernatant. Conventional techniques for releasing the periplasmic contents, such as sucrose/lysozyme spheroplasting or osmotic shock, resulted in only a limited release of the available protein. Freeze–thawing or sonication of cells to release total cytoplasmic material did not result in an increased yield of functional fusion protein. It was found that a higher yield of fusion protein could be obtained by treating cell pellets with a solution of the detergent Nonidet-P-40. The levels of L49-sFv-bL in samples that were treated with this detergent ranged from 2.5 to 8 mg/L culture, approximately 4 times the amount extracted by other techiques. Western analysis (Figure 5B) with rabbit polyclonal antiserum raised to bL showed that most of the bL-containing protein in the preparation was approximately 63 kDa in molecular mass (theoretical molecular mass 66.5 kDa). Small amounts of truncated fragments and aggregated material were also detected.

Purification of L49-sFv-bL. The purification of L49-sFv-bL was achieved according to a two-step affinity chromatography procedure. Periplasmic preparations from shake flask cultures were first applied to an immobilized sp97 affinity column that could bind the L49 portion of the fusion protein. After extensive washing, bound material was eluted at pH 11.2 (Figure 5C). Acidic pH conditions (pH 2.2) also eluted the fusion protein, but caused protein precipitation. The sp97 chromatography purified material was approximately 70% pure by size exclusion HPLC and SDS–PAGE, with the contaminants

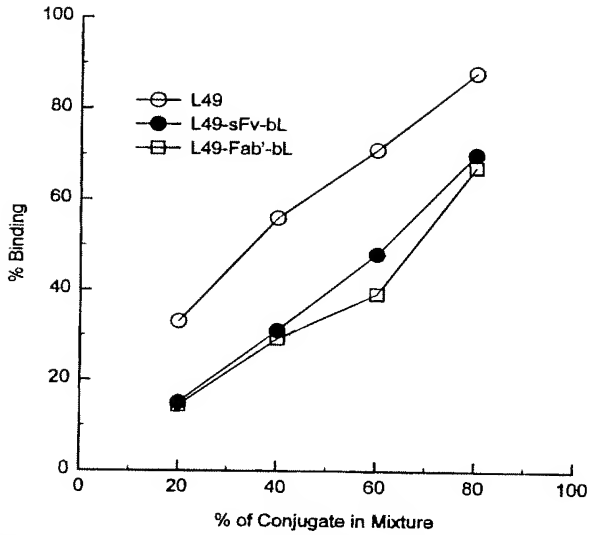

Figure 6. Competition binding assay. 3677 cells were incubated with various combinations of the test samples (L49, L49-sFv-bL, L49-Fab'-bL, and FITC-modified whole L49), keeping the total mAb concentration (test sample + L49-FITC) constant at 400 nM. Fluorescence intensity was determined by fluorescence activated cell sorter analysis.

consisting of two bands of approximately 33 kDa molecular mass. The second step of the purification involved binding the material to immobilized phenylboronic acid, a resin that binds to the active sites of β-lactamases. This led to the recovery of protein that was pure by SDS–PAGE analysis (Figure 5C,D). Size exclusion chromatographic analysis of the fusion protein indicated the presence of a single component that eluted in the expected molecular mass range (data not shown). In contrast, L49-Fab'-bL, which was prepared by combining maleimide-substituted bL with L49-Fab'-SH according to previously described methods (*10*, *23*), displayed significant levels of heterogeneity by SDS–PAGE (Figure 5D).

L49-sFv-bL Characterization and Activity. In view of the detergent-based release of L49-sFv-bL from the bacteria, it was important to demonstrate that isolated fusion protein had been correctly processed and transported into the periplasm, such that the pelB leader sequence was cleaved from the amino terminus of the V_H region. This was determined by subjecting the purified fusion protein to N-terminal amino acid sequence analysis. The sequence obtained (EVQLQES) was identical to the expected V_H amino terminal sequence, indicating that the leader sequence was proteolytically clipped, as designed.

The binding characteristics of the sFv portion of the fusion protein were determined using a fluorescence-activated cell sorting assay in which fusion protein and FITC-modified whole L49 competed for binding to cell-surface antigens on SK-MEL 28 melanoma cells. L49-sFv-bL and the L49 Fab'-bL chemical conjugates bound equally well to the cell line, but not as well as bivalent whole L49 mAb (Figure 6). More detailed information about binding was obtained using surface plasmon resonance, which allowed the measurement of the on and off rates of L49-sFv-bL binding to the p97 antigen immobilized on a gold surface (Table 1). This assay established that the binding affinity of the fusion protein to the p97 antigen (K_D = 1.0 nM) was comparable to those of L49 Fab' (K_D = 0.73 nM) and chemically produced L49-Fab'-bL conjugate (K_D = 1.3 nM).

Enzymatic activity assays of the bL portion of L49-sFv-bL were undertaken using nitrocefin as the substrate

Table 1. Binding and Enzyme Kinetic Parameters of L49- and bL-Containing Proteins[a]

sample	k_{on} ($M^{-1}\cdot s^{-1}$)	k_{off} (s^{-1})	K_D (nM)	k_{cat} (s^{-1})	K_m (μM)
L49 Fab′	2.3×10^5	1.7×10^{-4}	0.73	na[b]	na
r2-1 bL[c]	na	na	na	261	19
L49-Fab′-bL[d]	1.8×10^5	2.4×10^{-4}	1.3	nd[e]	nd
L49-sFv-bL[c]	4.1×10^5	4.2×10^{-4}	1.0	232	19

[a] Values shown are the average of a minimum of two independent experiments, except for L49-Fab′-bL (binding experiment performed once). The range of values obtained in Michaelis–Menten kinetic analyses was within 5% of the means. Nitrocefin was used as an enzyme substrate. [b] Not applicable. [c] The r2-1 bL contains mutations at positions 286–290 compared to the wild type enzyme (*22*). [d] Chemically prepared conjugate containing the wild type enzyme. [e] Not determined.

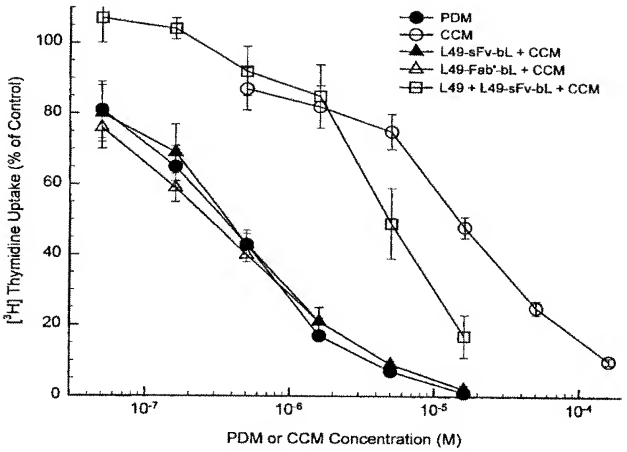

Figure 7. Cytotoxic effects of mAb–bL + CCM combinations on 3677 melanoma cells as determined by the incorporation of [^{3}H]thymidine into DNA. 3677 cells were incubated with the mAb–bL conjugates, washed, and treated with CCM for 1 h. The effects were compared to cells treated with CCM or PDM for 1 h without prior conjugate exposure and to cells that were treated with saturating amounts of unconjugated L49 prior to conjugate treatment.

(Table 1). Michaelis–Menten kinetic analyses confirmed that the fusion protein retained the full enzymatic activity of the mutant bL enzyme from which it was derived (*22*). Thus, both the binding of the L49 mAb and the enzymatic activity of the *E. cloacae* r2-1 bL were preserved in the fusion protein.

The cytotoxic effects of L49-sFv-bL in combination with CCM were determined on 3677 human melanoma cells, which express the p97 antigen (Figure 7). The experiments were performed by treating the cells with the conjugates, washing off unbound material, adding various concentrations of CCM, and using [^{3}H]thymidine incorporation as a measure of cytotoxic activity. The prodrug CCM ($IC_{50} = 16\ \mu M$) was approximately 50-fold less toxic to 3677 cells than the drug PDM ($IC_{50} = 0.3\ \mu M$). As expected, L49-sFv-bL and L49-Fab′-bL were equally effective at prodrug activation, and the combinations were equivalent in activity to PDM. This indicates that prodrug conversion by both conjugates was efficient under the conditions tested. In addition, it was found that activation was immunologically specific, since L49-sFv-bL did not activate CCM on cells that were saturated with unconjugated L49 before being exposed to the fusion protein.

***In Vivo* Localization.** Biodistribution studies of L49-sFv-bL and L49-Fab′-bL were carried out in nude mice bearing sc 3677 melanoma tumor xenografts. The conjugates were injected iv, and at various time points

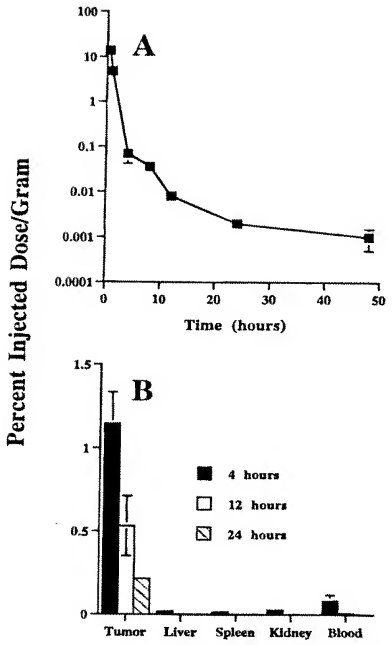

Figure 8. Pharmacokinetics of L49-sFv-bL in nude mice (three animals/group). L49-sFv-bL was injected intravenously, tissues were removed and extracted at the indicated times, and the β-lactamase activity was determined using nitrocefin as a substrate. (A) Clearance of L49-sFv-bL from the blood. Injected dose was 4 mg/kg. (B) L49-sFv-bL levels in subcutaneous 3677 melanoma tumors and in normal tissues. Injected dose was 1 mg/kg.

tissues were removed and extracted under alkaline conditions to disrupt antigen–antibody interactions. The samples were then trapped with polyclonal antiserum to bL, and bL activity was measured using nitrocefin as a colorimetric indicator (*37*). Control experiments in which L49-sFv-bL was directly injected into excised tumors and tissues indicated that this extraction procedure recovered 90% of the injected bL activity.

L49-sFv-bL cleared very rapidly from the blood (Figure 8A). The initial and terminal clearance half-lives ($t_{1/2}\alpha$ and $t_{1/2}\beta$, respectively) were 0.3 and 2.5 h, respectively, leading to a 10^4 reduction of L49-sFv-bL blood levels within 24 h of conjugate administration. In spite of this rapid clearance, relatively high intratumoral levels of L49-sFv-bL were measured compared to normal tissues, and the ratio remained high for 24 h (Figure 8B). At 4 h post L49-sFv-bL administration, the tumor to blood ratio was 13:1. The ratio increased substantially with time and was 105:1 within 24 h of conjugate administration (Table 2). Similar results were obtained using L49-sFv-bL doses of 4 mg/kg. At this dose, very high tumor to blood ratios (141–150:1) were measured 24–48 h after the conjugate was administered. Interestingly, chemically produced L49-Fab′-bL cleared quite slowly from the blood and had only a 5.6:1 tumor to blood ratio 72 h after administration. Thus, L49-sFv-bL localizes in tumors, clears rapidly from the systemic circulation, and has significantly improved pharmacokinetic properties compared to the chemically produced L49-Fab′-bL conjugate.

Therapeutic Activity. *In vivo* therapy experiments were performed using the L49-sFv-bL/CCM combination in nude mice with established sc 3677 tumors. This particular tumor model has previously been shown to be resistant to treatment with doxorubicin, PDM, and CCM (*10*). In the experiments reported here, conjugate treatment was initiated 7–8 days after tumor implant, at which time the tumors were approximately 130 mm^3 in

Table 2. Tissue Distribution of Immunoconjugates

		% injected dose/g (SD)				
treatment[a]	time (h)	tumor	liver	spleen	kidney	blood
L49-sFv-bL, 1 mg/kg	4	1.1 (0.2)	0.021 (0.002)	0.014 (0.008)	0.027 (0.015)	0.084 (0.04)
tumor/tissue ratios		1	52	79	41	13
L49-sFv-bL, 1 mg/kg	12	0.53 (0.17)	<0.003	<0.003	<0.003	0.008 (0.001)
tumor/tissue ratios		1	>177	>177	>177	66
L49-sFv-bL, 1 mg/kg	24	0.21 (0.01)	<0.003	<0.003	<0.003	0.002 (0.001)
tumor/tissue ratios		1	>70	>70	>70	105
L49-sFv-bL, 4 mg/kg	12	0.73 (0.02)	<0.003	<0.003	<0.003	0.009 (0.001)
tumor/tissue ratios		1	>240	>240	>240	81
L49-sFv-bL, 4 mg/kg	24	0.29 (0.05)	<0.001	<0.001	<0.001	0.002 (0.0002)
tumor/tissue ratios		1	>290	>290	>290	141
L49-sFv-bL, 4 mg/kg	48	0.15 (0.07)	nd[b]	nd	nd	0.001 (0.0002)
tumor/tissue ratios		1				150
L49-Fab'-bL, 1.8 mg/kg	72	0.28 (0.26)	0.015 (0.003)	0.010 (0.006)	0.016 (0.005)	0.05 (0.015)
tumor/tissue ratios		1	19	28	18	5.6

[a] Mice (three animals/group) were injected with conjugates, and at the times indicated, tissues were excised and extracted to remove the conjugate. The percent injected dose was based on the measured bL activity compared to standard curves obtained from extracted tissues that were spiked with known amounts of L49-sFv-bL or L49-Fab'-bL. [b] Not determined.

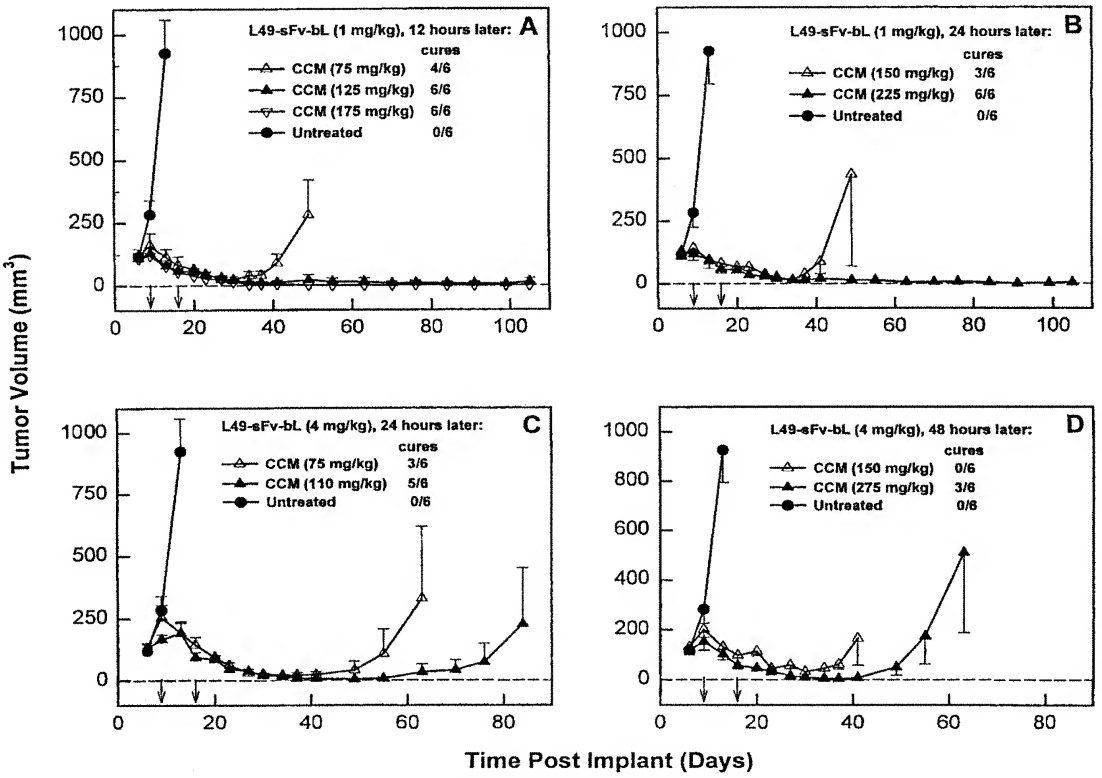

Figure 9. Therapeutic effects of L49-sFv-bL/CCM combinations in nude mice (six mice/group) with sc 3677 melanoma xenografts. Conjugates were injected, followed at various times by CCM (arrows on the *X*-axis). The average tumor volumes are reported until most or all of the animals were cured (tumors that became nonpalpable for ≥10 tumor volume doubling times) or until an animal was removed from the experiment due to tumor outgrowth. (A) L49-sFv-bL (1 mg/kg/injection) 12 h before CCM; (B) L49-sFv-bL (1 mg/kg/injection) 24 h before CCM; (C) L49-sFv-bL (4 mg/kg/injection) 24 h before CCM; (D) L49-sFv-bL (4 mg/kg/injection) 48 h before CCM.

volume. CCM was then administered 12, 24, or 48 h later, and the treatment protocol was repeated after 1 week. Maximum tolerated doses are defined as those that led to <20% weight loss and no treatment-related deaths and were within 50% of the dose at which such events took place. A tumor was considered as having been cured once it was not palpable for at least 10 tumor volume doubling times, based on the tumor growth of untreated animals (tumor volume doubling time was 4 days). If an animal was removed from the experiment because of tumor growth, the data from the entire group were no longer plotted, but the remaining animals were followed for tumor size and general health.

The maximum tolerated doses of CCM (300 mg/kg/injection) and PDM (3 mg/kg/injection) when administered weekly for three rounds induced 2 and 6 day delays in tumor outgrowth, respectively (data not shown). In contrast, pronounced antitumor activity was obtained in mice that received L49-sFv-bL prior to treatment with CCM (Figure 9). Therapeutic efficacy was schedule and dose dependent. Tumor cures were obtained in all of the animals that received CCM (125 and 175 mg/kg/injection) 12 h after treatment with L49-sFv-bL (Figure 9A). In this dosing schedule, significant antitumor activity including four cures in the group of six mice was obtained when the CCM dose was reduced to 75 mg/kg/injection.

The remaining two animals in this group had tumors that underwent partial regressions but eventually began to grow after the last prodrug treatment. There were no apparent toxicities in any of these treatment groups.

Significant antitumor activity could also be achieved when the prodrug was administered 24 h post conjugate administration, either by increasing the prodrug dose and keeping the conjugate dose constant at 1 mg/kg/injection (Figure 9B) or by increasing the conjugate dose to 4 mg/kg/injection (Figure 9C). In both cases, the majority of tumors were cured, again with no evidence of toxicity. Finally, therapeutic efficacy was also obtained with a 48 h interval between conjugate and prodrug administration (Figure 9D). Tumor regressions were obtained in all of the mice in these groups, and three of six animals that received 275 mg/kg/injection CCM were cured. Thus, the antitumor activities of L49-sFv-bL in combination with CCM were pronounced, and therapeutic efficacy was achieved in a variety of dosing schedules.

DISCUSSION

We have previously demonstrated that mAb–bL conjugates activate cephalosporin-containing prodrugs in an immunologically specific manner and such combinations lead to regressions and cures of established tumors in mice (*6*, *10*, *24*, *36*). These conjugates were prepared by combining maleimide-substituted bL with thiol-containing mAbs and then subjecting the resulting mixtures to purification procedures that involved affinity and size exclusion chromatographic steps. Although care was taken to control the degree of protein modification and to isolate principally monomeric material, SDS–PAGE analysis generally has indicated the presence of aggregates, dimers and lower molecular mass components in the conjugate preparations. This is exemplified in Figure 5D, which shows that chemically produced L49-Fab′-bL contains several species besides the expected product at 92 kDa. Such heterogeneity is most likely due to the lack of specificity inherent in the reagents used for protein modification (*39*). While a number of elegant methods, such as reverse proteolysis (*16*, *40–42*) and terminal amino acid group modification (*43*), have been devised to overcome this problem, these techniques can still lead to considerable product heterogeneity.

An alternative approach toward the preparation of uniform and well-defined antibody–enzyme immunoconjugates has involved recombinant technology for the production of fusion proteins. This has led to the development of L6-sFv-*Bacillus cereus* β-lactamase (*19*) and anti-p185HER2-Fv-*E. coli* β-lactamase (*20*) fusion proteins, both of which were capable of effecting prodrug activation *in vitro*. More detailed biological studies have been reported with a recombinant anti-CEA-Fab-β-glucuronidase fusion protein, which activated a doxorubicin prodrug *in vitro* and *in vivo* (*4*). The distinguishing features of these fusion proteins are that they are homogeneous and potentially can be made in reproducible and economical manners. In the work described here, we have utilized recombinant methodology for the production of L49-sFv-bL. It was possible to express soluble fusion protein in *E. coli* such that denaturation or refolding was not required for activity. L49-sFv-bL was purified using a two-stage affinity chromatography method leading to the isolation of a homogeneous product that was fully active with respect to both the L49 and bL components. As expected, the fusion protein was able to bind to melanoma cells that expressed the p97 antigen and activate a cephalosporin mustard in an immunologically specific manner.

To minimize systemic, nontargeted drug release *in vivo*, a high mAb–enzyme tumor to normal tissue ratio is needed before the prodrug is administered. To attain the required localization index in mice, the time between conjugate and prodrug administration has varied significantly from one system to another. For example, the delay between conjugate and prodrug was 3 days for 96.5-Fab′-bL (molecular mass 92 kDa) (*10*), 1 week for the anti CEA-Fab-β-glucuronidase fusion protein (molecular mass 250 kDa) (*4*), and 2 weeks for the ICR12–carboxypeptidase G2 conjugate (molecular mass range of 233–316 kDa) (*9*). In some cases, it has even been necessary to accelerate systemic conjugate clearance in a separate step involving the formation of immune complexes before prodrug could be administered (*5*, *44*, *45*). Here, we have shown that L49-sFv-bL not only clears very rapidly from the systemic circulation (Figure 8A) but also preferentially localizes into subcutaneous tumor xenografts (Figure 8B; Table 2). The very high tumor to nontumor fusion protein ratios obtained within 4–12 h of conjugate treatment would lead to the prediction that, in contrast to other enzyme/prodrug systems (*4*, *9*, *10*), therapeutic efficacy would not require protracted time intervals between conjugate and prodrug administration. This has now been experimentally confirmed, since cures of established tumors were obtained when CCM was administered 12 h following the conjugate (Figure 9A).

It is noteworthy that a correlation can be made between the outcome in the therapy experiments (Figure 9) and the pharmacokinetic data (Figure 8; Table 2). At a given conjugate dose, the intratumoral concentration decreased with a half-life of approximately 8 h (Table 2). This may be due to a variety of factors such as dissociation of the conjugate from the antigen, membrane recycling, enzyme metabolism, and rapid tumor growth. The net result is that longer time intervals between conjugate and prodrug administration require that the amount of either prodrug or conjugate be increased to maintain therapeutic efficacy (Figure 9).

In conclusion, we have shown that recombinant L49-sFv-bL has properties that are well suited for site-selective anticancer prodrug activation. The fusion protein is homogeneous, localizes in solid tumor masses, and clears very rapidly from the systemic circulation. In these respects, L49-sFv-bL has significant advantages over the L49-Fab′-bL chemically produced conjugate. Finally, we have shown that L49-sFv-bL/CCM combinations lead to cures of established melanoma tumors without toxic side effects. Currently, we are optimizing the treatment protocols and are investigating the effects of L49-sFv-bL/prodrug combinations in several carcinoma tumor models.

ACKNOWLEDGMENT

We thank William Bear, Joseph Cook, Wes Cosand, John Emswiler, Perry Fell, Deb Mahan, Hans Marquardt, Michael Neubauer, Hong Nguyen, Clay Siegall, Joseph Sundstrom, Håkan Svensson, and Trent Youngman for expert advice and assistance.

LITERATURE CITED

(1) Senter, P. D., Wallace, P. M., Svensson, H. P., Vrudhula, V. M., Kerr, D. E., Hellström, I., and Hellström, K. E. (1993) Generation of cytotoxic agents by targeted enzymes. *Bioconjugate Chem. 4*, 3–9.

(2) Jungheim, L. N., and Shepherd, T. A. (1994) Design of anticancer prodrugs: substrates for antibody targeted enzymes. *Chem. Rev. 94*, 1553–1566.

(3) Bagshawe, K. D., Sharma, S. K., Springer, C. J., and Rogers, G. T. (1994) Antibody directed enzyme prodrug therapy

(ADEPT). A review of some theoretical, experimental and clinical aspects. *Ann. Oncol. 5*, 879–891.
(4) Bosslet, K., Czech, J., and Hoffmann, D. (1994) Tumor-selective prodrug activation by fusion protein-mediated catalysis. *Cancer Res. 54*, 2151–2159.
(5) Wallace, P. M., MacMaster, J. F., Smith, V., Kerr, D. E., Senter, P. D., and Cosand, W. L. (1994) Intratumoral generation of 5-fluorouracil mediated by an antibody-cytosine deaminase conjugate in combination with 5-fluorocytosine. *Cancer Res. 54*, 2719–2723.
(6) Svensson, H. P., Vrudhula, V. M., Emswiler, J. E., MacMaster, J. F., Cosand, W. L., Senter, P. D., and Wallace, P. M. (1995) In vitro and in vivo activities of a doxorubicin prodrug in combination with monoclonal antibody β-lactamase conjugates. *Cancer Res. 55*, 2357–2365.
(7) Springer, C. J., Bagshawe, K. D., Sharma, S. K., Searle, F., Boden, J. A. Antoniw, P., Burke, P. J., Rogers, G. T., Sherwood, R. F., and Melton, R. G. (1991) Abalation of human choriocarcinoma xenografts in nude mice by antibody-directed enzyme prodrug therapy (ADEPT) with three novel compounds. *Eur. J. Cancer 27*, 1361–1366.
(8) Meyer, D. L., Jungheim, L. N., Law, K. L., Mikolajczyk, S. D., Shepherd, T. A., Mackensen, D. G., Briggs, S. L., and Starling, J. J. (1993) Site-specific prodrug activation by antibody-β-lactamase conjugates: regression and long-term growth inhibition of human colon carcinoma xenograft models. *Cancer Res. 53*, 3956–3963.
(9) Eccles, S. A., Court, W. J., Box, G. A., Dean, C. J., Melton, R. G., and Springer, C. J. (1994) Regression of established breast carcinoma xenografts with antibody-directed enzyme prodrug therapy against c-erbB2 p185. *Cancer Res. 54*, 5171–5177.
(10) Kerr, D. E., Schreiber, G. L., Vrudhula, V. M., Svensson, H. P., Hellström, I., Hellström, K. E., and Senter, P. D. (1995) Regressions and cures of melanoma xenografts following treatment with monoclonal antibody β-lactamase conjugates in combination with anticancer prodrugs. *Cancer Res. 55*, 3558–3563.
(11) Woodbury, R. G., Brown, J. P., Yeh, M.-Y., Hellström, I., and Hellström, K. E. (1980) Identification of a cell surface protein, p97, in human melanomas and certain other neoplasms. *Proc. Natl. Acad. Sci. U.S.A. 77*, 2183–2187.
(12) Brown, J. P., Nishiyama, K., Hellström, I., and Hellström, K. E. (1981) Structural characterization of human melanoma-associated antigen p97 with monoclonal antibodies. *J. Immunol. 127*, 539–545.
(13) Brown, J. P., Woodbury, R. G., Hart, C. E., Hellström, I., and Hellström, K. E. (1981) Quantitative analysis of melanoma-associated antigen p97 in normal and neoplastic tissues. *Proc. Natl. Acad. Sci. U.S.A. 78*, 539–543.
(14) Rose, T. M., Plowman, G. D., Teplow, D. B., Dreyer, W. J., Hellström, K. E., and Brown, J. P. (1986) Primary structure of the human melanoma-associated antigen p97 (melanotransferrin) deduced from the mRNA sequence. *Proc. Natl. Acad. Sci. U.S.A. 83*, 1261–1265.
(15) Mikolajczyk, S. D., Meyer, D. L., Starling, J. J., Law, K. L., Rose, K., Dufour, B., and Offord, R. E. (1994) High yield, site-specific coupling of N-terminally modified β-lactamase to a proteolytically derived single-sulfhydryl murine Fab'. *Bioconjugate Chem. 5*, 636–646.
(16) Werlen, R. C., Lankinen, M., Rose, K., Blakey, D., Shuttleworth, H., Melton, R., and Offord, R. E (1994). Site-specific conjugation of an enzyme and an antibody fragment. *Bioconjugate Chem. 5*, 411–417.
(17) Werlen, R. C., Lankinen, M., Smith, A., Chernushevich, I., Standing, K. G., Blakey, D. C., Shuttleworth, H., Melton, R. G., Offord, R. E., and Rose, K. (1995) Site-specific immunoconjugates. *Tumor Targeting 1*, 251–258.
(18) Bosslet, K., Czech, J., Lorenz, P., Sedlacek, H. H., Shuermann, M., and Seemann, G. (1992) Molecular and functional characterization of a fusion protein suited for tumor specific prodrug activation. *Br. J. Cancer 65*, 234–238.
(19) Goshorn, S. C., Svensson, H. P., Kerr, D. E., Somerville, J. E., Senter, P. D., and Fell, H. P. (1993) Genetic construction, expression, and characterization of a single chain anticarcinoma antibody fused to β-lactamase. *Cancer Res. 53*, 2123–2127.
(20) Rodrigues, M. L., Presta, L. G., Kotts, C. F., Wirth, C., Mordenti, J., Osaka, G., Wong, W. L. T., Nuijens, A., Blackburn, B., and Carter, P. (1995) Development of a humanized disulfide-stabilized anti-p185 HER2 Fv-β-lactamase fusion protein protein for activation of a cephalosporin doxorubicin prodrug. *Cancer Res. 55*, 63–70.
(21) Galleni, M., Lindberg, F., Normark, S., Cole, S., Honore, N., Joris, B., and Frère, J. M. (1988) Sequence and comparative analysis of three *Enterobacter cloacae* ampC beta-lactamase genes and their products. *Biochem. J. 250*, 753–760.
(22) Siemers, N. O., Yelton, D. E., Bajorath, J., and Senter, P. D. (1996) Modifying the specificity and activity of the *Enterobacter cloacae* P99 β-lactamase by mutagenesis within an M13 phage vector. *Biochemistry 35*, 2104–2111.
(23) Svensson, H. P., Wallace, P. M., and Senter, P. D. (1994) Synthesis and characterization of monoclonal antibody-β-lactamase conjugates. *Bioconjugate Chem. 5*, 262–267.
(24) Vrudhula, V. M., Svensson, H. P., Kennedy, K. A., Senter, P. D., and Wallace, P. M. (1993) Antitumor activities of a cephalosporin prodrug in combination with monoclonal antibody-β-lactamase conjugates. *Bioconjugate Chem. 4*, 334–340.
(25) Everett, J. L., and Ross, W. C. R. (1949) Aryl-2-halogenoalkylamines. Part II. *J. Chem. Soc.*, 1972–1983.
(26) Yeh, M. Y., Hellström, I., Brown, J. P., Warner, G. A., Hansen, J. A., and Hellström, K. E. (1979) Cell surface antigens of human melanoma identified by monoclonal antibody. *Proc. Natl. Acad. Sci. U.S.A. 76*, 2927–2931.
(27) Trucco, M., and dePetris, S. (1981) Determination of equilibrium binding parameters of monoclonal antibodies specific for cell surface antigens. *Immunological Methods* (I. Lefkovits and B. Pernis, Eds.) pp 1–26, Academic Press, New York.
(28) Alemany, R., Rosa Vila, M., Franci, C., Egea, G., Real, R. X., and Thomson, T. M. (1993) Glycosyl phosphatidylinositol membrane anchoring of melanotransferrin (p97): apical compartmentalization in intestinal epithelial cells. *J. Cell Sci. 104*, 1155–1162.
(29) Food, M. R., Rothenberger, S., Gabathuler, R., Haidl, I. D., Reid, G., and Jefferies, W. A. (1994) Transport and expression in human melanomas of a transferrin-like glycosylphosphatidylinositol-anchored protein. *J. Biol. Chem. 269*, 3034–3040.
(30) Cockett, M. I., Bebbington, C. R., and Yarranton, G. I. (1990) High level expression of tissue inhibitor of metalloproteinases in Chinese hamster ovary cells using glutamine synthetase gene amplification. *Biotechnology 8*, 662–667.
(31) Stephens, P. E., and Cockett, M. I. (1989) The construction of a highly efficient and versatile set of mammalian expression vectors. *Nucleic Acids Res. 17*, 7110.
(32) Baker, E. N., Baker, H. M., Smith, C. A., Stebbins, M. R., Kahn, M., Hellström, K. E., and Hellström, I. (1992) Human melanotransferrin (p97) has only one functional binding site. *FEBS Lett. 298*, 215–218.
(33) Jones, S. T., and Bendig, M. M. (1991) Rapid PCR-cloning of full-length mouse immunoglobulin variable regions. *Biotechnology 9*, 88–92.
(34) Whitlow, M., Bell, B. A., Feng, S-L., Fipula, D., Hardman, K. D., Hubert, S. L., Rollence, M. L., Wood, F. F., Schott, M. E., Milenic, D. E., Yokota, T., and Schlom, J. (1993) An improved linker for single-chain Fv with reduced aggregation and enhanced proteolytic stability. *Protein Eng. 6*, 989–995.
(35) Cartwright, S. J., and Waley, S. G. (1984) Purification of β-lactamases by affinity chromatography on phenylboronic acid-agarose. *Biochem. J. 221*, 505–512.
(36) Svensson, H. P., Kadow, J. F., Vrudhula, V. M., Wallace, P. M., and Senter, P. D. (1992) Monoclonal antibody-β-lactamase conjugates for the activation of a cephalosporin mustard prodrug. *Bioconjugate Chem. 3*, 176–181.
(37) O'Callaghan, D. E., Morris, A., Kirby, S., and Shingler, A. H. (1972) Novel method for detection of β-lactamases by using a chromogenic cephalosporin substrate. *Antimicrob. Agents Chemother. 1*, 283–288.
(38) Plückthun, A. (1992) Mono- and bivalent antibody fragments produced in *E. coli*: engineering, folding, and antigen binding. *Immunol. Rev. 130*, 151–188.

(39) Adamczyk, M., Gebler, J. C., and Mattingly, P. G. (1996) Characterization of protein-hapten conjugates. 2. Electrospray mass spectrometry of bovine serum albumin-hapten conjugates. *Bioconjugate Chem. 7*, 475−481.

(40) Chang, T. K., Jackson, D. Y., Burnier, J. P., and Wells, J. A. (1994) Subtiligase: a tool for semisynthesis of proteins. *Proc. Natl. Acad. Sci. U.S.A. 91*, 12544−12548.

(41) Jackson, D. Y., Burnier, J., Quan, C., Stanley, M., Tom, J., and Wells, J. A. (1994) A designed peptide ligase for total synthesis of ribonuclease A with unnatural catalytic residues. *Science 266*, 243−247.

(42) Schwarz, A., Wandrey, C., Bayer, E. A., and Wilchek, M. (1991) Enzymatic C-terminal biotinylation of proteins. *Methods Enzymol. 184*, 160−162.

(43) Rose, K., Vilaseca, L. A., Werlen, R., Meunier, A., Fisch, I., Jones, R. M. L., and Offord, R. E. (1991) Preparation of well-defined protein conjugates using enzyme-assisted reverse proteolysis. *Bioconjugate Chem. 2*, 154−159.

(44) Kerr, D. E., Garrigues, U. S., Wallace, P. M., Hellström, K. E., Hellström, I., and Senter, P. D. (1993) Application of monoclonal antibodies against cytosine deaminase for the *in vivo* clearance of a cytosine deaminase immunoconjugate. *Bioconjugate Chem. 4*, 353−357.

(45) Rogers, G. T., Burke, P. J., Sharma, S. K., Koodie, R., and Boden, J. A. (1995) Plasma clearance of an antibody-enzyme conjugate in ADEPT by monoclonal anti-enzyme: its effect on prodrug activation in vivo. *Br. J. Cancer 72*, 1357−1363.

BC9700751